UNIVERSITÀ
DEGLI STUDI
DI PADOVA

Head office: Università degli Studi di Padova

Department of Chemical Sciences

Ph.D. course in: Molecular Sciences

Curriculum: Pharmaceutical Sciences

Series XXXII

EVALUATION OF THE ACTIVITY OF PHOTOACTIVATABLE COMPOUNDS UNDER DIFFERENT IRRADIATION CONDITIONS ON HUMAN CANCER CELL LINES FOR PHOTOCHEMOTHERAPEUTIC APPLICATIONS

Coordinator: Ch.mo Prof. Leonard Jan Prins

Supervisore: Ch.mo Prof. Giorgia Miolo

Ph.D. Student: Luca Menilli

ABSTRACT

During these 3 years of PhD course, my research activity has focused on the evaluation of the antiproliferative activity of known photosensitizing compounds, using activation under different selected wavelengths.

Evaluation of 8-Methoxypsoralen (8-MOP) and 4,6,6'-Trimethylangelicin (TMA) antiproliferative activity in combination with Blue Light irradiation

Psoralens and angelicins are known photosensitizing agents, used in combination with UVA light (PUVA) for the treatment of a variety of diseases (*i.e.* psoriasis, vitiligo, mycosis fungoides, Graft-versus-Host disease, cutaneous T-cell lymphoma). Although this therapeutic approach proved to be highly effective, side effects may occur with PUVA therapy, including skin cancer (squamous cell carcinoma and basal cell carcinoma). The use of UVA irradiation also limits the light penetration into tissues, restricting the application of this therapeutic approach to superficial areas and it is known to cause DNA damages.
Previous studies indicated that psoralens can be activated with longer wavelengths (417 nm), with a reduced formation of mutagenic lesions, such as DNA crosslinks. These evidences gave us the idea to use blue light (BL) for the activation of psoralens, in order to reduce the toxicity of the treatment and to extend the application of this therapeutic approach to solid tumors as BL is also more penetrating than UVA.
Thus, the antiproliferative activity of 8-MOP and TMA was evaluated in combination with blue light on DU145 human prostate cancer cell line, along with the detection of DNA damages, ROS generation inside the cells and western blot analysis of proapoptotic, prosurvival and proliferative molecular pathways. Flow cytometry was used for the determination of cell death mechanism and to analyse the expression of CD44 receptors, which are markers for stem cell features.

Potential anticancer activity of Fluphenazine activated with UVA light

Fluphenazine (FPZ) is an antipsychotic agent from the phenothiazine family. It exerts its activity by blocking postsynaptic D2 dopamine receptors in the limbic, cortical system and basal ganglia areas of the brain. Blocking the action of dopamine, it reduces the hallucinations and delusions that are associated with schizophrenia. FPZ has a wide adverse effect profile, including extrapyramidal symptoms (akathisia, tremors, dyskinesia). In particular, fluphenazine induces photosensitization in patients exposed to sunlight as adverse effect.

Exploiting this last side effect of FPZ under light exposure, its cytotoxic activity in combination with UVA light was investigated on three different cell line.

TABLE OF CONTENTS

INTRODUCTION

1. Cancer

Cancer is a broad term used to describe a disease that results in uncontrolled cell growth and division. It is considered a major public health problem and leading cause of death worldwide. In 2018, 18.1 millions new cancer cases and 9.6 millions of death were estimated. In particular, lung cancer is the most commonly diagnosed type of cancer (11.6%), followed by breast cancer (11.6%), prostate cancer (7.1%), colorectal cancer (6.1%), stomach cancer (8.2%) and liver cancer (8.2%).[1]

Cancer can affect potentially any part of the body and can invade surrounding tissues, rapidly spreading to other organs, thus leading to the formation of metastasis. The development of a tumour arises from the mutation of one single cell and it can be triggered by a pre-cancerous lesion. In fact, tumorigenesis is a multifactorial process, involving dynamic changes in the genome, that accompanies the transformation of normal human cells into tumoral cells.[2] There are more than 100 known types of cancer, and subtypes can be found within specific organs. This wide collection of tumoral genome can be considered to be the manifestation of eight different alterations in cell physiology as reported by Hanahan *et al.*[3]

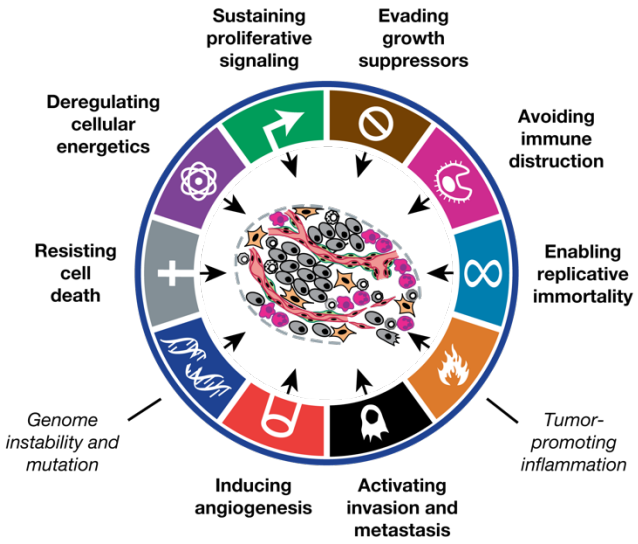

Figure 1. *Schematic representation of the necessary conditions to manifest malignant diseases.*

Genetic alteration can occur by chance or following exposure to cancer-causing agents, called carcinogens. Cancer risk factors can be divided into the following groups:

- Biological or internal factors, such as age, gender, inherited genetic defects and skin type;
- Environmental exposure to physical or chemical agents (*i.e.* UV or ionising radiation, radon, fine particulate matter, etc.);
- Bacterial or viral agents, such as Helicobacter pylori and Human Papilloma Virus (HPV);
- Lifestyle-related factors, such as smoking and alcohol abuse.

The possibilities of treating cancer have increased during the last decade and this has allowed improvements in lifespan and life quality of cancer patients. The most common types of cancer have a high cure rate when detected early and treated to best evidence. Cancer diagnosis can be performed by means of optical microscopy techniques or immunological assays. Several therapeutic approaches are available, and they are still improving, with enhanced selectivity and less side effect. The principal treatments are surgery, radiotherapy, chemotherapy and immunotherapy.

2. Treatment options

2.1 Surgery

Surgery can be used to treat many types of cancer and works best when the tumour is localized in a single area.[4] Surgeons are able to physically remove the tumour from the body, practising cuts through the skin, muscles and bones. During surgery, anaesthesia is administered to the patient using three different approaches, depending on the localization and the extension of the tumour:[5]

- Local anaesthesia: loss of feeling of small area of the body:
- Regional anaesthesia: loss of feeling of a part of the body (*i.e.* a leg or an arm);
- General anaesthesia: complete loss of feeling and awareness of the patient.

While being quite effective, surgery comes with a number of drawbacks. For instance, pain is the most common adverse effect of surgery, and its severity is strictly related to the extent of the surgery, the part of the body affected and the individual sensitivity to pain. Other common risks after surgery are the development of an infection, bleeding and reaction to the anaesthesia.

2.2 Radiation therapy

Radiation therapy is a cancer treatment in which a high dose of radiation is used to kill cancer cells or slow their growth. After radiation exposure, cancer cells DNA is damaged to an extent that results difficult to repair, leading to inhibition of cell proliferation and cell death in the irradiated area. Once damaged cells die, they are broken down and removed by the immune system.[6]

Radiotherapy can be delivered using an external or an internal approach, and that depends on many factors, such as the type of cancer, the size and location of the tumour. Briefly:

- External beam radiation therapy:[7,8] a machine is used as source of radiations, that are aim directly to the tumour. No surgical cuts are required. It is a local treatment, enabling to treat only selected areas of the body. It can treat many types of cancer;
- Internal radiation therapy:[9] the source of radiation is delivered to the patient as a solid or a liquid. It is also called brachytherapy or implant radiation therapy, and needles, seeds, wires or catheters containing the radioactive material are placed near o into the tumour. Like external beam radiotherapy, it can be used to treat only local parts of the body. The radiation source will remain active for a while. When the treatment is delivered as a liquid, it is called systemic radiation therapy.

It can be administered either orally or intravenously (IV). Body fluids like urine, sweat and saliva will contain radioactive material for a while. This kind of treatment id often used for head and neck, breast, cervix and prostate cancer. Systemic radiation therapy using radioactive iodine (^{131}I) is the most used for the treatment of thyroid cancer.

Radiation therapy is not selective, as it can damage not only malignant cells, but also healthy surrounding tissues, and that can be involved in the manifestation of several side effects: fatigue, hair loss, nausea and vomiting, skin alteration, headache, blurry vision, swelling of the treated area, taste alteration, fertility problems, etc.

2.3 Chemotherapy

Chemotherapy works by stopping or slowing the growth of cancer cells using systemically administered drugs. In particular, it is very effective with tumoral cells with rapid growth and divide rate. It can be used to treat many types of cancer and it is widely used in combination with other treatments. For example, it can be performed after surgery or radiotherapy, in order to remove remaining malignant tissues. The success of chemotherapy strongly depends on the diversity between neoplastic formation and normal healthy cells. If the differences are few, as in the case of tumoral cells and cells with high proliferative index (*i.e*. cells found in bone marrow, skin, gastro-intestinal epithelia), a chemotherapeutic agent is not able to remove the malignant population without causing side effects, deriving from the affection of rapid proliferating healthy cells. The manifestation of these unwanted targeting of healthy cells includes hair loss, nausea, infection, immune system suppression, etc.
Currently available chemotherapeutic drugs can be classified according to their main target as following:

- **Alkylating agents:** alkylating agents were better known as chemical weapon (sulphur mustard) in World War I. Nitrogen mustard were then used for medical purpose, as first modern cancer chemotherapeutic. This class of compounds works by attaching alkyl groups to DNA bases. Since cancer cells replicate faster than normal cells, with less error-correcting mechanisms, they are more sensitive to this kind of DNA damage.[10] In particular, reactions occur at N7 of the purine ring of a guanine nucleobase; monoalkylating agents can only react with a single guanine, forming monoadducts, while dialkylating agents are able to attack two different guanines, resulting in DNA crosslinkage. DNA alkylation affects DNA replication: monoadducts introduce replication errors, while crosslinks prevent DNA uncoiling and separation, thereby arresting DNA replication and RNA transcription, followed by arrested protein synthesis and cell division. Alkylating agent can be further classified as classical alkylating agents (nitrogen mustards, nitrosureas, alkyl sulphonates) and alkylating-like agents (platinum derivatives), that do not alkylated DNA directly, but permanently coordinate it, impeding DNA-related processes. The DNA damage induced by alkylating agents slows cell growth or triggers apoptotic signalling, leading to apoptosis. The effectiveness of these antineoplastic drugs strongly depends on the presence of specific DNA repair enzymes: for example, O-6-methylguanine-DNA methyltransferase (MGMT) can remove DNA crosslinks;

- **Cytotoxic antibiotics:** this class of drugs comprise a wide range of natural and semi-synthetic compounds, that works by interfering with DNA transcription, producing strand cuts or inducing DNA mutations, or inhibiting crucial DNA replication-involved enzymes. Antibiotics that directly interact with DNA intercalate between double helix bases couples, forming strong interaction that can deform or unwind DNA, thus preventing its replication. Some other antibiotics act as topoisomerase II inhibitors, an enzyme in charge of the maintenance of the DNA structure during replication. Briefly, this enzyme cuts DNA to unwind it, in order to allow the reading of DNA by replication-involved enzymes. Once this process completes, topoisomerase II repairs the cut produce before, restoring the original DNA conformation. Anti-topoisomerase II compounds induce the enzyme to produce a DNA breakage, inhibiting its repair, leaving it irreversibly damaged and thus replication is prevented. Another class of cytotoxic antibiotics acts as free-radical generators, able to produce DNA cuts as well. Anthracyclines, chromomycins, mitomycin and bleomycin are just a few examples of cytotoxic antibiotics;
- **Antimitotic agents:** during cellular division, tubulin polymerization is one of the key steps for the success of the process. Dynamic instability is the term used to describe the intense phenomena that involves tubulin polymerization and depolymerization, and their mechanism is strongly dependent on the presence of guanosine triphosphate and Ca^{2+}. Antimitotic agents act stabilizing tubulin polymers, inducing the blockage of the mitosis, with the production of large aberrant cellular structures.[11] When the cell is locked in the mitotic fuse, the situation can evolve in different ways: cell death through apoptosis or mitotic catastrophe or formation of aneuploid cells, posing a risk of oncogenesis. The main exponents of this class of drug are the taxans, natural or semi-synthetic (paclitaxel), and *Catharanthus roseus* alkaloids (vincristine, vinblastine, etc.);
- **Antimetabolites:** this class of anticancer drugs act as false substrates for enzymes involved in the biosynthesis of nucleotides. The design of these enzyme inhibitors favours their use over their endogenous analogues, binding irreversibly with the target enzyme. Being the synthesis of the building blocks of the DNA blocked, DNA synthesis is blocked as well.[12] The growth and division of tumoral cells are also arrested. Methotrexate and fluorouracil are the most used antimetabolites for cancer treatment.

The availability of different types of chemotherapeutics, combined with a better understanding of the genetic polymorphism and its impact on target proteins and metabolic enzymes, helps selecting a more efficient therapy based on the specific tumoral characteristics. Unfortunately, chemotherapeutics represents a class of very toxic compound that are not able to discriminate healthy cells from malignant ones. The affection of healthy tissues is responsible for the severe side effects mentioned above that arise even after a single treatment. Patients must be allowed to recover from these side effects before proceeding with another administration. This implies that chemotherapy must be performed over a great amount of time, and during therapy suspension tumoral growth can be restored.

2.4 Immunotherapy

The immune system plays a critical role in the regulation of tumour biology, inhibiting or supporting its development, growth, invasiveness and the ability to infiltrate other organs and tissues. The immune system actively surveys for malignant transformation and can be trained to recognise and eradiate abnormal cells.[13] However, one of the reasons that cancer cells can grow in an uncontrolled way is because they are able to escape the action of the immune system. Indeed, the immune system can't only protect against tumour development, but can also select for tumours with reduced antigenicity or immunogenicity, thus promoting tumour outgrowth. In this process called "cancer immunoediting", cancer cell clones evolve to avoid the attack and their elimination by leukocytes with anti-tumor activity.[14] Another strategy adopted by malignant cells to escape the immune system is the recruitment of immunosuppressive leukocytes, thus creating a microenvironment that weakens the anti-tumour immune response.[15] Recent strategies for cancer immunotherapy include the stimulation of the immune system, improving its natural ability to fight cancer. Cancer cells often express very specific antigens (proteins or other macromolecules) that can be used to mark them for the immune system to inhibit or kill. Cancer immunotherapy can be classified as:

- Active: directs the immune system to the tumoral cells by attacking tumour antigens;
- Passive: existing anti-tumour response is enhanced using monoclonal antibodies, lymphocytes and cytokines;
- Hybrid: combined action of both active and passive immunotherapy.

Active immunotherapy uses modified cells to exert its activity. Immune cells from the blood or the tumour are retrieved and grown in culture. During culturing, cells are induced to attack selected tumour antigens and then are reinfused into the patient. Alternatively, immune cells can be genetically engineered to express a tumor-specific receptor, cultured and returned to the patient. The most used cells are natural killer (NK) cells, lymphokine-activated killer cells, cytotoxic T-cells and dendritic cells.

Passive immunotherapy targets cell surface receptors, and include CD20, CD274, and CD279 antibodies. Once bound to the cancer antigen, monoclonal antibodies can induce antibody-dependent cell-mediated cytotoxicity, activate the complement system, or prevent the interaction between a ligand and its receptor, all which can lead to cell death.

Despite being a specific and effective approach, immunotherapy presents an heterogenic response, reflecting the ability of tumours to adapt to the immune action through the loss of antigenicity and immunogenicity, as well as their ability to establish an immunosuppressive microenvironment. Thus, predicting which patient will benefit from the action of immunotherapy remains a big challenge.

2.5 Hormone therapy

Hormones are endogenous compounds produced by different types of glands present in the human body. They are distributed through the bloodstream and they act as messengers, permitting the communication between differ parts of the body. Hormones are also responsible for many other functions, including growth and activity regulation of certain cells and organs. Some types of cancer are influenced by the action of hormones, which can promote their growth and development. These tumours are called hormone-sensitive

or hormone-dependent and some examples are breast cancer, prostate cancer, ovarian cancer and endometrial cancer. Hormone therapy is used to target these specific cancers, using drugs designed to block or lower the amounts of circulating hormones to reduce or arrest the growth of hormone-sensitive tumours.[16]

2.6 Alternative cancer therapies

All the therapies indicated above are currently used and approved. They all come with great efficacy, along with important side effects in most cases. Cancer patient face a very difficult journey. The diagnosis of tumour can have a negative impact on the patient's quality of life, especially from a psychological point of view. A very aggressive therapy with important side effects can only deteriorate the situation. Considering the repercussions of cancer therapy on the quality of life, it is extremely important to find new solutions, with reduced side effects, while maintaining the effectiveness of the treatment. Alternative strategies have been developed in the recent years. New surgical techniques that do not require cuts has been developed: the most common are cryosurgery, in which extreme cold produced by liquid nitrogen is used to destroy malignant tissues[17,18], and hyperthermia, where small affected areas of the body are exposed to high temperature, in order to thermally ablate cancer cells[19,20] or make them more sensitive to radiation[21] or chemotherapeutic drugs.[22]

This thesis will focus on photochemotherapy, which is a promising cancer treatment, and its features are the main topic of this thesis.

3. Photochemistry

Photochemistry is the study of chemical processes that occur following the absorption of light. Many biological processes are based on photochemical reactions. The most important one is photosynthesis, a process used by plant to convert light energy into chemical energy. The stored energy can then be used to fuel plants activities. The biological process of vision is also based on photochemical reactions, as well as the formation of vitamin D by the skin when exposed to sunlight.

Photochemical reactions proceed in a different way as compared to conventional chemical reactions, as the high energy intermediates generated by light absorption are completely different from the ones obtained increasing the temperature of a reaction system. The processes involved in light absorption and generation of excited states are summarized in Figure 2.

The first law of photochemistry (Grotthuss-Draper law) states that light must be absorbed by a chemical compound for a photochemical reaction to take place. This first step is known as excitation or photoexcitation. Mostly all molecules (except molecular oxygen O_2) are found in their ground state in standard ambient conditions (25°C, 1 bar) as a singlet (S_0). Singlet state refers to a system in which all electrons are paired, and the term “singlet” indicates a set of particles (electrons) whose net angular momentum zero (all electrons are in an antiparallel conformation) and overall spin quantum number *s* is zero. Light absorption is a very quick process (10^{-15} s) and promotes a molecule from the S_0 ground singlet state to an excited singlet state (S_x). In this state, an electron is promoted to a higher orbital level, maintaining its spin, according to spin selection rules. This electronic transition can proceed from HOMO to LUMO ($S_0 \rightarrow S_1$), or to higher orbitals, S_1,

S_2, S_3, etc. The second law of photochemistry (Stark-Einstein law) states that for each photon of light absorbed by the system, no more than one molecule is activated. The quantum yield (Φ) is a parameter used to determine the efficiency of a photochemical process. A molecule in its excited state is instable, due to its high energy content. Higher singlet states quickly relax (10^{-11} - 10^{-9} s) to S_1 by radiationless decay or internal conversion (IC), in which energy is dissipated via thermal emission (vibration deactivation). S_1 is usually the only relevant singlet excited state and from this point further events may occur:

- The excited state is deactivated via IC. This is the case of flexible molecules. The lowest vibrational levels of the S_1 state overlap with the higher vibrational levels of the S_0 state, thus internal conversion can proceed down to the ground state;
- In a rigid molecule, S_1 and S_0 levels are distant from each other. The vibrational levels of the two singlet states don't overlap and thus the energy of the excited singlet state can't be dissipated through internal conversion. In this case, energy dissipation happens through a radiative process, known as fluorescence. Fluorescence is a fast process (10^{-10} - 10^{-7} s), accompanied by the emission of light. The wavelength of the emitted radiation is always higher than the absorbed one, considering that it carries a lower amount of energy (part of the absorbed energy is converted to heat);
- It is possible for the excited S_1 state to undergo spin inversion, generating an excited triplet state T_1, with two unpaired electrons possessing the same spin. This violation of the spin selection rules is made possible by a phenomenon called intersystem crossing (ISC, 10^{-12} - 10^{-4} s), an isoenergetic radiationless transition between two electronic states having different multiplicities. As the energetic levels of the T_1 and S_1 excited states are closer to each other, this forbidden process is more likely to take place thanks to a partial overlapping of their vibrational sublevels. The relaxation of the T_1 state to the ground S_0 state is also forbidden, and so this process is slower as compared to fluorescence (10^{-6} – 10^{-1} s). Thus, excited triplet states have longer lifetimes than excited singlet states. The dissipation of the energy content may happen through radiationless IC or, alternatively, by a radiative pathway called phosphorescence.

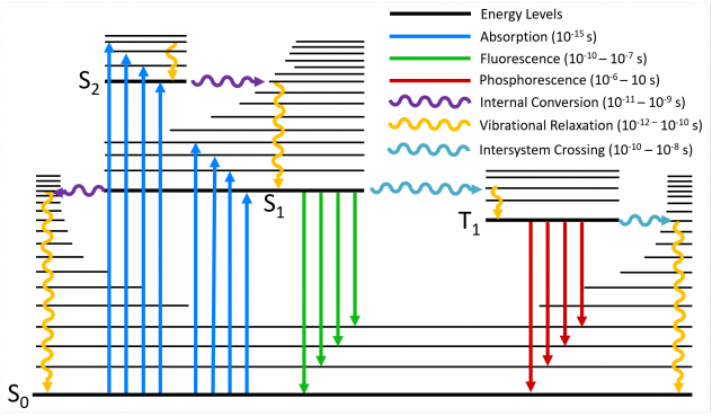

Figure 2. *Jablonski diagram.*

The energy absorbed by a molecule after light irradiation can be released through radiative or non-radiative processes, as described above, or it can be transferred to acceptor, non-absorbing molecules. The longer the lifetime of the excited state, the higher are the possibilities of encountering an acceptor molecule,

triggering the production of chemically reactive species. The related photoreactions can be classified in four main categories:

- Type I (electron transfer): a compound in its T_1 state induce the formation of ROS (hydroxyl radical $^{\bullet}OH$, superoxide anion $^{\bullet}O_2^-$ and others) by transferring one electron to molecular oxygen (O_2 ground state is a triplet);
- Type II (energy transfer): a compound in its T_1 state transfers its energy to molecular oxygen, forming singlet oxygen $^1O_2$;
- Type III: interaction between a compound in its T_1 state and native free radicals;
- Type IV: a compound in its S_1 state undergoes structural changes, enabling the direct interaction with a target. This process does not require the presence of oxygen.

The application of photochemical reactions for the treatment of human diseases and malignancies will be discussed in the next chapters.

4. Photomedicine

In photomedicine, light is used both as therapeutic and diagnostic. Photomedicine also studies the diseases caused by light. This interdisciplinary field of photobiology has found application in different branches of medicine, including surgery, dermatology, oncology, radiology, diagnosis and ophthalmology. Light plays an important role in the treatment of diseases and in the past therapeutic sunlight exposure was known with the name of heliotherapy. It was mainly used to cure skin disorders and the first registered use of heliotherapy comes from the 15th century BC and was still used until the mid-19th century. With the advent of modern technology, artificial light sources were created, and this was the first step toward the medical application of phototherapy. The first application of artificial ultraviolet light was in 1896 for the treatment of lupus vulgaris by Finsen. In the late 1950s, a treatment for new-born jaundice was developed: reduced levels of bilirubin were found in samples exposed to sunlight, indicating a possible effectiveness for the treatment of infantile hyperbilirubinemia and in 1956, at Rochford General Hospital in Essex, England, it was confirmed that exposure to sunlight was effective in reducing new-born jaundice. Further development in photomedicine lead to the combined use of light and a photoactive chemical compound, with the introduction of photochemotherapy.

4.1 Light and phototherapy

In photobiology, the most relevant part of the electromagnetic spectrum includes wavelengths from 100 to 800 nm. This range of wavelengths can be subdivided in ultraviolet spectrum (100 – 400 nm) and visible spectrum (400 - 800 nm). The UV spectrum presents three groups: UVC (100 – 290 nm), UVB (290 – 320 nm) and UVA (320-400 nm). From a biological point of view, the UVC region is too dangerous to be used for therapeutic purposes. It acts directly on DNA bases, leading to the formation of photodimers, which are then excised by the action of the endonuclease Ape1, resulting in DNA single-strand breaks, checkpoint activation

and cell cycle arrest.[23] Considering its elevated germicidal potential, UVC finds application in disinfection and sterilization of surfaces and instrumentation.

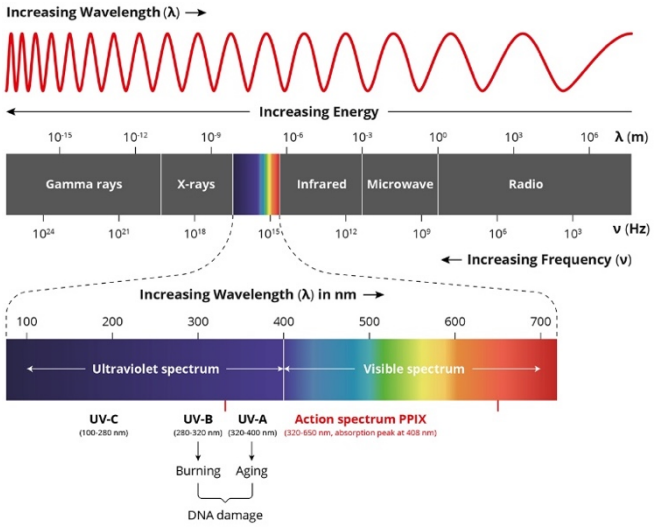

Figure 2. *Electromagnetic spectrum.*

The UVB region is commonly used in phototherapy for the treatment of various skin diseases, including psoriasis, atopic dermatitis and vitiligo.[24] Its penetration into biological tissues is limited to the papillary dermis. Although conventional UVB phototherapy (or broadband UVB phototherapy) proved to be very effective in the management of the aforementioned skin conditions, DNA nucleotides of skin cells strongly absorb the UVB radiation, inducing the formation of cyclobutane pyrimidine dimers (CPD) and pyrimidine 6,4-photoproduct (6,4-PPs), responsible for both UVB therapeutic and toxic effects.[25] The activation of the tumor suppressor gene p53 following DNA damage lead to the removal of the aberrant cells through the activation of the death receptor Fas and proapoptotic effector proteins Bax (Bcl-2–associated X protein), Bak, Bid, and PUMA.[26] UVB radiation is a known carcinogen and it is associated with skin burning. To reduce the occurrence of cutaneous cancers and phototoxicity, narrowband UVB (311 – 313 nm) lamps were developed for the treatment of psoriasis.[27]

UVA range of the ultraviolet spectrum can reach deeper regions of the skin, down to the subcutis. As with UVB, UVA radiation can affect DNA as well, forming CPDs and 6,4-PPs, but probably with less efficiency than UVB. Monotherapy with broadband UVA (320 – 400 nm) and UVA1 (340 – 400 nm) were reported to be effective in the treatment of skin diseases such as systemic sclerosis (SSc)[28–32], localized scleroderma (LS)[33], chronic graft-vs-host disease (GvHD)[34–36], extragenital lichen sclerosus et atrophicus (LSA)[37], sclerodermoid rarities (eosinophilic fasciitis)[38] and other disorders affective the connective tissue, including systemic lupus erythematosus (SLE)[39–41]. UVA1 is however safer than broadband UVA, considering that the formation of DNA damages is maximum at 320 nm.[42]

The visible part of the electromagnetic spectrum includes all the wavelength visible to the human eye. A number of biological chromophores (*i.e.* protoporphyrin IX, melanin, riboflavin, hemoglobin, bilirubin) can absorb visible light. Although wavelengths ranging from 400 to 800 nm are considered to be harmless toward biological systems, their interaction with endogenous chromophores can result in their activation and formation of excited states or reactive species, and thus could induce a biological response.

4.2 Psoralen photochemotherapy

The first photochemotherapeutic treatment was done in the 1970s, with orally administered 8-methoxypsoralen and consequent irradiation with UVA. This combination is termed Psoralen + UVA or PUVA, and proved to be very effective in the management of psoriasis[43,44], mycosis fungoides, vitiligo, atopic dermatitis and cutaneous graft-vs-host disease.

Psoralens are naturally occurring compounds, that can produce photochemical reactions after irradiation with UVA. Three psoralens are used in PUVA therapy: 8-methoxypsoralen or Methoxalen (8-MOP), 5-methoxypsoralen or bergapten (5-MOP) and 4,5',8-trimethylpsoralen or trioxalen (TMP).

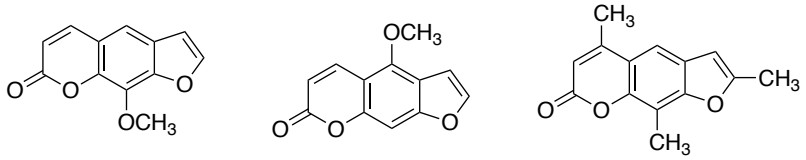

8-methoxypsoralen 5-methoxypsoralen 4,5',8-trimethylpsoralen

Figure 4. *Chemical structure of psoralens used in PUVA therapy.*

PUVA therapy induces the remission of skin diseases by repeated and controlled phototoxic reactions, that occur exclusively after photoactivation with UVA radiation (Fig. 5). Psoralens intercalate between two base pairs in the DNA double helix in the absence of UVA. The absorption of a UV photon results in the activation of the 3,4 or 4',5' double bond in the psoralen, with the consequent formation of a 3,4- or 4,5-cyclobutane addition product with pyrimidine DNA bases. In this first step, a monofunctional adduct with cytosine or thymine is formed. Some psoralens, including 8-MOP, 5-MOP and TMP, can absorb a second photon, activating the remaining double bond, and leading to the formation of a bifunctional adduct with the 5,6-double bond of a pyrimidine base of the opposite DNA strand. In this case, an interstrand crosslink is formed, suppressing DNA synthesis and replication, as well as cell division. All these processes take place in the absence of oxygen, and the involved reactions fall into the Type IV photochemical reactions.

The complete photoaddiction of psoralens to DNA was assumed as the main mechanism of action of PUVA therapy.[45] However, DNA crosslinking seems to be not crucial for the desired therapeutic effect. Indeed, photoactivated psoralens can also interact with RNA, lipids and proteins, along with the production of singlet oxygen and ROS. Probably, the action of psoralens is mediated by a mixture of the described processes, and that could explain the contribution of PUVA therapy in non-hyperproliferative diseases.

The formation of monoadducts and crosslinks immediately inhibit DNA synthesis. The interstrand crosslink are considered the main responsible for linear psoralen skin photosensitization. A great amount of cyclobutane adducts results in cell death or skin carcinogenesis and mutagenicity, considering that cells surviving this DNA damage tend to repair it through an error-prone repair process.

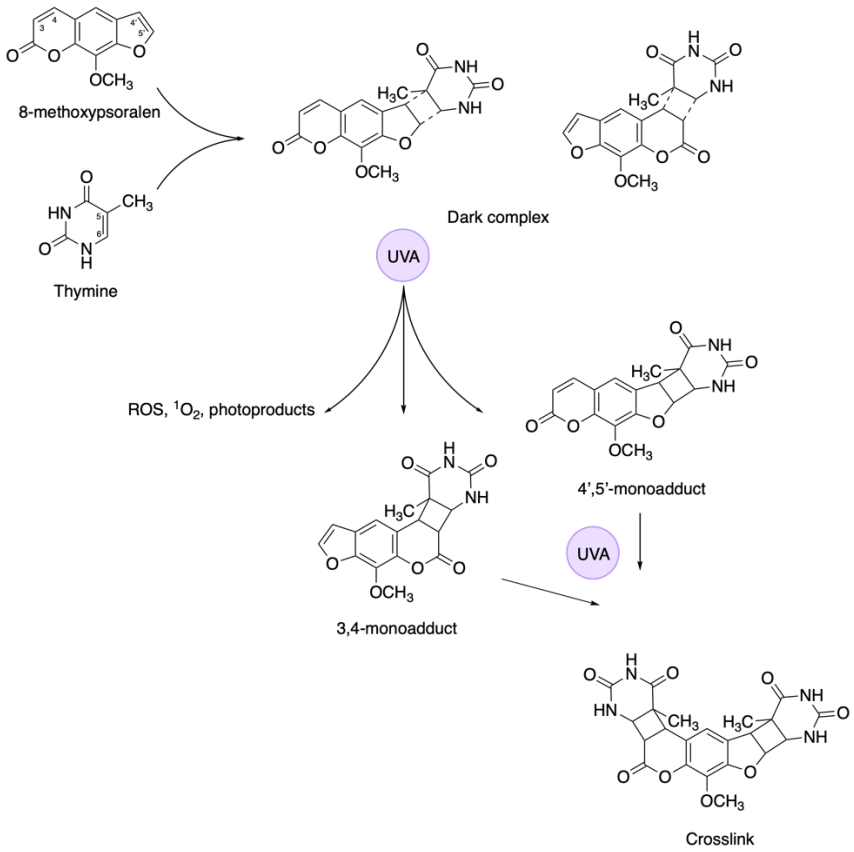

Figure 5. *Photochemistry of the psoralen 8-MOP. A dark complex with thymine DNA bases is formed, and upon UVA irradiation 8-MOP reacts with thymine, forming either the 3,4- or the 4',5'-monoadduct. After absorption of a second UVA photon, the monoadduct can further react, forming a crosslink. Aside from the Type IV mechanism of action of psoralen, they can also undergo Type I and II mechanisms, forming respectively reactive oxygen species and singlet oxygen.*

Psoralens photoactivity also involve Type I and II photochemical reactions. Indeed, the formation of ROS and singlet oxygen induce the oxidation of cellular components, such as membrane lipids and membrane bound cytochrome P-450. This cellular insult triggers the activation of arachidonic acid metabolism pathway, resulting in increased generation of secondary oxidation products that contribute to the increased synthesis of eicosanoids, responsible for different biological response, including inflammation. Reactive oxygen species can also directly damage DNA, oxidising bases and producing DNA strand breaks.

The underlying mechanism of action of psoralens relies on the photoconjugation of the psoralen to the DNA, suppressing mitosis, DNA synthesis and cell proliferation, and this should play a major role in decreasing proliferation rates in hyperproliferative diseases back to normal, as happens in psoriasis. PUVA alters the expression of cytokines and their receptors, downregulates certain lymphocytes and antigen-presenting cell functions, influences cellular adhesion, and lowers the count of Langerhans cell within the epidermis. The immune effector cells, such as lymphocytes and leukocytes, are affected by PUVA as well. Given that psoriasis is primarily caused by the action of blood-derived immunocytes, it is reasonable to suppose that PUVA may also act affecting immune functions through a direct phototoxic effect on lymphocytes in skin infiltrates, according to evidences that reports the successful treatment of non-hyperproliferative, immune-

mediated disorders. Infiltrating lymphocytes are strongly affected by PUVA, with variable effects on the different subsets. Also, lymphocytes more likely to undergo apoptosis than keratinocytes, which could explain the great efficacy of PUVA in treating cutaneous T-cell lymphoma (CTCL), as well as inflammatory skin diseases including psoriasis, given that its mechanism is in part T-cell mediated. Although the pathways and mechanisms of psoralen photosensitization are well understood, the contribution of the treatment for the definitive resolution of a specific disease remains to be investigated.

Psoralens stimulate melanogenesis, and this is linked to their action on melanocytes DNA. This involves photoconjugation of psoralens to DNA, mitosis and further proliferation of melanocytes, an increased formation and melanization of melanosomes, an increased transfer of melanosomes to keratinocytes and an increased activation of tyrosine synthesis mediated in part by cAMP stimulation. This latter effect of psoralens has been exploited in the treatment of vitiligo, inducing the pigmentation of the affected areas of the skin.

4.3 Extracorporeal Photopheresis

A modified version of PUVA therapy was introduced in the 1980s, with the name of extracorporeal photochemotherapy or photopheresis (ECP). The first disease treated with ECP was cutaneous T-cel lymphoma[46] and ECP was then approved by FDA. In 2006, ECP was recommended as first line treatment for patients with CTCL.

ECP originally involved the oral administration of 8-MOP, followed by phlebotomy passage of blood fractions from one arm vein through a photopheresis device and subsequent reinfusion to the patient. The photopheresis machine is equipped with a discontinuous flow cell separator that is used to harvest peripheral blood mononuclear cells (PBMCs) in a buffy coat collection (fraction of anticoagulated blood enriched in white cells and platelets) through density gradient centrifugation of blood. This blood fraction is then exposed to 2.0 J cm^{-2} of UVA radiation, pumping it through a thin UVA-transparent chamber, in order to ensure the correct exposure of each cell. After irradiation, blood is reconstituted and reinfused into the patient. Nowadays, 8-MOP administration is performed directly into the heparinized plasma and buffy coat fraction, right before UVA exposure, thereby avoid systemic phototoxicity of 8-MOP following accidental exposure to sunlight.[47] This therapy proved to be very effective and is currently used in clinical practise was elucidated by Edelson *et al.*[48], in which dendritic cells are involved in both antigen presentation and suppression of transplant immunopathology. PUVA induce apoptosis in circulating malignant lymphocytes. However, it has been demonstrated that the infusion of cells in which apoptosis was triggered by 8-MOP and UVA induces immunologic tolerance, probably due to the activation regulatory T-cells. ECP is also successfully used to reduce the effects observed after organ transplantation, including graft-vs-host disease and organ rejection, allowing the reduction or the total discontinuation of an immunosuppressive therapy.

4.4 Photodynamic therapy (PDT)

The first report on the application of photodynamic therapy dates back to 1978, when Dougherty clinically tested PDT by treating 113 cutaneous or subcutaneous malignant tumors with HpD-PDT, observing total or partial resolution of 111 tumors.[49] PDT aims to the destruction of the diseased tissues while minimizing the damage to normal tissues and its underlying photodynamic reaction consists of the excitation of a

photosensitizer (*i.e.* porphyrins and chlorins) by visible light in the presence of molecular oxygen (Fig. 6). The excited photosensitizer transfers its acquired energy to the molecular oxygen, resulting in the generation of reactive oxygen species, particularly singlet oxygen.

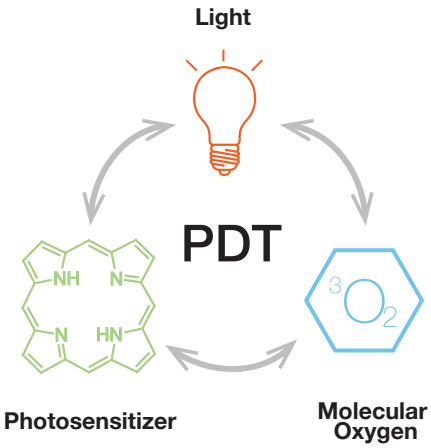

Figure 6. Basic elements for PDT. For a photodynamic reaction to take place, three elements are required: light of appropriate wavelength, a photosensitizer absorbing the light and molecular oxygen as final energy acceptor. When one of these three elements is missing, the photodynamic process can't be performed.

These highly reactive species are responsible for cellular and vascular effects, resulting in direct or indirect cytotoxicity on target cells.[50] Precancerous and malignant conditions treated successfully with PDT comprise actinic keratosis,[51] basal cell carcinoma,[52] Bowen's disease,[53] superficial squamous cell carcinoma.[54] PDT is indicate for inflammatory and infectious dermatoses as well, such as scleroderma[55] and acne vulgaris.[56] A relatively new employment of photodynamic therapy is photochemorejuvenation of the skin.[57]

Focusing on photosensitizers, they should meet the following criteria: high singlet oxygen production, significant light absorbance at wavelength that can penetrate deeply into biological tissues and high tissue selectivity. First generation PDT photosensitizers (*i.e.* Photofrin, HpD) lack tissue selectivity and lead to long-lasting photosensitization, indicating that the patient should avoid exposure to sunlight for a long time. On the contrary, second generation photosensitizers (*i.e.* 5-aminolevulinic acid, 5-ALA and its methyl ester) act as precursors of the synthesis of heme, leading to the selective accumulation of protoporphyrin IX (PpIX) in target tissues.[58] Indeed, an exogenous dose of 5-ALA bypasses the feedback control of the enzyme 5-aminolevulinic acid synthase, and proceeds into the biosynthesis pathway all the way to PpIX. At this point, ferrochelatase coordinates an iron ion inside PpIX, producing the final product, heme. A strong accumulation of PpIX coupled with a reduced activity of ferrochelatase leads to the accumulation of the photosensitizer. However, this works only in determined tissues and cell types.

A photosensitizer with a high quantum yield can produce noticeable biological effects with at low concentration and the majority of photosensitisers absorb light within the visible range (400 - 800 nm). Visible light penetration in tissues is only up to 3-6 mm, limiting the application of PDT to superficial tumours, unless interstitial light propagation is used. It is really important that a photosensitizer accumulate in a target tissue with a high selectivity, in order to avoid damaging surrounding healthy tissues, particularly when larger areas are treated, as in actinic keratosis. Second generation photosensitizers show interesting selectivity towards

tumoral tissues, with a ratio of porphyrins production in tumour to the surrounding tissue higher than 10:1, likely due to altered metabolism and accumulation within the premalignant or malignant cells.[59]

Light penetration into tissues increases with longer wavelengths up to 1100 nm. Porphyrins presents a absorption maximum around 400 nm (Soret band) along with minor peaks at longer wavelengths (Q bands). However, Soret band are usually not used for the excitation of photosensitizers, considering that the therapeutic optical window is located between 620 and 1200 nm (Fig. 7).

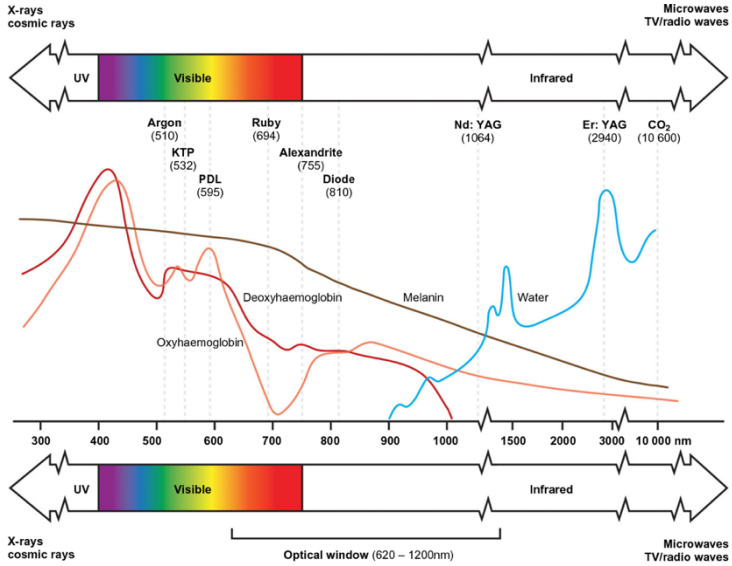

Figure 7. *Therapeutic optical window.*

To increase the depth of light penetration and match photosensitizer absorption maxima, wavelengths around 600 nm are used. Laser sources are the most efficient light source used in PDT, but they are expensive and come with high maintenance costs, along with a narrowband light emission. Incoherent sources, such as fluorescent lamps and light-emitting diodes, are getting more and more consent in their use in photodynamic therapy. Many solutions are available commercially, with blue or red emission, and are designed for the treatment of large areas. Light dosimetry strictly depends on the photosensitizer used and the light source used, as well as the disorder to be treated.

The biological effect of PDT can be divided into primary cellular and secondary vascular damage. The first noticeable effect involves cell membrane integrity, as lipid peroxidation may lead to cell lysis. Depending on the subcellular localization of the photosensitizer, cellular death may be caused by damage to mitochondria, lysosomes or the endoplasmic reticulum. DNA is not a direct target for PDT but can be oxidized anyway. Vascular effects manifest themselves with vasoconstriction, blood stasis, and thrombosis of tumoral vessels, thus interrupting the nutritional intake of a tumour with subsequent ischemia and necrosis.[60]

PDT was also reported to be capable of causing immunogenic apoptosis, mainly due to the release of damage-associated signals such as calreticulin (CRT) and heat shock proteins 70 and 90 (Hsp70 and Hsp90). These signalling proteins have various effects on dendritic cells (DCs), including antigen presentation, and once released are able to interact with DCs membrane bound or vesicular pattern-recognition receptors (PRRs). Cancer cells undergoing immunogenic apoptosis also downregulate the expression of “don’t eat me” signals, such as surface integrin-associated protein CD47. Evidences shows that these immune-related

effects of PDT can be exploited to prepare cancer vaccine using in vitro PDT of cultured cells.[61] The use of PDT for the production of cancer vaccines could open new fields of application for this type of therapeutic strategy, enhancing the action of the individual's immune system and eliminating the main limitations of PDT, including the penetration of light into the tissues and a narrow optical therapeutic window.

5. Cell death

Cell death is the aim of anti-cancer therapy, and it strictly depends on its mechanism of action. Cell death may follow two pathways: regulated cell death (RCD), in which a set of genetically encoded mechanisms for targeted elimination of altered or superfluous cells is activated,[62–65] or accidental cell death (ACD), which consists in the instantaneous autolysis and death of a cell following its exposure to severe damage, due to physical, chemical or mechanical agents.

RCD is a complicated event, acted through a dedicated molecular network and can be influenced by exogenous or endogenous factors. RCD can be activated in the absence of external stimuli and plays an important role in tissue turnover or development[66,67] and this form of RCD is referred to programmed cell death (PCD). However, RCD can also arise from modification of intra- or extracellular microenvironment, especially when the injuries exceed a certain threshold level above which the repair and restoration mechanisms are no longer sufficient to restore the homeostasis.[68] It can therefore also be said that RCD is a key factor for maintaining the biological equilibrium of an organism, mimicking the action of an adaptive stress response. This complex system not only operates eliminating useless of potentially dangerous cells, but also permits the release or the exposure of signalling molecules from dying cells, alerting the organism about a potential threat. These signals are called damage-associated molecular patterns (DAMPs) or alarmins.[69–72]

Cell death is accompanied by morphological alterations and morphotypes are used to classify cell death modality in three categories (Fig. 8):

- *Type 1 cell death or apoptosis*: cytoplasmic shrinkage, chromatin condensation (pyknosis), nuclear fragmentation (karyorrhexis) and plasma membrane blebbing, terminating with the formation of small vesicles, called apoptotic bodies, phagocyted by neighbouring cells and degraded within lysosomes;
- *Type 2 cell death or autophagy*: extensive cytoplasm vacuolization, culminating in phagocytosis and lysosomal degradation;
- *Type 3 cell death or necrosis*: no distinctive features observed in Type 1 and 2 cell death, with an elimination of cell corpses different from phagocytosis or lysosomal degradation.

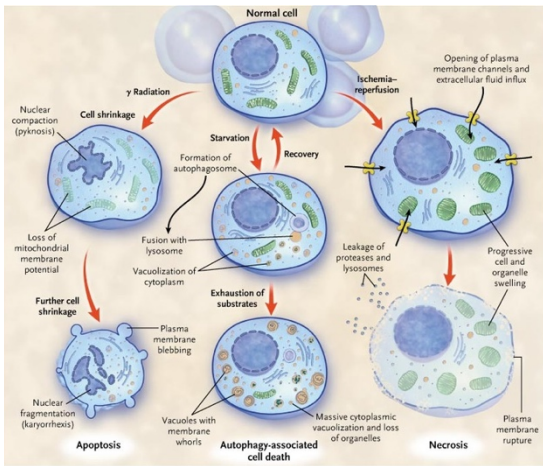

Figure 8. *Morphological classification of the three main types of cellular death. Apoptosis presents cytoplasmic shrinkage, chromatin condensation, nuclear fragmentation and membrane blebbing. Autophagy is recognized by the presence of extensive vacuolization of the cytoplasm. Necrosis do not exhibit clear morphological changes, except from swelling and loss of plasma membrane integrity.*

Focusing on apoptosis, two different modalities of activation can be distinguished:

- the *intrinsic pathway* involves a complex network of intracellular mitochondrial signaling, and it is also known as the mitochondrial pathway. Mitochondria are essential organelles that are involved in fundamental cell functions such as aerobic respiration. Indeed, a mitochondrial misfunctioning directly translates into quick cell death. Pro-apoptotic proteins interact with mitochondria and induce their swelling, probably following increased mitochondrial membrane permeability. This alteration lead to the release apoptotic effectors. During apoptosis, cytochrome c is released, and it binds with Apoptotic protease activating factor-1 (Apaf-1) and ATP, which then binds to pro-caspase-9, creating a protein complex known as apoptosome. The apoptosome convert pro-caspases to their active form caspase-9, which in turn activates the effector caspase-3, involved in the destruction of cellular components. Mitochondria also release second mitochondria-derived activator of caspases (SMACs), that are able to suppress apoptosis-inhibiting proteins (IAPs) activity, thus allowing apoptosis to proceed;
- the *extrinsic pathway* is activated by extracellular signaling, mediated by the interaction of ligands with cell-surface death receptors, that leads to the formation of Death-Inducing Signaling Complex (DISC). Two extrinsic activation theories have been suggested: tumor necrosis factor-induced (TNF) model and Fas-ligand mediated model, both involving the TNF receptor.
    - TNF path: TNF-α is major mediator of apoptosis, a cytokine produced by activated macrophages. Human cells express two types of TNF receptor: TNFR1 and TNFR2. The activation of TNFR1 leads to caspase activation, mediated by the intermediate membrane protein TNF receptor-associated death domain protein (TRADD) and Fas-associated death domain protein (FADD). The apoptotic process can be inhibited in ways, such as inhibition of TNF-α signaling following binding of Cellular Inhibitor of Apoptosis Protein 1 (cIAP1 or BIRC2)

to TNF receptor-associated factor 2 (TRAF2), or CASP8 and FADD-like apoptosis regulator (CFLAR) can inhibit caspase-8;[73]

- Fas path: the Fas receptor (First apoptosis signal) is a transmembrane receptor of the TNF family which binds the Fas ligand (FasL).[74] The formation of the ligand-receptor complex (DISC) leads to the activation of caspase-8 and caspase-10. In some types of cells, activated caspase-8 directly recruits other caspases, executing cellular apoptosis. In other types of cells, the DISC complex starts a signal leading to increased release of proapoptotic factors from mitochondria and amplified activation of caspase-8.

After apoptosis initiation, a cell undergoes a process of organized disassembly, detectable by the morphological changes described above, and in the final stages phagocytic molecules are displayed (*i.e.* phosphatidylserine) on the cell surface. These molecules mark the cell for phagocytosis and recruits the activation of macrophages. DNA and RNA are fragmented and sorted in distinct apoptotic bodies and the cell removal occurs in an ordinate process, without triggering an inflammatory response.

References

1. Bray, F. *et al.* Global cancer statistics 2018: GLOBOCAN estimates of incidence and mortality worldwide for 36 cancers in 185 countries. *CA. Cancer J. Clin.* **68**, 394–424 (2018).

2. Hanahan, D. & Weinberg, R. A. The Hallmarks of Cancer. *Cell* **100**, 57–70 (2000).

3. Hanahan, D. & Robert A, W. Biological Hallmarks of cancer. *Holland-Frei cancer Med.* 1–10 (2017). doi:10.1002/9781119000822.hfcm002

4. Arruebo, M. *et al.* Assessment of the Evolution of Cancer Treatment Therapies. *Cancers (Basel).* **3**, 3279–3330 (2011).

5. Gudaitytė, J., Dvylys, D. & Šimeliūnaitė, I. Anaesthetic challenges in cancer patients: current therapies and pain management. *Acta medica Litu.* **24**, (2017).

6. Chen, H. H. W. & Kuo, M. T. Improving radiotherapy in cancer treatment: Promises and challenges. *Oncotarget* **8**, (2017).

7. Shirato, H. *et al.* Selection of external beam radiotherapy approaches for precise and accurate cancer treatment. *J. Radiat. Res.* **59**, i2–i10 (2018).

8. Chino, F. *et al.* The role of external beam radiotherapy in the treatment of hepatocellular cancer. *Cancer* **124**, 3476–3489 (2018).

9. Wang, T.-H. *et al.* Combined Yttrium-90 microsphere selective internal radiation therapy and external beam radiotherapy in patients with hepatocellular carcinoma: From clinical aspects to dosimetry. *PLoS One* **13**, e0190098 (2018).

10. More, G. S., Thomas, A. B., Chitlange, S. S., Nanda, R. K. & Gajbhiye, R. L. Nitrogen Mustards as Alkylating Agents: A Review on Chemistry, Mechanism of Action and Current USFDA Status of Drugs. *Anticancer. Agents Med. Chem.* **19**, (2019).

11. van Vuuren, R. J., Visagie, M. H., Theron, A. E. & Joubert, A. M. Antimitotic drugs in the treatment of cancer. *Cancer Chemother. Pharmacol.* **76**, 1101–1112 (2015).

12. Asuncion, M. M. Antimetabolite Treatment for Pancreatic Cancer. *Chemother. Open Access* **03**, (2014).

13. Farkona, S., Diamandis, E. P. & Blasutig, I. M. Cancer immunotherapy: the beginning of the end of cancer? *BMC Med.* **14**, 73 (2016).

14. Schreiber, R. D., Old, L. J. & Smyth, M. J. Cancer immunoediting: integrating immunity's roles in cancer suppression and promotion. *Science* **331**, 1565–70 (2011).

15. Ferrone, C. & Dranoff, G. Dual roles for immunity in gastrointestinal cancers. *J. Clin. Oncol.* **28**, 4045–51 (2010).

16. Decruze, S. B. & Green, J. A. Hormone therapy in advanced and recurrent endometrial cancer: a systematic review. *Int. J. Gynecol. Cancer* **17**, 964 LP – 978 (2007).

17. Tarkowski, R. & Rzaca, M. Cryosurgery in the treatment of women with breast cancer-a review. *Gland Surg.* **3**, 88–93 (2014).

18. Gao, L. *et al.* Cryosurgery would be An Effective Option for Clinically Localized Prostate Cancer: A Meta-analysis and Systematic Review. *Sci. Rep.* **6**, 27490 (2016).

19. van der Horst, A. *et al.* The clinical benefit of hyperthermia in pancreatic cancer: a systematic review. *Int. J. Hyperth.* **34**, 969–979 (2018).

20. Oei, A. L. *et al.* Targeting therapy-resistant cancer stem cells by hyperthermia. *Int. J. Hyperth.* **33**, 419–427 (2017).

21. Peeken, J. C., Vaupel, P. & Combs, S. E. Integrating Hyperthermia into Modern Radiation Oncology: What Evidence Is Necessary? *Front. Oncol.* **7**, (2017).

22. Issels, R. D. Hyperthermia adds to chemotherapy. *Eur. J. Cancer* **44**, 2546–2554 (2008).

23. Mullenders, L. H. F. Solar UV damage to cellular DNA: from mechanisms to biological effects. *Photochem. Photobiol. Sci.* **17**, 1842–1852 (2018).

24. Gambichler, T., Breuckmann, F., Boms, S., Altmeyer, P. & Kreuter, A. Narrowband UVB phototherapy in skin conditions beyond psoriasis. *J. Am. Acad. Dermatol.* **52**, 660–670 (2005).

25. Bhana, S. & Lloyd, D. R. The role of p53 in DNA damage-mediated cytotoxicity overrides its ability to regulate nucleotide excision repair in human fibroblasts. *Mutagenesis* **23**, 43–50 (2008).

26. Raj, D., Brash, D. E. & Grossman, D. Keratinocyte apoptosis in epidermal development and disease. *J. Invest. Dermatol.* **126**, 243–57 (2006).

27. Simon, J. C., Pfieger, D. & Schöpf, E. Recent advances in phototherapy. *Eur. J. Dermatol.* **10**, 642–5 (2000).

28. Blann, A. D., Illingworth, K. & Jayson, M. I. Mechanisms of endothelial cell damage in systemic sclerosis and Raynaud's phenomenon. *J. Rheumatol.* **20**, 1325–30 (1993).

29. Rose, N. R. & Leskovsek, N. Scleroderma: immunopathogenesis and treatment. *Immunol. Today* **19**, 499–501 (1998).

30. Ferrarini, M., Steen, V., Medsger, T. A. & Whiteside, T. L. Functional and phenotypic analysis of T lymphocytes cloned from the skin of patients with systemic sclerosis. *Clin. Exp. Immunol.* **79**, 346–52 (1990).

31. Scaletti, C. *et al.* Th2-oriented profile of male offspring T cells present in women with systemic sclerosis and reactive with maternal major histocompatibility complex antigens. *Arthritis Rheum.* **46**, 445–50 (2002).

32. von Kobyletzki, G., Uhle, A., Pieck, C., Hoffmann, K. & Altmeyer, P. Acrosclerosis in patients with systemic sclerosis responds to low-dose UV-A1 phototherapy. *Arch. Dermatol.* **136**, 275–6 (2000).

33. Falanga, V., Medsger, T. A., Reichlin, M. & Rodnan, G. P. Linear scleroderma. Clinical spectrum, prognosis, and laboratory abnormalities. *Ann. Intern. Med.* **104**, 849–57 (1986).

34. Feldmann, R. & Harms, M. Lichen sclerosus et atrophicus. *Hautarzt.* **42**, 147–53 (1991).

35. Glockenberg, A., Cohen-Sobel, E., Caselli, M. & Chico, G. Rare case of lichen sclerosus et atrophicus associated with morphea. *J. Am. Podiatr. Med. Assoc.* **84**, 622–4 (1994).

36. Meyrick Thomas, R. H., Ridley, C. M. & Black, M. M. Clinical features and therapy of lichen sclerosus et atrophicus affecting males. *Clin. Exp. Dermatol.* **12**, 126–8 (1987).

37. Kreuter, A. *et al.* Low-dose ultraviolet-A1 phototherapy for lichen sclerosus et atrophicus. *Clin. Exp. Dermatol.* **26**, 30–2 (2001).

38. Cardozo, T. J. Eosinophilic fasciitis. *Dermatol. Online J.* **9**, 33 (2003).

39. Sönnichsen, N., Meffert, H., Kunzelmann, V. & Audring, H. [UV-A-1 therapy of subacute cutaneous lupus erythematosus]. *Hautarzt.* **44**, 723–5 (1993).

40. McGrath, H., Martínez-Osuna, P. & Lee, F. A. Ultraviolet-A1 (340-400 nm) irradiation therapy in systemic lupus erythematosus. *Lupus* **5**, 269–74 (1996).

41. Polderman, M. C., Huizinga, T. W., Le Cessie, S. & Pavel, S. UVA-1 cold light treatment of SLE: a double blind, placebo controlled crossover trial. *Ann. Rheum. Dis.* **60**, 112–5 (2001).

42. Sinha, R. P. & Häder, D. P. UV-induced DNA damage and repair: a review. *Photochem. Photobiol. Sci.* **1**, 225–36 (2002).

43. Parrish, J. A., Fitzpatrick, T. B., Tanenbaum, L. & Pathak, M. A. Photochemotherapy of psoriasis with oral methoxsalen and longwave ultraviolet light. *N. Engl. J. Med.* **291**, 1207–11 (1974).

44. Wolff, K. W. *et al.* Photochemotherapy for psoriasis with orally administered methoxsalen. *Arch. Dermatol.* **112**, 943–50 (1976).

45. Averbeck, D. Recent advances in psoralen phototoxicity mechanism. *Photochem. Photobiol.* **50**, 859–882 (1989).

46. Edelson, R. *et al.* Treatment of cutaneous T-cell lymphoma by extracorporeal photochemotherapy. Preliminary results. *N. Engl. J. Med.* **316**, 297–303 (1987).

47. Knobler, R. M. *et al.* Parenteral administration of 8-methoxypsoralen in photopheresis. *J. Am. Acad. Dermatol.* **28**, 580–4 (1993).

48. Edelson, R. L. Mechanistic insights into extracorporeal photochemotherapy: Efficient induction of monocyte-to-dendritic cell maturation. *Transfus. Apher. Sci.* **50**, 322–329 (2014).

49. Dougherty, T. J. *et al.* Photoradiation Therapy for the Treatment of Malignant Tumors. *Cancer Res.* **38**, 2628–2635 (1978).

50. Pass, H. I. Photodynamic therapy in oncology: mechanisms and clinical use. *J. Natl. Cancer Inst.* **85**, 443–56 (1993).

51. Heerfordt, I. M. & Wulf, H. C. Daylight photodynamic therapy of actinic keratosis without curettage is as effective as with curettage: a randomized clinical trial. *J. Eur. Acad. Dermatology Venereol.* jdv.15744 (2019). doi:10.1111/jdv.15744

52. de Albuquerque, I. O., Nunes, J., Figueiró Longo, J. P., Muehlmann, L. A. & Azevedo, R. B. Photodynamic therapy in superficial basal cell carcinoma treatment. *Photodiagnosis Photodyn. Ther.* **27**, 428–432 (2019).

53. O'Connell, K. A., Okhovat, J.-P. & Zeitouni, N. C. Photodynamic therapy for Bowen's Disease (squamous cell carcinoma in situ) current review and update. *Photodiagnosis Photodyn. Ther.* **24**, 109–114 (2018).

54. Jerjes, W., Yousif, A. A., Hamdoon, Z. & Hopper, C. Non-metastatic cutaneous squamous cell carcinoma treated with photodynamic therapy using intravenous mTHPC. *Photodiagnosis Photodyn. Ther.* (2019). doi:10.1016/j.pdpdt.2019.08.004

55. Wen, X., Li, Y. & Hamblin, M. R. Photodynamic therapy in dermatology beyond non-melanoma cancer: An update. *Photodiagnosis Photodyn. Ther.* **19**, 140–152 (2017).

56. Serini, S. M. *et al.* The efficacy and tolerability of 5-aminolevulinic acid 5% thermosetting gel photodynamic therapy (PDT) in the treatment of mild-to-moderate acne vulgaris. A two-center, prospective assessor-blinded, proof-of-concept study. *J. Cosmet. Dermatol.* **18**, 156–162 (2019).

57. Le Pillouer-Prost, A. & Cartier, H. Photodynamic Photorejuvenation. *Dermatologic Surg.* **42**, 21–30 (2016).

58. Kennedy, J. C. & Pottier, R. H. Endogenous protoporphyrin IX, a clinically useful photosensitizer for photodynamic therapy. *J. Photochem. Photobiol. B.* **14**, 275–92 (1992).

59. Fritsch, C. *et al.* Ex vivo Application of δ-Aminolevulinic Acid Induces High and Specific Porphyrin Levels in Human Skin Tumors: Possible Basis for Selective Photodynamic Therapy. *Photochem. Photobiol.* **66**, 114–118 (1997).

60. Fingar, V. H. Vascular Effects of Photodynamic Therapy. *J. Clin. Laser Med. Surg.* **14**, 323–328 (1996).

61. Zheng, Y. *et al.* Photodynamic-therapy Activates Immune Response by disrupting Immunity Homeostasis of Tumor Cells, which Generates Vaccine for Cancer Therapy. *Int. J. Biol. Sci.* **12**, 120–132 (2016).

62. Conrad, M., Angeli, J. P. F., Vandenabeele, P. & Stockwell, B. R. Regulated necrosis: disease relevance and therapeutic opportunities. *Nat. Rev. Drug Discov.* **15**, 348–66 (2016).

63. Weinlich, R., Oberst, A., Beere, H. M. & Green, D. R. Necroptosis in development, inflammation and disease. *Nat. Rev. Mol. Cell Biol.* **18**, 127–136 (2017).

64. Fuchs, Y. & Steller, H. Live to die another way: modes of programmed cell death and the signals emanating from dying cells. *Nat. Rev. Mol. Cell Biol.* **16**, 329–344 (2015).

65. Pasparakis, M. & Vandenabeele, P. Necroptosis and its role in inflammation. *Nature* **517**, 311–320 (2015).

66. Conradt, B. Genetic Control of Programmed Cell Death During Animal Development. *Annu. Rev. Genet.* **43**, 493–523 (2009).

67. Fuchs, Y. & Steller, H. Programmed Cell Death in Animal Development and Disease. *Cell* **147**, 742–758 (2011).

68. Galluzzi, L., Bravo-San Pedro, J. M., Kepp, O. & Kroemer, G. Regulated cell death and adaptive stress responses. *Cell. Mol. Life Sci.* **73**, 2405–2410 (2016).

69. West, A. P. & Shadel, G. S. Mitochondrial DNA in innate immune responses and inflammatory pathology. *Nat. Rev. Immunol.* **17**, 363–375 (2017).

70. Krysko, D. V. *et al.* Immunogenic cell death and DAMPs in cancer therapy. *Nat. Rev. Cancer* **12**, 860–875 (2012).

71. Galluzzi, L., Kepp, O. & Kroemer, G. Mitochondria: master regulators of danger signalling. *Nat. Rev. Mol. Cell Biol.* **13**, 780–788 (2012).

72. McDonald, B. *et al.* Intravascular Danger Signals Guide Neutrophils to Sites of Sterile Inflammation. *Science (80-.).* **330**, 362–366 (2010).

73. Chen, G. & Goeddel, D. V. TNF-R1 signaling: a beautiful pathway. *Science* **296**, 1634–5 (2002).

74. Wajant, H. The Fas signaling pathway: more than a paradigm. *Science* **296**, 1635–6 (2002).

AIM OF THE PROJECT

The best cancer treatment leads to tumoral cells destruction without significant side effects. In this connection, photochemotherapy could represent the ideal cancer treatment, as most photosensitizers show no toxicity until light is applied in the area to be treated. In this project, two classes of compounds have been studied as photochemotherapeutic compounds against cancer:

- 8-methoxypsoralen, already used in PUVA and ECP, and 4,6,6'-trimethylangelicin, a very potent psoralen derivative, currently under study for the treatment cystic fibrosis;
- Fluphenazine: a neuroleptic drug, whose major adverse effect is phototoxicity.

The main aim of this study was to evaluate the optimal combination of light sources with the photoactive test compounds to trigger biological effects on cancer cells to shed light on mechanisms involved in their antiproliferative activity.

SCIENTIFIC PUBLICATIONS

Antiproliferative activity of 8-methoxypsoralen on DU145 prostate cancer cells under UVA and blue light

Giulio Sturaro, Giulia Cigolini, Luca Menilli, Fabio Cola, Rosa Di Liddo, Alessia Tasso, Maria Teresa Conconi and Giorgia Miolo

Antiproliferative activity of 8-methoxypsoralen on DU145 prostate cancer cells under UVA and blue light.
Photochem Photobiol Sci. 2017 Jul 1;16(7):1182-1193. doi: 10.1039/c7pp00116a

Abstract

The use of photoactivatable 8-methoxypsoralen (8-MOP) as potential focal treatment towards prostate cancer cells is proposed here. Our results, obtained on isolated DNA and DU145 cells, indicate that blue light, besides UVA, is able to activate 8-MOP. When compared to UVA, blue light irradiation led to a modulation of the extent and the types of 8-MOP-DNA damage, specially cross-links, coupled to a still valuable antiproliferative effect. Our data suggest that the proapototic activity of 8-MOP is related not only to DNA damage and reactive oxygen species generation but also to the modulation of cell signalling pathways. In particular, a different activation of p38 and p44/42 mitogen-activated protein kinases was detected depending on the light wavelengths.

1. Introduction

Prostate cancer (PCa) is the most common non-cutaneous male malignancy and the second leading cause of cancer related deaths in males. External beam radiotherapy, brachytherapy or radical prostatectomy are the main options for localized PCa. Chemotherapy is also used for patients with recurrent PCa after prostatectomy. However, recurrence and progression of disease occur in a high percentage of patients.[1] In the last few years, interstitial photodynamic therapy (PDT) has also been proposed for the treatment of recurrent PCa and has entered clinical trials.[2] PDT involves a photosensitizer that upon activation by visible light, leads to cell death through the production of reactive oxygen species (ROS). Furocoumarins are natural and synthetic compounds whose structure consists of a furan ring fused with coumarin leading to several isomers, i.e. linear molecules, so called psoralens, and the angular ones, angelicins. 8-Methoxypsoralen (8-MOP), 5-methoxypsoralen (5-MOP) and 4,5,8-trimethylpsoralen (TMP) are commonly used with ultraviolet A (UVA) light in PUVA (psoralen plus UVA) therapy to treat a number of skin conditions, i.e. psoriasis, vitiligo, and cutaneous T-cell lymphoma (CTCL).[3] Another application is extracorporeal photopheresis (ECP), which involves exposure of white blood cells to UVA with 8-MOP, for the treatment of autoimmune disorders, such as variants of cutaneous T cell lymphomas, graft-versus-host disease, rheumatoid arthritis, systemic lupus erythematosus, systemic sclerosis and Crohn's disease.[4] Furthermore, linear furocoumarins have been used for sterilising blood components under UV irradiation[5] and some of them are also active without light activation, showing some activity against psychological depression.

As the photosensitizers used in PDT, furocoumarins produce ROS, singlet oxygen ($^1O_2$) or superoxide (O_2^-), that impair cellular functions through lipid peroxidation, oxidation of guanine, strand breaks in nucleic acids, oxidation of proteins, and inactivation of enzymes.[6] However, the photobiological effects of furocoumarins are mainly related to their capacity to bind DNA and form monoadducts and interstrand crosslinks, mainly with

pyrimidine bases, under UVA irradiation (320–400 nm), a region of the electromagnetic spectrum in which nucleic acids are transparent. Moreover, furocoumarins photobind lipids and intra- and extra-cellular proteins, localize in mitochondria and, upon UVA irradiation, they are able to damage these organelles leading to cell death by apoptosis.[7] Photoactivation of furocoumarins also yields stable species (photoproducts, mainly formyl-derivatives and dimers) which are cytotoxic products considered to play a relevant role in PUVA therapy.[8] Although some long-term side-effects, such as skin phototoxicity, have been observed after PUVA therapy, it has been acknowledged that long-term multiple exposures appear to be necessary for a clinical meaningful increase of risk of genotoxicity and skin cancer.[9,10] Furthermore, it has been proposed that photoactivation of furocoumarins under longer wavelengths than the UVA range leads to less mutagenic lesions in the DNA, i.e. preferential formation of psoralen monoadducts over crosslinks.[11] Herein, this work aimed to verify whether 8-MOP activated by UVA or blue light could target prostate cancer cells, providing some insights into mechanisms underlying the antiproliferative effect.

2. Materials and methods

2.1 Irradiation procedure

For UVA irradiation, a Philips HPW 125 lamp was used, mainly emitting at 365 nm. The total energy hitting the sample was monitored by means of a radiometer (Variocontrol, Waldmann, Villingen-Schwenningen, Germany), equipped with a Variocontrol UV Sensor (Waldmann). The radiant power emitted by the UVA lamp was about 8 mW cm^{-2}. For blue light (BL) experiments, samples were irradiated using Waldmann UV436HF apparatus, mainly emitting at around 420 nm (radiant power 20 mW cm^{-2}). The total energy hitting the sample was monitored by means of the same radiometer equipped with a Variocontrol blue_v Sensor (Waldmann). The samples were maintained at room temperature during irradiation.

2.2 Isolation of photoadducts with salmon testes DNA

The volumes of 8-MOP (Sigma-Aldrich, St. Louis, MO-USA) ethanol concentrated solution were added dropwise to salmon testes DNA (Sigma-Aldrich) in 10 mM NaCl and 1 mM EDTA (1.5×10^{-3} M) solutions to achieve a DNA/compound ratio of about 40. The mixture was irradiated with 15 J cm^{-2} of blue or UVA light in a glass dish. After irradiation, the DNA was precipitated with 1 M NaCl and cold ethanol (2 volumes); the precipitated DNA was collected, washed with 80% ethanol, dried and then dissolved in water. The two final solutions were hydrolyzed with 0.5 M HCl, heated at 100 °C for 1 h, neutralized with NaOH and extracted three times with $CHCl_3$. Then, the organic layers were collected, dried under high vacuum and dissolved in ethanol. The hydrolyzed mixtures were separated by thin-layer chromatography (TLC; F254 plates, 0.25 mm, Merck, Darmstadt, Germany) eluting with ethyl acetate/ethanol (9 : 1).

2.3 pBR322 DNA strand break-relaxation assay

Each pBR322 DNA sample (150 ng) (Life Technologies, Monza, Italy) dissolved in TE buffer (10 mM Tris–HCl, 1 mM EDTA, pH 7.5) was irradiated with increasing blue and UVA radiation exposures (0, 2.0, 5.0, 7.5, 12.0, 15.0 J cm^{-2}) in the presence of 300 μM 8-MOP. The samples were loaded on 1% agarose gel, after addition of 1 μL of gel loading buffer (0.25% Bromophenol blue, BPB; 0.25% xylene cyanol; and 40%, w/v, sucrose) to each of them. The electrophoretic run was carried out in TAE buffer (40 mM Tris-acetate, 1 mM EDTA, pH 8.0)

at 25 V for 6 h, using GNA-100 electrophoretic apparatus (Pharmacia, Uppsala, Sweden). After staining with ethidium bromide solution (1 μg mL^{-1} in TAE buffer) for 20 min, the gel was washed with water, and the DNA bands were visualized under UV radiation with a UV transilluminator and detected with Bio-Rad GelDoc EZ (Bio-Rad Laboratories, Inc., Hercules, CA, USA). The fraction of undamaged DNA (supercoiled, SC) and damaged DNA (open circular, OC) was calculated by using ImageLab 5.2.1 (Bio-Rad). Samples of DNA alone in the dark and after irradiation were used as controls.

2.4 Photooxidation of pBR322 DNA

Each pBR322 DNA sample (200 ng) dissolved in phosphate buffer (10 mM, pH 7.2) was irradiated with UVA and BL (0, 2.0, 7.5 J cm^{-2}) in the presence of 300 μM 8-MOP. After irradiation, DNA was precipitated by ethanol/sodium acetate, dissolved in the reaction buffer (supplied by BioLabs: 10 mM Bis Tris propane–HCl, 10 mM $MgCl_2$, 1 mM DDT, pH 7.0). Each sample was incubated for 30 min at 37 °C with Endo III (New England BioLabs, Ipswich MA, USA), as previously described.[12]

Loading buffer (3 μL, 0.25% BPB, 0.25% xylene cyanol, 30% glycerol in water) was added to the samples, then loaded on 1% agarose gel. The run was carried out in TAE buffer at 80 V for 2 h. After staining with ethidium bromide solution, the gel was washed with water and the DNA bands were detected and quantified as described above. Samples of DNA alone in the dark and after irradiation were used as controls.

2.5 Cross-linking assay

pBR322 DNA dissolved in TE buffer (10 mM Tris–HCl, 1 mM EDTA, pH 7.4) was linearized using EcoRI restriction enzyme (New England BioLabs). DNA was precipitated and irradiated with increasing doses of blue and UVA light (0, 2.0, 5.0, 7.5, 12.0, 15.0 J cm^{-2}) in the presence of 300 μM 8-MOP. Half of the samples were denatured with NaOH (0.2 M final), then placed in water bath at 100 °C for 10 min and immediately placed in ice. Non-denatured UVA and blue light treated samples (the second half), UVA and blue light irradiated pBR322 linearized untreated samples and pBR322 kept in the dark were taken as controls. The samples were loaded on 1% agarose gel and run as described above.

2.6 Cell cultures

Human prostatic cell line DU145 (Cell Lines Service, GmbH, Eppelheim, GER) was cultured as a monolayer in a proliferation medium composed of Eagle's Minimum Essential Medium (MEM) supplemented with 10% fetal bovine serum (FBS), 1% L-glutamine, 0.1 mM non-essential amino acids,

0.1 mM sodium pyruvate and 1% antibiotics (Sigma-Aldrich) at 37 °C under a humidified atmosphere containing 5% CO2.

2.7 Cell treatments

Cells (2.6×10^4 cm^{-2}) were seeded into each well of 24-well plates (Sarstedt, Newton, NC, USA) in the proliferation medium. After 24 h, the medium was removed and replaced with MEM w/o phenol red (Sigma-Aldrich) containing various 8-MOP concentrations (ranging from 0.01 to 30 μM). After 1 h of incubation in the dark at 37 °C, cultures were irradiated with 2 J cm−2 of UVA or blue light. After irradiation, media were removed and replaced with proliferation media. At 48 h, CD44 expression, apoptosis rates and cell viability were determined.

2.8 Sphere forming assay

To evaluate sphere formation, immediately after irradiation the cells were detached, seeded (3.3×10^3 cm^{-2}) into each well of low attachment 24-well plates and cultured for 13 days with a sphere formation medium composed of DMEM/F-12 (3 : 1, v/v) (Gibco, Waltham, MA, USA) supplemented with 0.4% BSA (Sigma-Aldrich), 0.4% B27 (Gibco), 1% L-glutamine, and 1% antibiotics. Then, cultures were observed by using a phase contrast microscope Nikon T-s (Shinagawa, Tokyo, Japan) and photographed at 40× magnification. Spheres' diameters and number were determined using ImageJ tools.

2.9 ROS production

The assay was performed using the Abcam's DCFDA – Cellular Reactive Oxygen Species Detection Assay Kit (Cambridge, UK) according to the manufacturer's instructions. Briefly, the cells (2.5×10^4) were seeded into each well of a 96-well black plate with a clear bottom (Corning, New York, U.S.) in the proliferation medium. After 24 h, cultures were incubated with 20 μM 2′,7′-dichlorofluorescin diacetate (DCFDA) for 45 min and then treated with various concentrations of 8-MOP for 1 h. Afterwards the plate was irradiated with 2 J cm^{-2} of blue or UVA light. Data were collected using a fluorescence microplate reader (Ex/Em = 485/535) (Viktor, PerkinElmer, Waltham, Massachusetts, US). Cultures treated with 100 and 200 μM tertbutyl hydrogen peroxide (TBHP) were taken as positive controls.

2.10 CD44 expression

CD44 expression was evaluated by means of immunofluorescence and citofluorimetric analysis. The cells were detached, placed on glass slides using Cytospin 4 (Thermo Scientific, Waltham, Massachusetts, US) and fixed with 10% formalin (Sigma-Aldrich) in PBS for 15 min at 4 °C. Nonspecific binding sites were deactivated through incubation with 3% BSA (Sigma-Aldrich) for 1 h. Samples were treated overnight at 4 °C with a non-conjugated monoclonal mouse anti-CD44 antibody (1 : 100, v/v) (AbD Serotech, Hercules, CA, USA) and, after washings with PBS, treated with secondary antibody goat antimouse Alexa 488 (1 : 200 in 1.5% BSA) (Gibco) for 30 min at room temperature. The samples were mounted with an aqueous mounting medium containing DAPI (4′-6-diamidino-2-phenylindole) (Vector Laboratories, Peterborough, UK). For citofluorimetric analysis, cell suspensions were incubated with the primary antibody non-conjugated mouse anti-CD44 (AbD Serotech) for 15 min in the dark at room temperature. Afterwards, the samples were washed with 0.5% BSA and treated with the secondary antibody Alexa 488-conjugated (Santa Cruz Biotechnology, Dallas, Texas, USA). The cells were analysed by using a FACSCanto II (Becton Dickinson, San Jose, California, USA). Samples treated only with a secondary antibody were taken as controls.

2.11 Cell viability and apoptosis

Cell viability was assessed by trypan blue staining. Alternatively, cell suspensions were treated with FITC-Annexin V and propidium iodide (BD Biosciences, San Jose, CA, USA) and incubated in the dark for 15 min at room temperature. Data were collected with a FACSCanto II cytofluorimeter. Samples marked with only FITC-Annexin V or propidium iodide and not stained cells were used as control to set up the instrument.

2.12 Western blot

At 24 h from irradiation, cultures were treated with lysis buffer (0.3% Tris-Base, 1.4% Glycine, 0.1% SDS, 1% Triton X-100, protease and phosphatase inhibitors 1×). Proteins were quantified using a BCA Protein Assay Reagent Kit (Thermo Fisher Scientific, Waltham, MA, USA, Pierce Biotechnology) according to the manufacturer's protocols and then separated by 10% SDS/PAGE (Bio-Rad Laboratories). Electroblotting was performed by using a polyvinylidene difluoride membrane (Immobilon PVDF, Millipore, Watford, UK). Blocking of nonspecific binding was achieved by incubation with 5% BSA in Tris-buffered saline for 2 h at room temperature. Then, the membrane was incubated overnight, with gentle shaking, at 4 °C with primary polyclonal rabbit anti-human GAPDH, phospho(Thr180/Tyr182)-p38, phospho(Thr202/Tyr204)-p44/42 (1 : 500, v/v) (Cell Signaling, Danvers MA, USA) antibodies. The detection of target proteins was performed using peroxidase conjugated goat anti-rabbit secondary antibodies (Bio-Rad Laboratories). The development of immunoreactivity was enhanced by a chemiluminescence substrate (ECL) (Sigma-Aldrich) and then visualized by using the VersaDoc Imaging System (Bio-Rad, Hercules, CA, USA). The protein expression level was normalized to housekeeping protein GAPDH and quantified using the image processing software ImageJ. Data are reported as the ratio between target protein and relative housekeeping protein expression.

2.13 Statistical analysis

Data are expressed as mean ± the standard error of the mean. The difference between groups was evaluated using analysis of variance (ANOVA) and Student's t-test.

3. Results

3.1 Formation of monoadducts

The capacity of 8-MOP to photobind DNA under BL was verified by irradiating salmon testes DNA with 8-MOP and comparing the results obtained under UVA at the same dose (15 J cm^{-2}). DNA irradiated in the presence of 8-MOP acquired a violet fluorescence under both blue and UVA light, as it usually happens when fluorescent furocoumarins photobind to the macromolecule.[13] The corresponding fluorescent bandseparated through TLC after hot acid hydrolysis, presented not only the same kind of violet fluorescence but also the same Rf = 0.52. Moreover, they showed the same capacity to photoreverse under mineral light (254 nm), giving rise to thymine and 8-MOP (visualized through two-dimensional chromatography), thus showing the typical behaviour of the C4-furan side cycloadduct between thymine and 8-MOP.[14] This common behaviour indicated that 8-MOP was able to form cycloadducts with thymine through the furan side double bond (4′,5′-monoadducts) even under BL. However, the lower fluorescence intensity of the band formed under BL with respect to UVA indicated that the formation of this monoadduct was less efficient under longer wavelengths. The 8-MOP pyrone side photoadducts (3,4-monoadducts) were not visualized on the TLC plate in the sample after BL irradiation. In contrast, a low amount of 3,4-monoadducts was formed under UVA light.

3.2 Interstrand cross-linking detection

Since the furan side monoadducts of psoralens, by absorbing a further photon, are able to form cross-links (XLs) through the photobinding to another front pyrimidine in the complementary DNA strand, the capacity of 8-MOP to crosslink DNA under BL was investigated with plasmid pBR322 DNA by alkaline agarose gel

electrophoresis and compared with the experiment under UVA light. The treatment of double-stranded DNA (ds-DNA) with a base (NaOH) destroys the H-bonds of the two strands linked together, thus leading to the denaturation and separation of the single-stranded DNA (ss-DNA). ds-DNA
runs slower than ss-DNA and sometimes the two single strands which run separately in the agarose gel can be easily seen (Fig. 1). Consequently, ds-DNA, which has been covalently cross-linked through 8-MOP cycloaddition, is unable to alkali denature and remains double stranded. In our experiment, denaturation of photosensitized pBR322 DNA, previously linearized with EcoRI restriction enzymes and irradiated in the presence of 8-MOP with the two lights, proved that 8-MOP produced a growing amount of XLs under increasing BL doses, i.e. a growing amount of both crosslinked DNA molecules and XLs inside the same molecule. These can be seen from the presence of the upper band (double strand DNA, ds-DNA) of increasing intensity, corresponding to non-denatured-cross linked DNA. This DNA should contain both monoadducts and at least one cross-link per molecule. It is interesting to note that in all the samples irradiated with UVA light the only band present was the ds-DNA at all the light doses used, indicating that 8-MOP is a very efficient bifunctional agent under the conditions used, even at the lowest dose of light. Moreover, looking at the position of the ds-DNA bands it can be seen that, as the light increased, the ds-crosslinked DNA moved slightly slower under the effect of the increasing number of
monoadducts and XLs formed. In contrast, at the BL dose of 2.0 J cm^{-2}, corresponding to the dose used in the photoantiproliferative experiments, the XLs were hardly detectable. Looking at the ss-DNA, this is split into the two complementary strands in the alkaline gel. The percentage of ss- (denatured, summing the two separate bands) and ds-DNA (non-denatured) of the blue and UVA light irradiated samples in the presence of 8-MOP with respect to the control are reported in Fig. 1.

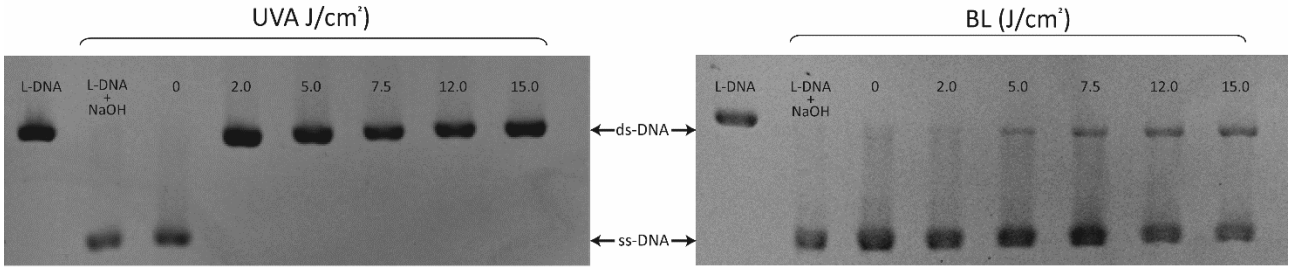

Samples	UVA		BL	
	% ds-DNA	% ss-DNA	% ds-DNA	% ss-DNA
L-DNA	100.0	\	100.0	\
L-DNA + NaOH	\	100.0	\	100.0
0 J/cm^2	\	100.0	\	100.0
2.0 J/cm^2	100.0	\	4.4 ± 0.2*	95.6 ± 0.2*
5.0 J/cm^2	100.0	\	9.9 ± 0.5*	90.1 ± 0.5*
7.5 J/cm^2	100.0	\	15.3 ± 1.1*	84.7 ± 1.1*
12.0 J/cm^2	100.0	\	24.4 ± 0.8*	75.6 ± 0.8*
15.0 J/cm^2	100.0	\	28.0 ± 0.4*	72.0 ± 0.4*

Figure 1. *Photosensitization of linearized pBR322 DNA (L) with 300 μM 8-MOP under increasing UVA and blue light (BL) radiant exposures. The samples were treated with 0.2 M NaOH, boiled for 10 min, placed quickly on ice, and loaded in alkaline 1% agarose. L: non-denatured DNA sample. L + UVA + NaOH and L + BL + NaOH: denatured and irradiated (15.0 J cm^{-2}) L samples. ds: double strand. ss: single strand. *p < 0.05 vs. non-treated L sample taken as control.*

3.3 Frank strand breaks on pBR322 DNA

We further investigated and compared the possible photodamage of 8-MOP to the nucleic acid with the two light conditions. In particular, we performed the relaxation assay on pBR322 plasmid DNA, through which single strand breaks induced directly (frank strand breaks) from the photosensitizing agent converted a supercoiled (SC) DNA molecule to a relaxed single strand form (open circular, OC) that migrates separately in an agarose gel (Fig. 2). Relaxation assay showed that 8-MOP did not damage plasmid DNA under 2 J cm^{-2} of BL and barely cleaved DNA under higher BL doses (5.0, 7.5, 12 and 15 J cm^{-2}), as indicated by the presence of a very slight band corresponding to the OC form. In contrast, under UVA light 8-MOP started to directly induce single strand cleavage at the lowest dose of 2 J cm^{-2}. The damage was much more evident at 5.0 J cm^{-2} and augmented at increasing UVA doses (12 and 15 J cm^{-2}). At these last UVA doses, the OC was the main lasting form of the DNA along with the increasing broader and slower moving SC band, reflecting the presence of a population of DNA molecules, which differ in their extent of covalent photomodification.[15] No double strand breaks, which convert the SC plasmid DNA in a linear form, were generated by 8-MOP under both light conditions. Therefore, under BL only a small effect was observed by irradiating pBR322 DNA in the presence of 8-MOP, with the formation of a very low amount of OC form, indicating that 8-MOP is not able to induce a significant yield of frank strand breaks inside DNA upon BL irradiation. It is therefore conceivable that the furan side monoadducts are the major lesions produced under this kind of light. The fractions of SC and OC DNA were quantified, and the results are reported in the table of Fig. 2 below the electrophoretic run. In the case of UVA irradiated samples (2.0, 5.0, 7.5, 12 and 15 J cm^{-2}) the quantification of the SC form was made including its smearing.

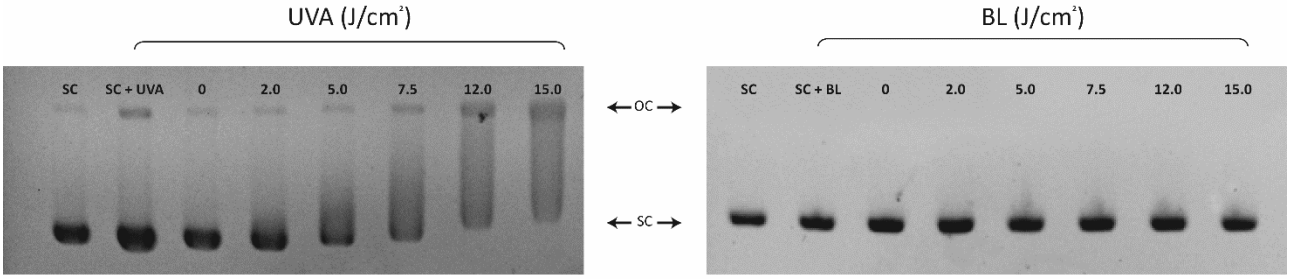

Samples	UVA		BL	
	% OC	% SC	% OC	% SC
SC	2.9 ± 0.6	97.1 ± 0.6	3.3 ± 0.3	96.7 ± 0.3
SC + Light 15.0 J/cm^2	10.3 ± 0.8*	89.7 ± 0.8*	4.5 ± 1.2	95.5 ± 1.2
0 J/cm^2	3.1 ± 0.4	96.9 ± 0.4	2.9 ± 0.8	97.1 ± 0.8
2.0 J/cm^2	4.8 ± 1.4	95.2 ± 1.4	2.4 ± 1.1	97.6 ± 1.1
5.0 J/cm^2	6.3 ± 0.5*	93.7 ± 0.5*	2.6 ± 0.8	97.4 ± 0.8
7.5 J/cm^2	5.8 ± 1.3*	94.2 ± 1.3*	3.3 ± 0.5	96.7 ± 0.5
12.0 J/cm^2	21.2 ± 0.8*	78.8 ± 0.8*	2.7 ± 0.5	97.3 ± 0.5
15.0 J/cm^2	27.8 ± 1.1*	72.2 ± 1.1*	2.5 ± 1.2	97.5 ± 1.2

***Figure 2**. Relaxation assay-frank strand breaks. pBR322 DNA in the presence of 300 μM 8-MOP was irradiated with increasing doses of UVA and blue light (BL). In the first two wells dark (SC) and irradiated pBR322 DNA samples (UVA and BL, 15 J cm^{-2}) were loaded. *p < 0.05 vs. non-treated DNA sample (SC) taken as control. OC: open circular. SC: super coiled.*

3.4 pBR322 DNA photooxidation

We further investigated the possible photooxidative damage on plasmid pBR322 DNA induced by 8-MOP under the two light conditions by using the Endonuclease III (Endo III) enzyme known to recognize 5,6-dihydropyrimidine derivatives, in addition to AP sites.[12] Single strand breaks (OC form) produced by 8-MOP under enzymatic incision at the endonuclease-sensitive sites were measured as in the previous experiments. Quantification of SC and OC DNA is shown in Fig. 3. The treatment with the base excision enzyme revealed that 8-MOP was able to photooxidize DNA bases under UVA light only under the highest UVA dose (7.5 J cm^{-2}) with respect to the UVA light alone. Indeed, UVA alone induced a photooxidative damage but besides the endonuclease revealed a small oxi-dative damage also in sample 0, thus present already in the DNA used although the sample was kept in the dark during the treatment (0 sample). The same behaviour was observed when DNA was irradiated under BL (see sample 0), but, in this case, 8-MOP did not produce a photooxidative damage higher than that of the light alone; rather it seemed to have a photoprotective effect likely through the absorption of the incoming radiation (Fig. 3). Therefore, no significant oxidative damage was induced by 8-MOP on the plasmid DNA and only a greater damage was present under a higher dose of UVA.

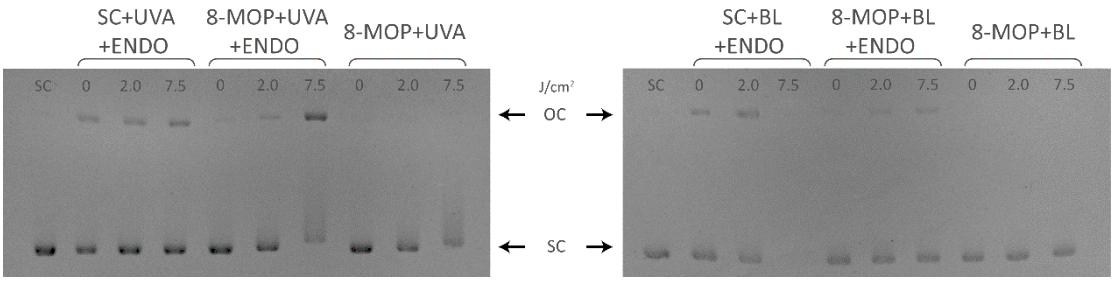

Figure 3. *Photooxidative DNA damage. DNA base modifications photoinduced by 8-MOP under increasing exposures (2.0 and 7.5 J cm^{-2}) to UVA light (left) and blue light (right). SC: non-treated SC plasmid pBR322 DNA; SC + ENDO: pBR322 DNA digested with Endo III in the dark (0) and upon irradiation (2.0, 7.5 J cm^{-2}); 8-MOP + ENDO: pBR322 DNA in the presence of 300 μM 8-MOP in the dark (0) and upon irradiation (2.0 and 7.5 J cm^{-2}) after treatment with the enzyme Endo III.*

3.5 Effects on DU145 prostate cancer cells

The antiproliferative activity of 8-MOP activated by both UVA and BL was evaluated on DU145 cells, derived from human prostate carcinoma. These small and flat cells formed good sized colonies when sub-confluent and a squamous layer when they reached confluence (Fig. 4A). The cultures comprised a high percentage (about 98%) of cells expressing CD44 that appeared mainly localized in the cytoplasmic membrane (Fig. 4C). When cultured in low attachment plates with serum free medium, DU145 cells were able to form spheres still expressing CD44 and their diameters ranged from 80 to 100 μm (Fig. 4B and D).

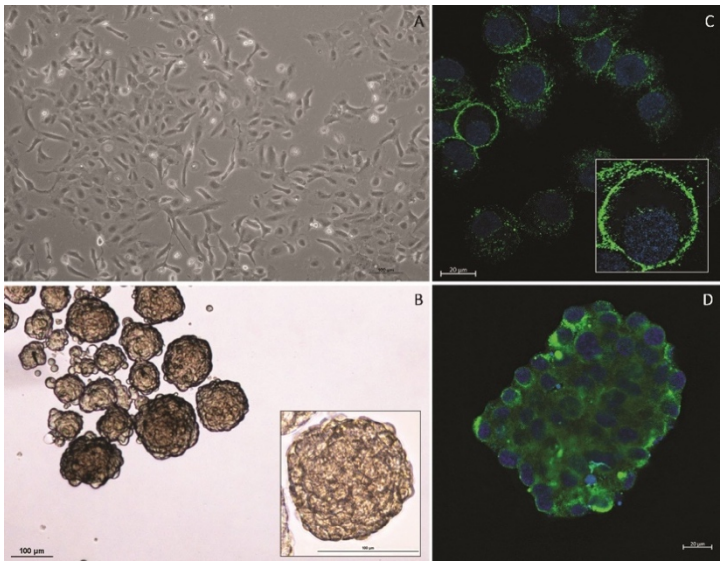

Figure 4. *Phase contrast microscopy (A, B) and immunofluorescence (C, D) of DU145 cell cultures as a monolayer (A, C) and under serum free conditions (B, D). Immunoreactivity towards CD44 stained green, whereas nuclei were labelled with DAPI (blue). Bars: 100 µm (A, B), 20 µm (C, D).*

Monolayer cultures were treated with various concentrations of 8-MOP and then irradiated with 2 J cm^{-2} UVA or BL. As shown in Fig. 5, 8-MOP was more effective after UVA irradiation than under BL one. Indeed, sphere formation was completely abrogated at 0.5 µM when activation was carried out with UVA light. In contrast, 30 µM 8-MOP was needed to achieve a 70% decrease in sphere number after BL activation. No significant

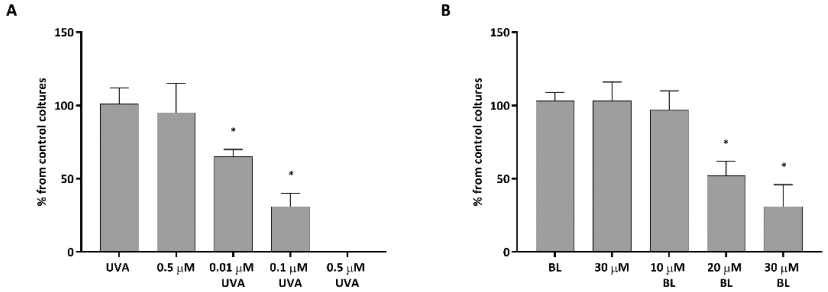

Figure 5. *Sphere forming assay. Cultures were irradiated with 2 J cm^{-2} of UVA (A) or blue light (B). Statistical significance was calculated using Student's t-test, *p < 0.05 vs. non-treated cultures taken as control. BL: blue light.*

variations were detected in cultures treated with light only or with 8-MOP kept in the dark. To elucidate the mechanism underlying the observed effects on sphere formation, further experiments were carried out by using 0.5 µM and 30 µM 8-MOP activated by UVA and BL, respectively. As expected, immediately after both irradiation, significant increases in ROS production were detected, being more pronounced under UVA activation (Fig. 6). At 48 h, two-dimensional cultures treated with photoactivated 8-MOP were less immunoreactive towards CD44 than control ones (Fig. 7).

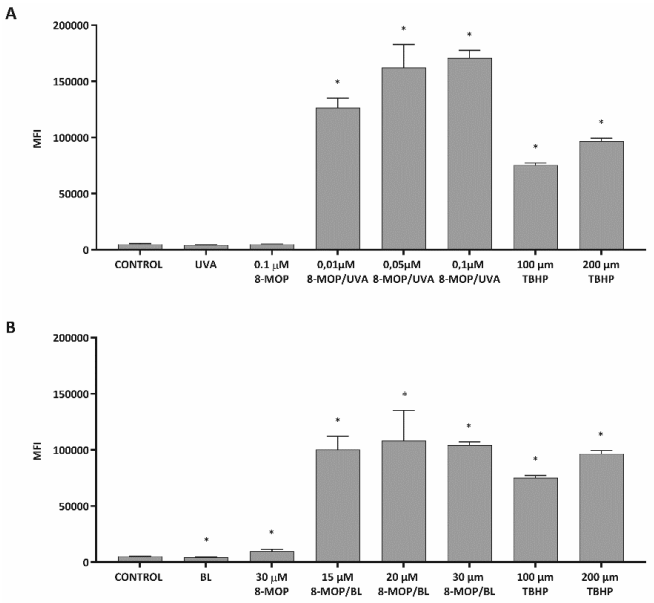

Figure 6. *ROS generation. Cultures were irradiated with 2 J cm^{-2} of UVA (A) or blue light (B). Statistical significance was calculated using Student's t-test, *p < 0.05 vs. non-treated cultures taken as control. BL: blue light.*

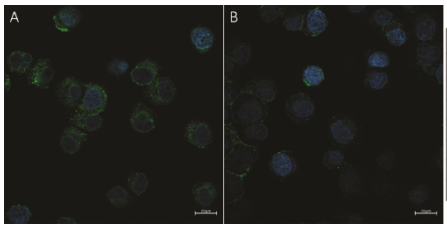

Samples	% CD44$^+$cells ± SD
Control	97.6% ± 1.2% *
UVA	96.7 ± 0.6
0.5 µM	96 ± 1.6
0.5 µM/UVA	75.3 ± 3.5 *
BL	91.2 ± 0.8 *
30 µM	91.5 ± 1 *
30 µM/BL	89.3 ± 2.7 *

Figure 7. *CD44 expression. Cultures were irradiated with 2 J cm^{-2} of UVA or blue light. Representative micrographs of untreated cell cultures (A) and cultures exposed to 8-MOP plus blue light. Immunoreactivity towards CD44 stained green, whereas nuclei were labelled with DAPI (blue). Bars: 20 µm. Cytofluorimetric data are reported as the percentage of CD44-positive cells. Statistical significance was calculated using Student's t-test, *p < 0.05 vs. non-treated cultures taken as control. BL: blue light.*

These findings are in agreement with cytofluorimetric analysis that showed significant decrease in the percentage of CD44-positive cells treated with the compound under both light conditions. However, a stronger variation was detected after UVA irradiation than under BL. Decrease in CD44 expression was also noted in cultures treated with BL only and 30 µM 8-MOP kept in the dark. Furthermore, the significant decrease in cell viability was coupled to the induction of cell apoptosis (Fig. 8). Indeed, as demonstrated by cytofluorimetric analysis, 8-MOP with both UVA and BL significantly enhanced the percentage of Annexin V-positive cells. However, the apoptosis rate was higher in cultures treated with 0.5 µM 8-MOP plus UVA that also induced a significant increase in necrotic cells (propidium iodide positive / Annexin V-negative). No significant variations were detected in control cultures, in those treated with UVA light only or with the compound kept in the dark. To investigate the mechanism underlying the antiproliferative and proapoptotic effects of 8-MOP under irradiation, the activation status of some mitogen-activated protein kinases (MAPKs) was evaluated by western blotting, using antibodies able to detect the phosphorylated forms of these proteins. The expression levels of phosphorylated p38 significantly increased in cultures treated with 8-MOP plus UVA compared to that revealed in non-treated cultures, whereas no variations of phosphorylated p44/42 were detected (Fig. 9). In contrast, after BL irradiation, 8-MOP enhanced p44/42 activation, without affecting the p38 one.

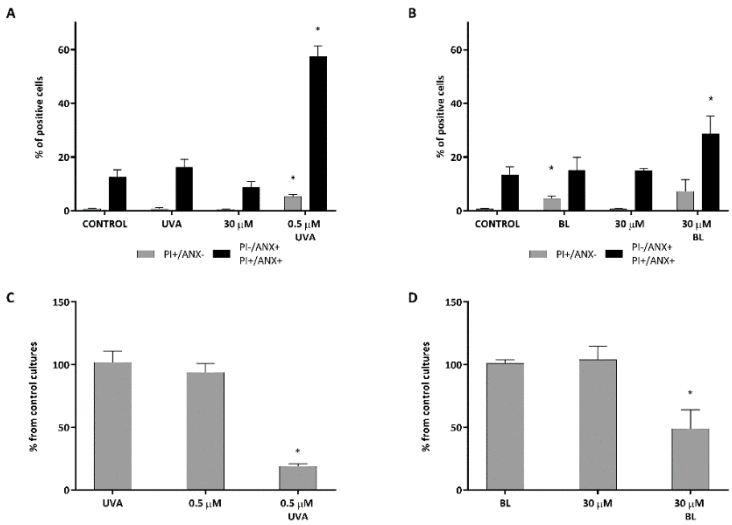

Figure 8. *Effects on apoptosis (A, B) and cell viability (C, D). Cultures were irradiated with 2 J cm^{-2} of UVA (A, C) or blue light (B, D). Statistical significance was calculated using Student's t-test, *p < 0.05 vs. non-treated cultures taken as control. BL: blue light; PI: propidium iodide; ANX: annexin V.*

4. Discussion and conclusion

Prostate cancer is a significant health problem due to its high incidence, mortality and cost associated with its diagnosis and treatment, and the lack of effective treatment for advanced disease. Thus, there is an urgent need for developing more effective anticancer modalities with minimal side effects.

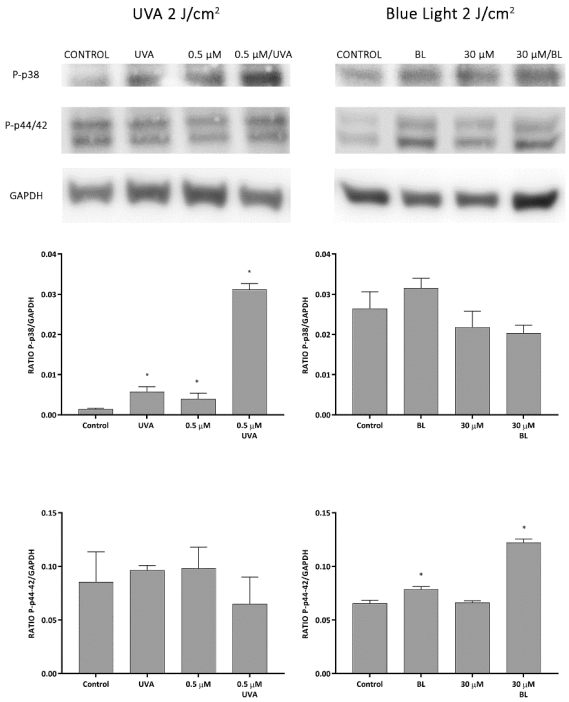

Figure 9*. WB analysis of the phosphorylation status of p38 and p44/42. Cultures were treated with 0.5 μM 8-MOP plus 2 J cm^{-2} of UVA or 30 mM 8-MOP plus 2 J cm^{-2} of blue light. The quantification of protein expression levels was performed by densitometric analysis of the bands using ImageJ processing software. Data are reported as the ratio between target protein and relative GAPDH expression. *p < 0.05 vs. non-treated cultures taken as control. BL: blue light.*

In this context, the use of naturally occurring dietary agents, suchas some bioactive compounds from Psoralea corylifolia, including flavonoids and coumarins (psoralidin, psoralen, isopsoralen and angelicin), has already been proposed as an effective strategy for prostate cancer chemoprevention.[16–18]In this work, our data have shown that 8-MOP activated by either UVA and blue light BL exerts antiproliferative effects on DU145 prostate cancer cells. Although inhibition of sphere formation under blue light was achieved at micromolar concentrations of the compound, 8-MOP was less cytotoxic on DU145 cells than when irradiated with UVA. Indeed, sphere formation inhibition of 70% was obtained with 2 J cm^{-2} of BL plus 8-MOP at a concentration about 60 times higher than that used with the same dose of UVA under which 100% of sphere inhibition was reached. From the experiments on isolatedDNA, the furan side monoadduct and cross-link
formation were detected, although to a lower extent under blue light than under UVA, thus showing that the photocytotoxic effect is strictly related to the number of DNA lesions. Similarly, the production of ROS measured both in the treated cancers cells and through the detection of photooxidized bases in plasmid DNA was less efficient under blue radiation than under UVA. These findings suggest that the photocytotoxic effects of 8-MOP on prostate cancer cells can be strictly related to the number of DNA lesions and the oxidation of cell targets. In accordance with the data of Gasparro et al.,[19] the XLs in plasmid DNA were hardly detectable at a blue light dose of 2.0 J cm^{-2}, corresponding to the dose we used in the cell-based assays. Therefore, we can assume that the formation of XLs could be very low even in the DU145 cells and that this lesion likely plays a minor role in the antiproliferative effects of 8-MOP on cancer cells.

Compelling evidence suggest that PCa stem cells (PCaSCs), a subset of cells possessing tumor-propagating ability and long-term self-renewal potential,[20] are resistant to conventional chemotherapy and radiation because they overexpress drug efflux pumps and possess an increased capacity to activateanti-apoptotic and pro-survival pathways as well as DNA repair.[21] They are responsible for recurrent hormone refractory PCa and the signatures of PCaSCs are associated with PCa bone metastasis and poor prognosis.[22] Our results indicate that photoactivated 8-MOP was also able to target PCaSCs, as demonstrated by the inhibitory activity in sphere forming assay and decreases in the percentage of CD44-positive cells. CD44, a receptor for hyaluronic acid and involved in cell adhesion and migration, is overexpressed by PCaSCs and plays an important role in the development and progression of cancer.[23] Since it is positively correlated with the PCa stage, its expression levels can be used to predict the therapeutic response to the treatment.[24] Furthermore, it has been demonstrated that monoclonal antibodies against CD44 and antisense oligonucleotides significantly reduce tumour progression.[25]

Our data show that 8-MOP activated by both UVA and blue light induced cell death by apoptosis as a result of DNA damage and the generation of a large amount of ROS. Nowadays, the release of high levels of ROS is the basis of PDT for cancer treatment. However, this may be not sufficient for successfully inhibiting tumor growth. Indeed, cancer cells overexpress antioxidant proteins to prevent ROS-induced
damage. Moreover, ROS levels inside tumor tissue must be finely tuned because low amounts of ROS can facilitate cancer cell survival and angiogenesis through the modulation of VEGF expression.[26,27] Thus, treatments possessing the mechanisms of action besides ROS generation might be more
effective than PDT.

To further elucidate the proapoptotic activity of 8-MOP, we investigated its effects on the activation of the MAPKs that modulate a wide range of processes, such as cell growth and differentiation, apoptosis, and gene expression, through the phosphorylation of target proteins. In particular, among MAPKs, extracellular signal-

regulated kinase (ERK1/2), also named p44/42, and p38 MAPK were here taken into account. Our data have shown that a different modulation of these signalling pathways occurred depending on the light used for the activation of 8-MOP. Indeed, the phosphorylation status of p38 was enhanced by 8-MOP plus UVA, whereas, under BL, it remained unchanged compared to control cultures. Our findings agree to that already reported by Cappellini et al.,[28] who demonstrated that PUVA treatment induced phosphorylation of p38, but not p42/44, in both Jurkat cells and normal human T lymphocytes. Modulation of cell cycle checkpoints, cell apoptosis and autophagy is closely related to the p38 MAPK signalling pathway similar to Jun amino-terminal kinases (JNKs), strongly activated by various extracellular stimuli, such as oxidative stress and UV radiation.[29] On the other hand, increased phosphorylation of p44/42 MAPK was detected only after activation of 8-MOP with BL. The ERK1/2 signalling pathway is usually activated by growth factors and mitogens, leading to anti-apoptotic effects by down-regulation of pro-apoptotic factors and/or upregulation of anti-apoptotic ones.[30] However, an ERK1/2 module can also act in a pro-apoptotic manner depending on cell types and under specific stimuli, such as DNA damage and some anticancer molecules. For example, Li et al.[31] have reported that angelicin, an angular furocoumarin, inhibits cell growth through the activation of the ERK pathway without any effect on the phosphorylation levels of p38 MAPK. Furthermore, it has been demonstrated that the activation of ERK1/2 may lead to toxicity in neuronal cells and its inhibition reduces apoptosis induced by adriamycin and platinum compounds.[32] Thus, we can suppose that in this study the observed different activations of MAPKs could be related to the different kinds of DNA damage and their extent. Nevertheless, further study is needed to confirm this hypothesis. Collectively, this work demonstrates, for the first time, that 8-MOP photoactivated by blue light exerts reliable antiproliferative effects on DU145 prostate cancer cells. The flexibility of 8-MOP photochemistry has allowed modulating the extent and the types of DNA damage through the delivery of blue light, thus controlling the ratio of monoaddition to the crosslinkage, mainly responsible for the mutagenicity of the DNA lesions. Moreover, in view of clinical applications, blue light may guarantee deeper penetration into the target tissue and it is also easier to be delivered by an optical fiber than UVA.

References

1. M. Valerio, H. U. Ahmed, M. Emberton, N. Lawrentschuk, M. Lazzeri, R. Montironi, P. L. Nguyen, J. Trachtenberg and T. J. Polascik, The role of focal therapy in the management of localised prostate cancer: A systematic review, *Eur. Urol.*, 2014, **66**, 732–751.

2. G. Shafirstein, D. Bellnier, E. Oakley, S. Hamilton, M. Potasek, K. Beeson and E. Parilov, Interstitial photodynamic therapy—a focused review, *Cancers (Basel).*, 2017, **9**, 12.

3. L. A. Schneider, R. Hinrichs and K. Scharffetter-Kochanek, Phototherapy and photochemotherapy, *Clin. Dermatol.*, 2008, **26**, 464–476.

4. F. Trautinger, U. Just and R. Knobler, Photopheresis (extracorporeal photochemotherapy), *Photochem. Photobiol. Sci.*, 2013, **12**, 22–28.

5. L. Lin, D. N. Cook, G. P. Wiesehahn, R. Alfonso, B. Behrman, G. D. Cimino, L. Corten, P. B. Damonte, R. Dikeman, K. Dupuis, Y. M. Fang, C. V. Hanson, J. E. Hearst, C. Y. Lin, H. F. Londe, K. Metchette, A. T. Nerio, J. T. Pu, A. A. Reames, M. Rheinschmidt, J. Tessman, S. T. Isaacs, S. Wollowitz and L. Corash, Photochemical inactivation of viruses and bacteria in platelet concentrates by use of a novel psoralen and long-wavelength ultraviolet light, *Transfusion*, 1997, **37**, 423–435.

6. D. Averbeck, Recent advances in psoralen phototoxicity mechanism, *Photochem. Photobiol.*, 1989, **50**, 859–882.

7. M. Canton, S. Caffieri, F. Dall'Acqua and F. Di Lisa, PUVA-induced apoptosis involves mitochondrial dysfunction caused by the opening of the permeability transition pore, *FEBS Lett.*, 2002, 168–172.

8. S. Caffieri, F. Di Lisa, F. Bolesani, M. Facco, G. Semenzato, F. Dall'Acqua and M. Canton, The mitochondrial effects of novel apoptogenic molecules generated by psoralen photolysis as a crucial mechanism in PUVA therapy, *Blood*, 2007, **109**, 4988–4994.

9. R. S. Stern, Photocarcinogenicity of drugs, *Toxicol. Lett.*, 1998, **102**, 389–392.

10. A. Hannuksela-Svahn, R. Sigurgeirsson, E. Pukkala, B. Lindelöf, B. Berne, M. Hannuksela, K. Poikolainen and J. Karvonen, Trioxsalen bath PUVA did not increase the risk of squamous cell skin carcinoma and cutaneous malignant melanoma in a joint analysis of 944 Swedish and Finnish patients with psoriasis, *Br. J. Dermatol.*, 1999, **141**, 497–501.

11. E. Sage and A. Bredberg, Damage distribution and mutation spectrum: the case of 8-methoxypsoralen plus UVA in mammalian cells, *Mutat. Res. Lett.*, 1991, **4**, 217–222.

12. B. Epe, M. Pflaum and S. Boiteux, DNA damage induced by photosensitizers in cellular and cell-free systems, *Mutat. Res. Toxicol.*, 1993, 135–145.

13. R. G. Dall'Acqua F, Vedaldi D, Caffieri S, Guiotto A, Bordin F, Chemical basis of the photosensitizing

activity of angelicins, *Natl Cancer Inst Monogr.*, 1984, **66**, 55–60.

14. D. Kanne, H. Rapoport and J. E. Hearst, 8-Methoxypsoralen-Nucleic acid Photoreaction. Effect of Methyl Substitution on Pyrone vs. Furan Photoaddition, *J. Med. Chem.*, 1984, **27**, 531–534.

15. X. Chen, J. Kagan, G. Miolo, F. Dall'Acqua, D. Averbeck and E. Bisagni, Photosensitized cross-linking and cleavage of pBR322 and M13 DNA: Comparison of 4,4′,6-trimethylangelicin and 3-carbethoxypsoralen, *J. Photochem. Photobiol. B Biol.*, 1994, **22**, 51–57.

16. E. Szliszka, Z. P. Czuba, Ł. Sędek, A. Paradysz and W. Król, Enhanced TRAIL-mediated apoptosis in prostate cancer cells by the bioactive compounds neobavaisoflavone and psoralidin isolated from Psoralea corylifolia, *Pharmacol. Reports*, 2011, **63**, 139–148.

17. Y. Wang, C. Hong, C. Zhou, D. Xu and H. Qu, Screening Antitumor Compounds Psoralen and Isopsoralen from Psoralea corylifolia L. Seeds, *Evidence-Based Complement. Altern. Med.*, , DOI:10.1093/ecam/nen087.

18. V. Carneiro Leite, R. Ferreira Santos, L. Chen Chen and L. Andreu Guillo, Psoralen derivatives and longwave ultraviolet irradiation are active in vitro against human melanoma cell line, *J. Photochem. Photobiol. B Biol.*, 2004, **76**, 49–53.

19. F. P. Gasparro, P. Gattolin, G. A. Olack, L. I. Deckelbaum and B. E. Sumpio, The excitation of 8-methoxypsoralen with visible light: reversed phase HPLC quantitation of monoadducts and cross-links, *Photochem. Photobiol.*, 1993, **57**, 1007–1009.

20. C. Yang, K. Jin, Y. Tong and W. C. Cho, Therapeutic potential of cancer stem cells, *Med. Oncol.*, 2015, **32**, 619.

21. J. Zhao, Cancer stem cells and chemoresistance: The smartest survives the raid, *Pharmacol. Ther.*, 2016, 145–158.

22. A. P. Rybak, R. G. Bristow and A. Kapoor, Prostate cancer stem cells: deciphering the origins and pathways involved in prostate tumorigenesis and aggression, *Oncotarget*, 2015, **6**, 1900–1919.

23. A. M. De Marzo, C. Bradshaw, J. Sauvageot, J. I. Epstein and G. J. Miller, CD44 and CD44v6 downregulation in clinical prostatic carcinoma: Relation to Gleason grade and cytoarchitecture, *Prostate*, 1998, **65**, 291–295.

24. K. Korski, A. Malicka-Durczak and J. Bręborowicz, Expression of stem cell marker CD44 in prostate cancer biopsies predicts cancer grade in radical prostatectomy specimens, *Polish J. Pathol.*, , DOI:10.5114/pjp.2014.48190.

25. D. Maisel, F. Birzele, E. Voss, A. Nopora, S. Bader, T. Friess, B. Goller, D. Laifenfeld, S. Weigand and V. Runza, Targeting Tumor Cells with Anti-CD44 Antibody Triggers Macrophage-Mediated Immune Modulatory Effects in a Cancer Xenograft Model, *PLoS One*, ,

DOI:10.1371/journal.pone.0159716.

26. P. Storz, Reactive oxygen species in tumor progression., *Front. Biosci.*, 2005, **10**, 1881–1896.

27. D. Zhu, Z. Shen, J. Liu, J. Chen, Y. Liu, C. Hu, Z. Li and Y. Li, The ROS-mediated activation of STAT-3/VEGF signaling is involved in the 27-hydroxycholesterol-induced angiogenesis in human breast cancer cells, *Toxicol. Lett.*, 2016, **264**, 79–86.

28. A. Cappellini, P. L. Tazzari, I. Mantovani, A. M. Billi, C. Tassi, F. Ricci, R. Conte and A. M. Martelli, Antiapoptotic role of p38 mitogen activated protein kinase in Jurkat T cells and normal human T lymphocytes treated with 8-methoxypsoralen and ultraviolet-A radiation, *Apoptosis*, 2005, **10**, 141–152.

29. A. Cuadrado and A. R. Nebreda, Mechanisms and functions of p38 MAPK signalling, *Biochem. J.*, 2010, **429**, 403–417.

30. Z. Lu and S. Xu, ERK1/2 MAP kinases in cell survival and apoptosis, *IUBMB Life*, 2006, **58**, 621–631.

31. G. Li, Y. He, J. Yao, C. Huang, X. Song, Y. Deng, S. Xie, J. Ren, M. Jin and H. Liu, Angelicin inhibits human lung carcinoma A549 cell growth and migration through regulating JNK and ERK pathways, *Oncol. Rep.*, 2016, **36**, 3504–3512.

32. A. Scuteri, A. Galimberti, M. Ravasi, S. Pasini, E. Donzelli, G. Cavaletti and G. Tredici, NGF protects Dorsal Root Ganglion neurons from oxaliplatin by modulating JNK/Sapk and ERK1/2, *Neurosci. Lett.*, 2010, **486**, 141–145.

4,6,4’-trimethylangelicin shows high antiproliferative activity on DU145 cells under both UVA and Blue Light

Giorgia Miolo, Giulio Sturaro, Giulia Cigolini, Luca Menilli, Alessia Tasso, Ilaria Zago, and Maria Teresa Conconi

4,6,4'-trimethylangelicin shows high anti-proliferative activity on DU145 cells under both UVA and blue light.
Cell Prolif. 2018 Apr;51(2):e12430. doi: 10.1111/cpr.12430

Abstract

Furocoumarins (psoralens and angelicins) have been already used under UVA for the treatment of skin diseases and cutaneous T cell lymphoma. Besides their high antiproliferative activity, some severe long-term side-effects have been observed, e.g., genotoxicity and mutagenicity, likely strictly related to the formation of crosslinks. It has been demonstrated that blue light (BL) activation of 8-methoxypsoralen (8-MOP), an FDA approved drug, leads to less mutagenic monoadducts in the DNA. So far, in this work the less toxic and more penetrating BL is proposed to activate 4,6,4’-trimethylangelicin (TMA), an already known UVA photoactivatable compound.

Photocleavage, crosslink formation, and oxidative damage were detected in pBR322 plasmid DNA treated with 300.0 μM TMA activated with various exposures of BL. Antiproliferative activity, ROS formation and activation status of some signaling pathways involved in cell growth and apoptosis were verified on DU145 cells treated with 5.0 μM TMA plus 2.0 J/cm^2 of BL.

Under BL-TMA no mutagenic crosslinks, no photocleavage and neither photooxidative lesions were detected on isolated plasmid DNA. TMA showed high antiproliferative activity on DU145 cells through induction of apoptosis. Besides ROS generation, the proapoptotic effect seemed to be related to activation of p38 and inhibition of p44/42 phosphorylation. Interestingly, the decrease of nuclear β-catenin was coupled with a significant dropping of CD44-positive cells.

Overall, our results indicate that TMA can be activated by BL and may be considered for targeted phototherapy of prostate cancer lesions.

1. Introduction

Prostate cancer (PCa) is one of the most frequent disease among male subjects. Conventional therapies may lead to recurrence and progression of disease[1], being necessary the development of new approaches. Among these, photodynamic therapy (PDT) is a promising strategy in delivering focal treatment in prostate cancer.[2] PDT involves the use of a photosensitizer, quite harmless in the dark, that generates cytotoxic reactive oxygen species (ROS) upon visible light irradiation. Besides porphyrin derivatives in PDT, furocoumarins (i.e. 8-methoxypsoralen, 8-MOP) are employed with ultraviolet A light (UVA) in PUVA (psoralen plus UVA) therapy to treat several skin diseases for patients with moderate to severe psoriasis, eczema, vitiligo, mycosis fungoides[3] and some autoimmune disorders

such as cutaneous T cell lymphomas, graft vs. host disease, systemic sclerosis, and Crohn's disease through an extracorporeal therapy called photopheresis.[4]

Furocoumarins comprise natural and synthetic compounds: linear molecules, so called psoralens, and the angular ones, the angelicins. The photobiological effects of furocoumarins plus UVA are mainly related to their capacity to bind DNA and form monoadducts (MAs) and interstrand crosslinks (XLs), mainly with pyrimidine bases. Furthermore, furocoumarins produce ROS that impair cellular functions through lipid peroxidation, oxidation of guanine and strand breaks in nucleic acids, oxidation of proteins and inactivation of enzymes.[5] It is known that the combination of 8-MOP and UVA radiation causes apoptosis of treated leukocytes and may cause preferential apoptosis of activated or abnormal T cells. Moreover, these apoptotic cells may promote immune tolerance, production of antigen-specific regulatory lymphocytes (CD4/8 T, B), and rebalance of immune system.[6]

Even though furocoumarins possess high chemotherapeutic potency under UVA and lack toxicity in the dark, genotoxicity, mutagenicity and skin phototoxicity have been observed.[7,8]

In the attempt to improve the activity of psoralens and avoid severe side effects thought to be mainly related to the formation of XLs, a variety of derivatives, hopefully monofunctionals, have been synthesized. Although angelicins, due to their angular geometry, do not generally form XLs, some of them, i.e. 4,6,4'-trimetylangelicin (TMA), are reported to crosslink certain types of folded DNA upon UVA irradiation.[9] 8-MOP was found to photoreact under blue light (BL) leading to less mutagenic lesions in the DNA, i.e. preferentially MAs over XLs.[10] Recently, we have demonstrated that 8-MOP, upon BL, exerts antiproliferative effects in DU145 PCa cells.[11] Furthermore, cells treated with 419 nm light resumed normal growth rates faster than cells which received the same UVA dose.[12]

2. Materials and methods

2.1 Irradiation apparatus

UVA irradiation was carried out by using one Philips HPW 125 lamp, mainly emitting at 365 nm. BL was delivered to the samples by the Waldmann UV436HF apparatus, mainly emitting at around 417 nm. The total energy hitting the sample was monitored by means of a radiometer (Variocontrol, Waldmann, Villingen-Schwenningen, Germany), equipped with a Variocontrol UV Sensor (Waldmann). The radiant power emitted by the UVA and BL lamp was about 8 mW cm^{-2} and 20 mW cm^{-2}, respectively. All samples (isolated DNA and cell cultures) were maintained at room temperature during irradiation.

2.2 Detection of interaction between TMA and isolated DNA

Strand breaks, photooxidative damage and XL formation were verified on pBR322 plasmid DNA as in [9]. DNA was irradiated with various BL and UVA radiant exposures (up to 15.0 J cm^{-2}) with 300.0 μM TMA (Fig. 1S), kindly provided by Professor Adriana Chilin (University of Padova). Samples kept in the dark or only irradiated were used as controls.

2.3 Cell cultures

Human PCa cell line DU145 (Cell Lines Service, GmbH, Eppelheim, GER) was cultured as in [9]. Cells ($2.6x10^4$ cm^{-2}) were seeded into 24-well plates. After 24 h, medium was removed and replaced with MEM w/o phenol red (Sigma-Aldrich) containing TMA concentrations up to 10.0 μM. After 1h of incubation in the dark, cultures were irradiated with UVA light or BL (2.0 J cm^{-2}). Then, media were removed and replaced with fresh medium. Sphere formation, ROS generation, CD44 expression, and apoptosis rate were determined as in [9]. Briefly, to evaluate sphere formation, immediately after irradiation cells were detached, seeded ($3.3x10^3$ cm^{-2}) into each well of low attachment 24-well plates and cultured for 13 days with sphere formation medium composed of DMEM/F-12 (3:1, v/v) (Gibco, Waltham, MA, USA) supplemented with 0.4 % BSA (Sigma-Aldrich), 0.4 % B27 (Gibco), 1 % L-glutamine, 1 % antibiotics. Then, cultures were observed by using phase contrast microscope Nikon T-s (Shinagawa, Tokyo, Japan) and photographed at 40x magnification. Spheres diameters and number were determined using ImageJ tools.

2.4 Western blot

At 24 h, total proteins were isolated by lysis buffer, whereas nuclear proteins by Nuclear and Cytoplasmic Extraction Reagents (Thermo Fisher Scientific, Waltham, MA, USA). Protein separation, electroblotting and detection of target proteins were carried out as in [9] with primary polyclonal rabbit anti-human GAPDH, phospho(Thr180/Tyr182)-p38, phospho(Thr202/Tyr204)-p44/42 (Cell Signaling Technologies, Danvers MA, USA), β-catenin, laminB1 (Santa Cruz, Dallas, Texas, USA) (1:500, v/v) antibodies. Data were reported as ratio within target protein and relative housekeeping protein expression.

2.5 Statistical analysis

Data, obtained from at least 3 experiments, were expressed as mean ± the standard error of the mean. The difference between groups was evaluated using analysis of variance (ANOVA) and Student's t-test.

3. Results

3.1 Lesions induced by TMA on DNA under BL and UVA irradiation

Thin layer chromatography followed by [H]NMR demonstrated that, although at a lower yield than under UVA, TMA plus BL was able to form MAs in salmon testes DNA (data not shown). To verify the ability of TMA to form XLs, alkali denatured linearized pBR322 DNA was loaded on denaturing agarose gel (Fig. 1A). When XLs were formed, double strand (ds) DNA was unable to denature and ran slower than the two single strands (ss). XLs formed even at the lowest UVA exposure (2.0 J cm^{-2}) along with the ss-DNA; their formation seemed complete upon 12.0 and 15.0 J cm^{-2}. The slower migration of cross-linked DNA was a function of the light dose reflecting the increasing number of XLs and MAs per molecule. On the contrary, at the highest doses of BL TMA behaved monofunctionally without any trace of undenatured crosslinked DNA. Moreover, the two ss-DNA bands appeared to run faster compared to the controls as the light increased, likely due to the presence of TMA-MAs containing furohydroxycinnamic derivatives resulting from the breakage of the pyrone ring by the alkali (Fig. 2S in

Supporting information-SI). Therefore, two more negative charges per TMA molecule bound to the DNA increased the migration of the separate strands towards the anode. These negative charges were surely present in the TMA crosslinked ds-DNA, that contains also MAs, but probably didn't increase its migration being masked inside the folded DNA. When irradiated with BL TMA did not induce any detectable cleavage on DNA and only the supercoiled (SC) form was present in all the samples (Fig. 1B). On the contrary, under UVA TMA relaxed the DNA with an increasing efficacy as the exposures augmented. Fragmentation of the strands was also visible as a smearing attesting the presence of multi forms of DNA differently modified by a varied number of photoadducts. It is noteworthy that as long as the SC DNA migrated slower as the UVA irradiation increased, under BL it happened the opposite. This behaviour is likely due to the different types of photoadducts formed under the two lights and the resulting structure acquired by the plasmid.

The detection of DNA oxidative damage was achieved by the base excision enzyme Endo III, which recognizes 5,6-dihydropyrimidines induced by hydroxyl radicals and removes the oxidized base, leaving abasic sites. Notably, TMA in combination with BL induced less oxidation than BL alone (Fig. 1C). However, both BL and UVA light alone were able to induce a remarkable oxidative damage, higher than in the presence of TMA. Indeed, TMA molecules by absorbing the incoming radiation likely protected the macromolecule from photooxidation. The quantification by densitometric analysis of each band of the gels shown in Fig. 1 is reported in Fig. 3S of the Supporting Information.

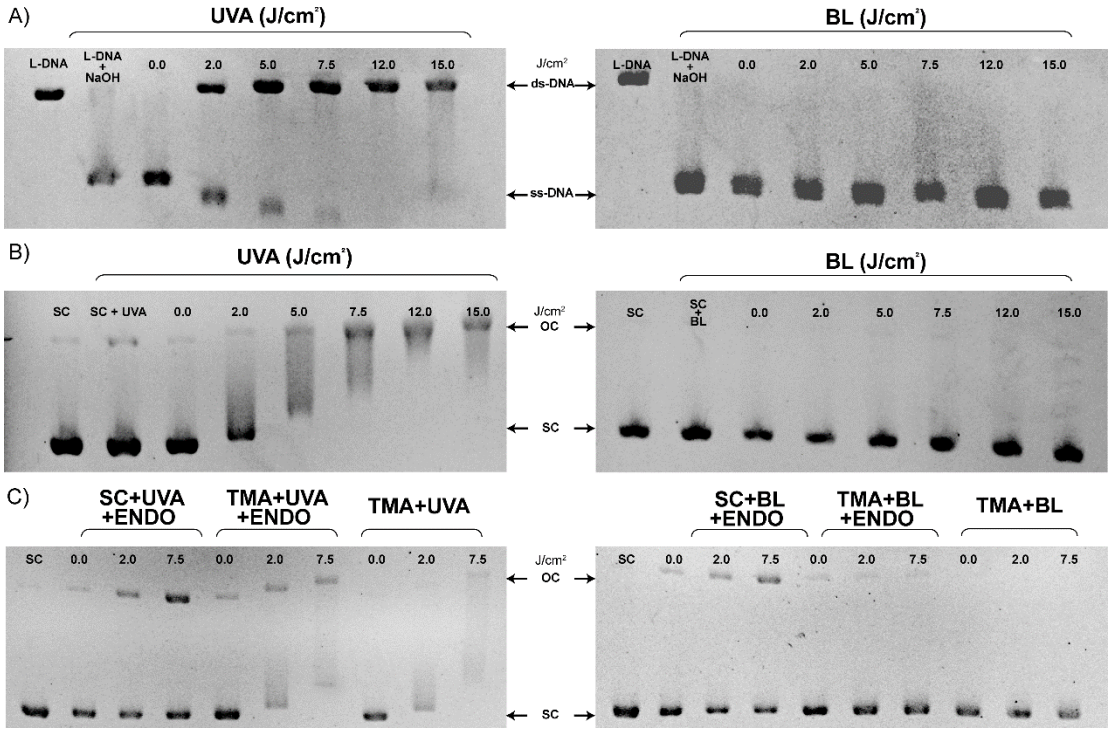

Figure 1. *(A) Photosensitization of linearized pBR322 DNA (L) with 300.0 μM TMA under UVA light and BL. The samples were treated with 0.2 M NaOH, boiled for 10 min, placed quickly in ice, and loaded in alkaline 1% agarose. L-DNA: undenatured DNA. L-DNA+UVA+NaOH and L-DNA+BL+NaOH: denatured and irradiated (15.0 J cm^{-2}) samples. ds: double strand. ss: single strand. (B) Relaxation assay in supercoiled pBR322 DNA. pBR322 DNA treated with 300.0 μM TMA was irradiated with UVA and BL. In the first two wells, dark (super coiled, SC) and irradiated pBR322 DNA samples (UVA and BL, 15.0 J cm^{-2}) were loaded. OC: open circular. (C) Photooxidative DNA damage. DNA base modifications photoinduced by TMA under UVA light and BL. SC:*

untreated SC plasmid pBR322 DNA; SC+ ENDO: pBR322 DNA digested with Endo III in the dark (0) and upon irradiation (2.0, 7.5 J cm^{-2}); TMA + ENDO: pBR322 DNA with 300.0 μM TMA in the dark (0) and upon irradiation after treatment with the enzyme Endo III.

3.2 Effects on DU145 PCa cells

To evaluate the antiproliferative activity of TMA, DU145 cells were incubated with TMA (0.01- 10.0 μM) and irradiated with 2.0 J cm^{-2} of UVA or BL. Then, detached cells were seeded to carry out the sphere forming assay. TMA was more effective after UVA irradiation than under BL one (Fig. 2). Lack of sphere formation was observed with 0.05 μM TMA upon UVA (IC_{50} = 0.017 μM), whereas 100-fold higher concentration (5.0 μM) was needed to achieve the same effect after BL (IC_{50} = 2.47 μM). No significant variation was detected with samples treated with light alone or TMA in the dark. Further experiments were performed by treating monolayer cultures with 0.05 μM and 5.0 μM TMA activated by UVA light and BL, respectively.

ROS generation, determined immediately after cell treatments, was significantly enhanced by photoactivated TMA. TMA plus UVA induced higher levels of ROS than plus BL (Fig. 3C).

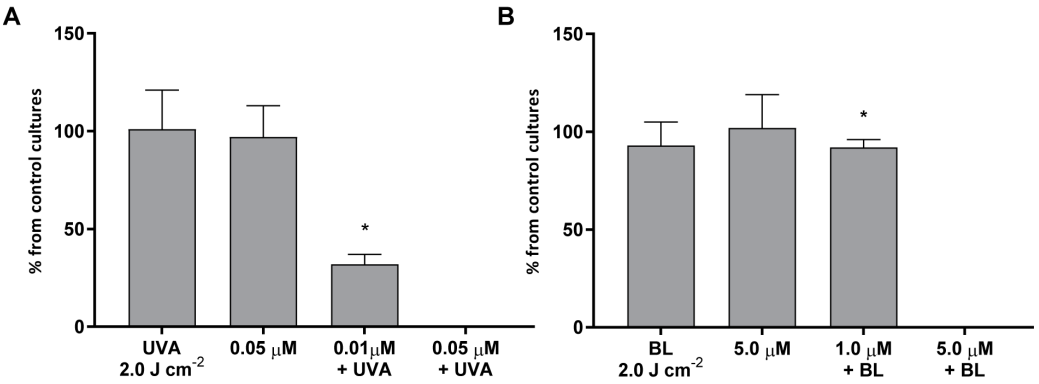

Figure 2. *Sphere forming assay. Cultures were irradiated with 2.0 J cm^{-2} of UVA light (A) or BL (B). Student's t-test, *p<0.05 vs untreated cultures taken as control.*

Small but significant increases were noted in cultures treated with the compound without light. ROS generation was unaffected by UVA light or BL alone.

At 48 h, TMA with either UVA light and BL significantly enhanced the percentages of apoptotic annexin V-positive cells and, at lower yield, those of necrotic propidium iodide- positive cells compared to non-treated cultures (fig. 3A and B). No significant variations were detected in cultures treated with light alone or TMA in the dark. Nevertheless, the presence of large vacuoles inside the treated cells suggests that also autophagy may contribute to the antiproliferative effects of TMA.[13]

DU145 cell cultures comprised a high percentage (about 98%) of cells expressing CD44 (fig. 3D). Significant decreases in CD44-positive cells were detected at 48 h from treatment with the TMA under both lights, being BL more effective (about 12%) than UVA light (about 35%). Although to a lesser extent than upon TMA photoactivation, 5.0 μM TMA in the dark and BL alone lowered CD44 expression.

The expression levels of phosphorylated p38 were significantly enhanced in cultures treated with TMA plus UVA light or BL compared to non-treated cells (Fig. 4, Fig. 4S). On the contrary, the amount of

phosphorylated p44/42 was decreased by photoactivated TMA. Notably, also cultures treated with TMA alone presented lower expression of ERK½ than controls. Nuclear β-catenin expression was significantly lowered by TMA plus UVA light or BL.

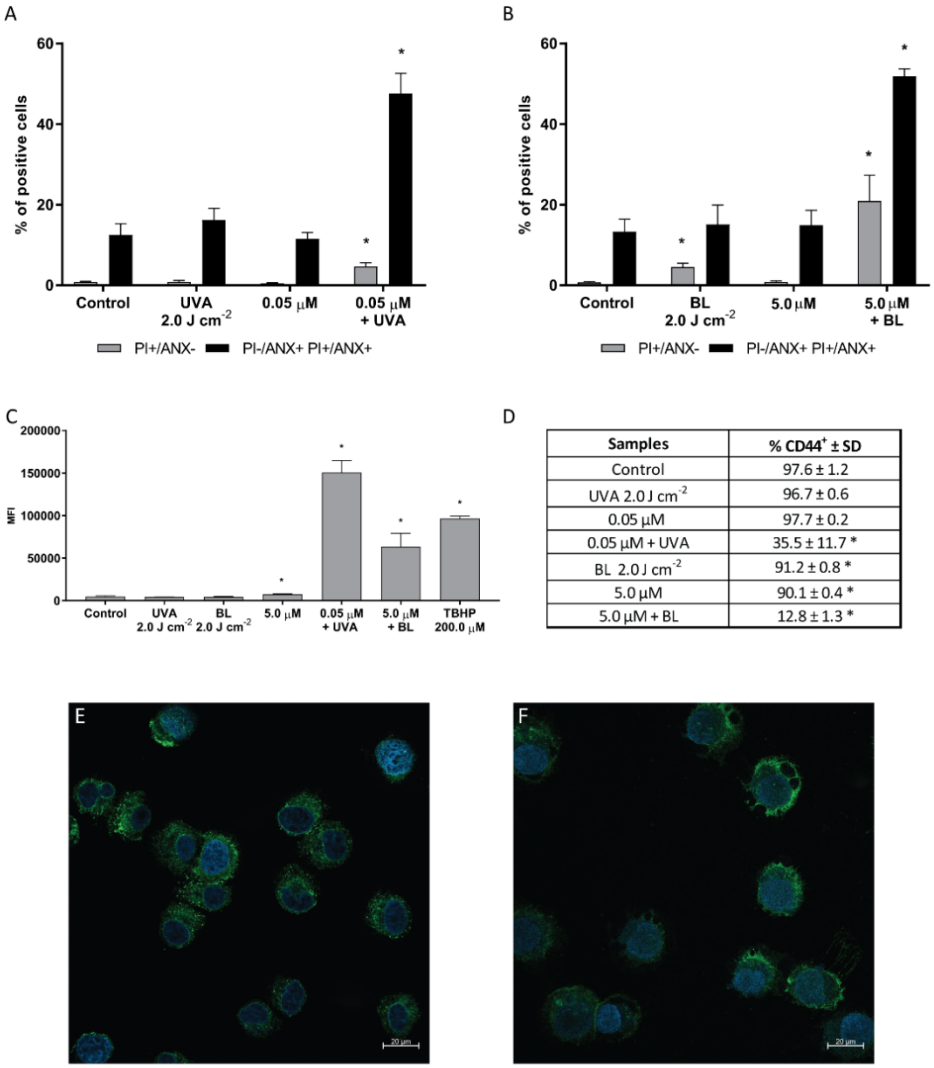

Samples	% CD44$^+$ ± SD
Control	97.6 ± 1.2
UVA 2.0 J cm^{-2}	96.7 ± 0.6
0.05 µM	97.7 ± 0.2
0.05 µM + UVA	35.5 ± 11.7 *
BL 2.0 J cm^{-2}	91.2 ± 0.8 *
5.0 µM	90.1 ± 0.4 *
5.0 µM + BL	12.8 ± 1.3 *

Figure 3. *Effects on cell apoptosis, ROS formation, and CD44 expression. Cultures were irradiated with 2.0 J cm^{-2} of UVA light or BL. (A, B) Cell apoptosis. PI: propidium iodide; ANX: annexin V (C) ROS generation. TBHP: tert-butyl hydrogen peroxide. (D) Cytofluorimetric data are reported as percentage of CD44-positive cells. Student's t-test, *p<0.05 vs untreated cultures taken as control. Representative micrographs of untreated cell cultures (E) and cultures exposed to 5.0 µM TMA plus BL (F). Immunoreactivity towards CD44 stained green, whereas nuclei were labelled with DAPI (blue). Bars: 20 µm*

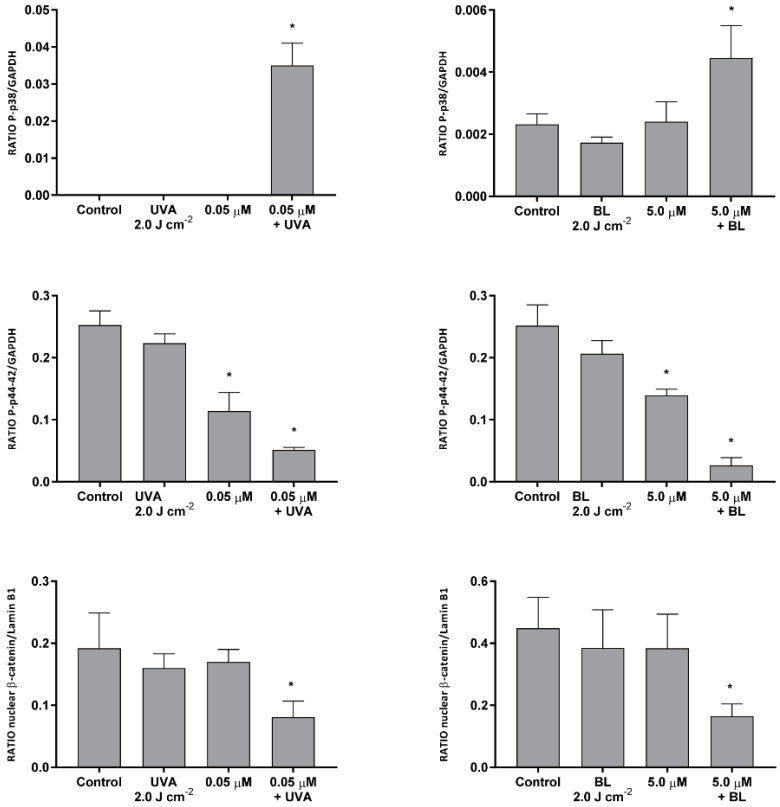

Figure 4. *WB analysis. Cultures were treated with 0.05 μM TMA plus 2.0 J/cm^2 UVA light or 5.0 μM plus BL. The quantification of protein expression levels was performed by densitometric analysis of the bands using ImageJ processing software. Data are reported as ratio between target protein and relative GAPDH expression. *p<0.05 vs untreated cultures taken as control.*

4. Discussion

Our data demonstrated that TMA activated by either UVA light and BL exerts strong antiproliferative effects on DU145 cells through induction of apoptosis. Although inhibition of sphere formation under BL was achieved at concentration 100-fold higher than under UVA, different kind of lesions were induced. Indeed, MAs were formed in salmon testes DNA under both lights, but XLs were detected in pBR322 DNA only under UVA light. Moreover, both TMA-induced DNA photocleavages and photooxidations under UVA were not detected under BL. Accordingly, the production of ROS measured in the TMA treated cells were less efficient under BL compared to UVA light. It is known that the oxidative lesions are as important as strand breaks for cellular function and survival.[14]

The results obtained under BL are very satisfactory assuming that the formation of less mutagenic lesions could be negligible and even absent in the DU145 cells when TMA activation is achieved through less noxious and more penetrating wavelengths. However, a significant amount of DNA lesions, *i.e.* MAs, can justify the effects on cell growth. In previous experiments with 8-MOP on the same cells we assumed that XLs likely play a minor role in the antiproliferative effects.[9]

Our findings indicate that the strong TMA photocytotoxicity can be related to the kind and number of DNA lesions; BL, compared to UVA light, can activate TMA as well, although at higher concentrations, but without the potential risk of mutagenic lesions.[15]

TMA activated by both UVA light and BL induced cell death by apoptosis enhancing the phosphorylation of p38 whose pathway modulates cell cycle checkpoints, cell apoptosis and autophagy. [16] Furthermore, as in photopheresis, apoptotic bodies induced by TMA treatment with BL and UVA light, and the following antigen presentation by dendritic cells (DCs), could modulate the immune system, increasing the photoantiproliferative effect. It must be also noted that, despite UVA light, BL irradiation (2.5 J cm^{-2}) does not impair the *in vitro* differentiation and maturation of human monocyte-derived dendritic cells and reduces the production of pro-inflammatory cytokines.[17]

On the contrary, cultures treated with photoactivated TMA showed decreases in phosphorylation of p44/42 MAPK (ERK½), usually activated by growth factors and mitogens leading to anti-apoptotic effects.[18] Taken together, our data agree to the observation that p38 signaling can indirectly regulate ERK½.[19]

Decreases in p44/42 phosphorylation were detected also in cultures treated with the compound in the dark suggesting that TMA could interact with molecular targets without photoactivation. It has been demonstrated that in the dark some angelicins are able to inhibit NF-kB/DNA interactions demonstrating anti-inflammatory profile[20] and TMA has shown to be an effective enhancer of Cystic Fibrosis Transmembrane Conductance Regulator (CFTR).[21]

Photoactivation of TMA by either UVA light and BL affected the canonical Wnt signaling pathway as the nuclear accumulation of β-catenin decreased. The binding of Wnt ligands to Frizzled (Fz) receptors or low-density lipoprotein receptor-related protein 5/6 (LRP5/6) co- receptors inhibits degradation of cytoplasmic β-catenin that translocates into the nucleus leading to transcription of genes. Dysregulation of Wnt signaling has been associated with several types of cancers, including PCa.[22]

Notably, the decrease in nuclear β-catenin was coupled to significant lowering of CD44- positive cells, being TMA plus BL more effective than TMA plus UVA light. The reduction of CD44-positive cells detected also in cultures treated with the compound alone may be related to the lowering of p44/42 MAPK phosphorylation, since pERK regulates CD44 expression.[23]

Several evidences have shown that CD44 is overexpressed in several cancers as marker of cancer stem cells (CSCs). Thus, in the last years, the therapeutically targeting of CD44 has been attempted through various approaches.[24] In PCa, CD44 expression levels positively correlates to the cancer stage and can predict the therapeutic response to the treatment.[25] Our findings suggest a relation between CD44 and Wnt pathway. CD44 is not only a Wnt target gene but also a positive regulator of Wnt pathway through interaction with LRP6.[26] Indeed, nuclear translocation of β-catenin is inhibited by silencing CD44 in several cancer cells, including PCa cell lines.[27]

Overall, our results indicate, for the first time, that TMA can be activated by BL, although at higher concentrations than UVA light, decreasing the risk of mutagenic lesions on treated cells. Thus, the toxicity of both light and compound itself on neighbouring healthy cells could be overcome with a BL-TMA targeted treatment in the site of the cancer lesions. Besides ROS generation, the proapoptotic effects on DU145 cells seems to be related to activation of p38 and inhibition of p44/42

phosphorylation. Interestingly, photoactivated TMA was able to affect Wnt signaling and CD44 expression, both involved in CSC growth and renewal. To investigate the interaction between these two hallmarks of CSCs after treatment with BL-TMA, molecular docking studies will be carried out to verify whether TMA can bind CD44 and expression levels of Wnt target genes as well as glycogen synthase kinase-3b, involved in β-catenin degradation, will be determined.

Supporting Information

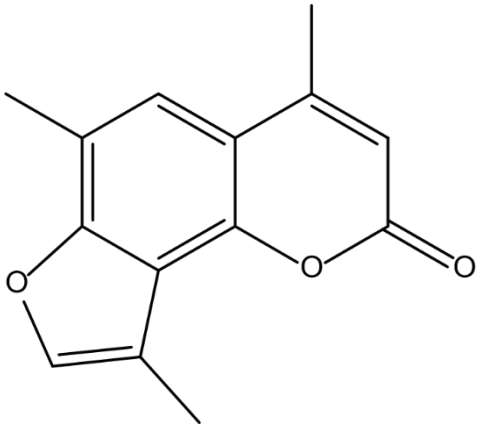

Figure 1S. *Molecular structure of 4,6,4'-trimethylangelicin (TMA).*

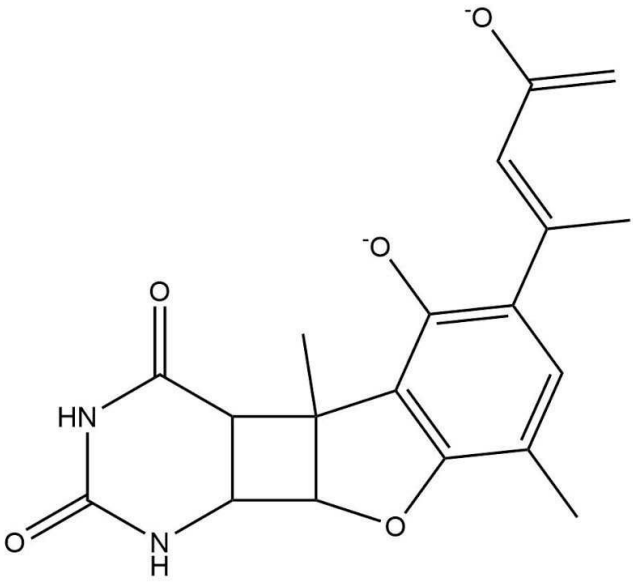

Figure 2S. *Supposed molecular structure of TMA-thymine monoadduct after alkali hydrolysis at the pyrone ring resulting in a furohydroxycinnamic derivative bearing two negative charges.*

Crosslinking Assay				
Samples	UVA		BL	
	% ds-DNA	% ss-DNA	% ds-DNA	% ss-DNA
L-DNA	*100.0*	*n.d.*	*100*	*n.d.*
L-DNA + NaOH	*n.d.*	*100.0*	*n.d.*	*100.0*
0.0 J/cm^2	*n.d.*	*100.0*	*n.d.*	*100.0*
2.0 J/cm^2	52.2 ± 2.3*	47.8 ± 2.3*	*n.d.*	*100.0*
5.0 J/cm^2	72.4 ± 1.5*	27.6 ± 1.5*	*n.d.*	*100.0*
7.5 J/cm^2	81.1 ± 3.5*	18.9 ± 3.5*	*n.d.*	*100.0*
12.0 J/cm^2	93.7 ± 2.7*	6.3 ± 2.7*	*n.d.*	*100.0*
15.0 J/cm^2	*100.0*	*n.d.*	*n.d.*	*100.0*

Relaxation Assay				
Samples	UVA		BL	
	% OC	% SC	% OC	% SC
SC	5.7 ± 1.7	94.3 ± 1.7	2.1 ± 1.5	97.9 ± 1.5
SC + Light 15.0 J/cm^2	13.6 ± 3.1*	86.4 ± 3.1*	2.2 ± 0.7	97.8 ± 0.7
0.0 J/cm^2	7.9 ± 1.2*	92.1 ± 1.2*	3.1 ± 1.2	96.9 ± 1.2
2.0 J/cm^2	5.6 ± 3.2	94.4 ± 3.2	3.3 ± 0.9	96.7 ± 0.9
5.0 J/cm^2	15.3 ± 2.6*	84.7 ± 2.6*	4.6 ± 1.6	95.4 ± 1.6
7.5 J/cm^2	55.5 ± 1.1*	44.5 ± 1.1*	4.0 ± 0.8	96.0 ± 0.8
12.0 J/cm^2	70.4 ± 2.9*	29.6 ± 2.9*	2.2 ± 1.4	97.8 ± 1.4
15.0 J/cm^2	82.4 ± 1.7*	17.6 ± 1.7*	5.4 ± 2.1	94.6 ± 2.1

Photooxidation Assay				
Samples	UVA		Blue Light	
	% OC	% SC	% OC	% SC
Control DNA	1.4 ± 0.2	98.6 ± 0.2	2.5 ± 0.6	97.5 ± 0.6
0.0 J/cm^2 + EndoIII	9.0 ± 2.3*	91.0 ± 2.3*	14.8 ± 1.7*	85.2 ± 1.7*
2.0 J/cm^2 + EndoIII	27.8 ± 1.8 *	72.2 ± 1.8 *	29.5 ± 3.1*	70.5 ± 3.1*
7.5 J/cm^2 + EndoIII	46.6 ± 1.4*	53.4 ± 1.4*	41.3 ± 2.7*	58.7 ± 2.7*
0 J/cm^2 + TMA + EndoIII	10.3 ± 1.6*	89.7 ± 1.6*	7.7 ± 0.5*	92.3 ± 0.5*
2.0 J/cm^2 + TMA + EndoIII	19.3 ± 2.2*	80.7 ± 2.2*	9.9 ± 1.6*	90.1 ± 1.6*
7.5 J/cm^2 + TMA + EndoIII	46.6 ± 3.1*	53.4 ± 3.1*	8.9 ± 0.7*	91.1 ± 0.7*
0.0 J/cm^2 + TMA	1.6 ± 0.4	98.4 ± 0.4	*n.d.*	*100.0*
2.0 J/cm^2 + TMA	3.5 ± 0.8*	96.5 ± 0.8*	*n.d.*	*100.0*
7.5 J/cm^2 + TMA	21.2 ± 2.7*	78.8 ± 2.7*	*n.d.*	*100.0*

Figure 3S. *Densitometric analysis of agarose gels reported in figure 1. The intensity of each band was calculated by using ImageLab 5.2.1 (Bio-Rad). *p<0.05 vs L-DNA (crosslinking assay) or supercoiled (SC) DNA (relaxation assay) or control DNA (photooxidation assay). OC: open circular; L: linearized; ds: double strand; ss: single strand.*

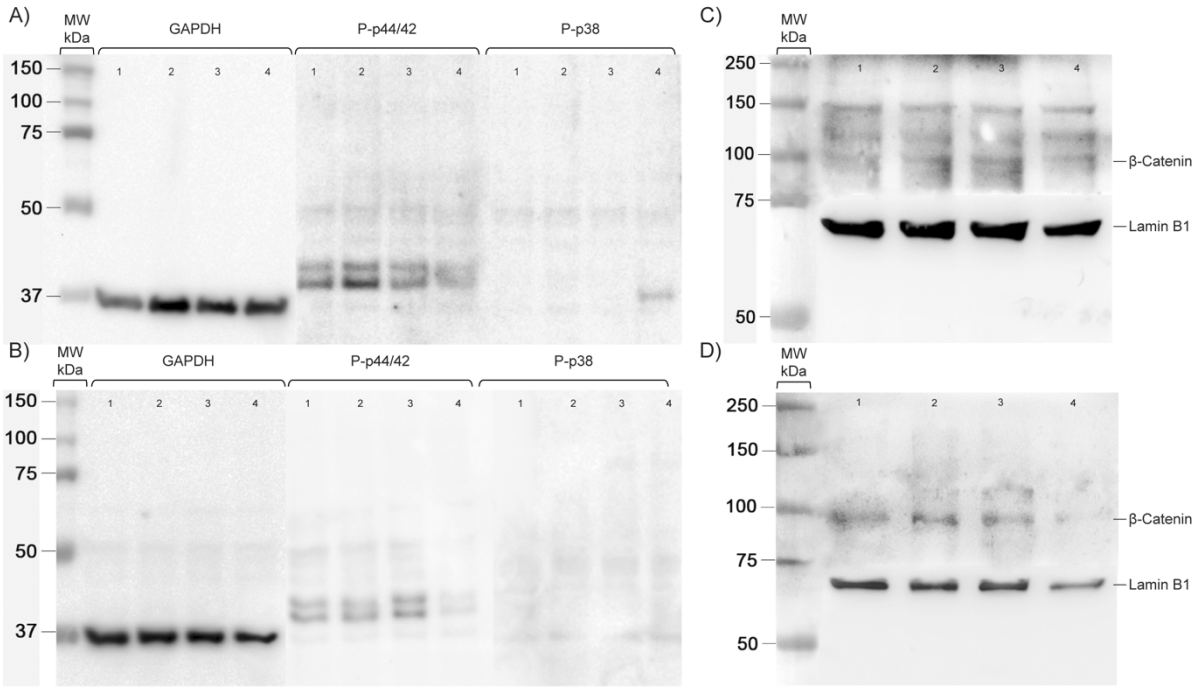

Figure 4S. *Western blot analysis. Cultures were treated with 0.05 μM TMA plus 2.0 J/cm^2 UVA light (A, C) or 5.0 μM plus BL (B, D). 1, untreated samples; 2, samples only irradiated; 3, samples treated with TMA in the dark; 4, samples treated with TMA plus light.*

References

1. Valerio, M., H.U. Ahmed, M. Emberton, N. Lawrentschuk, M. Lazzeri, R. Montironi, P.L. Nguyen, J. Trachtenberg, and T.J. Polascik, *The role of focal therapy in the management of localised prostate cancer: a systematic review.* Eur Urol, 2014. **66**(4): p. 732-51.

2. Gheewala, T., T. Skwor, and G. Munirathinam, *Photosensitizers in prostate cancer therapy.* Oncotarget, 2017. **8**(18): p. 30524-30538.

3. Schneider, L.A., R. Hinrichs, and K. Scharffetter-Kochanek, *Phototherapy and photochemotherapy.* Clin Dermatol, 2008. **26**(5): p. 464-76.

4. Trautinger, F., U. Just, and R. Knobler, *Photopheresis (extracorporeal photochemotherapy).* Photochem Photobiol Sci, 2013. **12**(1): p. 22-8.

5. Averbeck, D., *Recent advances in psoralen phototoxicity mechanism.* Photochem Photobiol, 1989. **50**(6): p. 859-82.

6. Xia, C.Q., K.A. Campbell, and M.J. Clare-Salzler, *Extracorporeal photopheresis-induced immune tolerance: a focus on modulation of antigen-presenting cells and induction of regulatory T cells by apoptotic cells.* Curr Opin Organ Transplant, 2009. **14**(4): p. 338-43.

7. Walker, D. and H. Jacobe, *Phototherapy in the age of biologics.* Semin Cutan Med Surg, 2011. **30**(4): p. 190-8.

8. Averbeck, D., *Relationship between lesions photoinduced by mono- and bi-functional furocoumarins in DNA and genotoxic effects in diploid yeast.* Mutat Res, 1985. **151**(2): p. 217-33.

9. Chen, X., J. Kagan, G. Miolo, F. Dall'Acqua, D. Averbeck, and E. Bisagni, *Photosensitized cross-linking and cleavage of pBR322 and M13 DNA: comparison of 4,4',6-trimethylangelicin and 3-carbethoxypsoralen.* J Photochem Photobiol B, 1994. **22**(1): p. 51-7.

10. Gasparro, F.P., P. Gattolin, G.A. Olack, L.I. Deckelbaum, and B.E. Sumpio, *The excitation of 8-methoxypsoralen with visible light: reversed phase HPLC quantitation of monoadducts and cross-links.* Photochem Photobiol, 1993. **57**(6): p. 1007-10.

11. Sturaro, G., G. Cigolini, L. Menilli, F. Cola, R. Di Liddo, A. Tasso, M.T. Conconi, and G. Miolo, *Antiproliferative activity of 8-methoxypsoralen on DU145 prostate cancer cells under UVA and blue light.* Photochem Photobiol Sci, 2017. **16**(7): p. 1182-1193.

12. Schmitt, I.M., V.M. Maxwell, G.A. Olack, R.L. Edelson, S. Chimenti, and F.P. Gasparro, *The specific effects of 8-methoxypsoralen photoadducts on cell growth: HPLC analysis of monoadduct and crosslink formation in cells exposed to split-dose treatment.* J Photochem Photobiol B, 1994. **22**(1):

p. 17-21.

13. Lin, S.R., Y.S. Fu, M.J. Tsai, H. Cheng, and C.F. Weng, *Natural Compounds from Herbs that can Potentially Execute as Autophagy Inducers for Cancer Therapy.* Int J Mol Sci, 2017. **18**(7).

14. Wallace, S.S., *Biological consequences of free radical-damaged DNA bases.* Free Radic Biol Med, 2002. **33**(1): p. 1-14.

15. Bjelland, S. and E. Seeberg, *Mutagenicity, toxicity and repair of DNA base damage induced by oxidation.* Mutat Res, 2003. **531**(1-2): p. 37-80.

16. Cuadrado, A. and A.R. Nebreda, *Mechanisms and functions of p38 MAPK signalling.* Biochem J, 2010. **429**(3): p. 403-17.

17. Monfrecola, G., S. Lembo, M. Cantelli, E. Ciaglia, L. Scarpato, G. Fabbrocini, and A. Balato, *The effect of visible blue light on the differentiation of dendritic cells in vitro.* Biochimie, 2014. **101**: p. 252-5.

18. Lu, Z. and S. Xu, *ERK1/2 MAP kinases in cell survival and apoptosis.* IUBMB Life, 2006. **58**(11): p. 621-31.

19. Li, S.P., M.R. Junttila, J. Han, V.M. Kahari, and J. Westermarck, *p38 Mitogen-activated protein kinase pathway suppresses cell survival by inducing dephosphorylation of mitogen-activated protein/extracellular signal-regulated kinase kinase1,2.* Cancer Res, 2003. **63**(13): p. 3473-7.

20. Marzaro, G., A. Guiotto, M. Borgatti, A. Finotti, R. Gambari, G. Breveglieri, and A. Chilin, *Psoralen derivatives as inhibitors of NF-kappaB/DNA interaction: synthesis, molecular modeling, 3D-QSAR, and biological evaluation.* J Med Chem, 2013. **56**(5): p. 1830-42.

21. Favia, M., M.T. Mancini, V. Bezzerri, L. Guerra, O. Laselva, A.C. Abbattiscianni, L. Debellis, S.J. Reshkin, R. Gambari, G. Cabrini, and V. Casavola, *Trimethylangelicin promotes the functional rescue of mutant F508del CFTR protein in cystic fibrosis airway cells.* Am J Physiol Lung Cell Mol Physiol, 2014. **307**(1): p. L48-61.

22. Kypta, R.M. and J. Waxman, *Wnt/beta-catenin signalling in prostate cancer.* Nat Rev Urol, 2012. **9**(8): p. 418-28.

23. Roeder, S.S., T.J. Barnes, J.S. Lee, I. Kato, D.G. Eng, N.V. Kaverina, M.W. Sunseri, C. Daniel, K. Amann, J.W. Pippin, and S.J. Shankland, *Activated ERK1/2 increases CD44 in glomerular parietal epithelial cells leading to matrix expansion.* Kidney Int, 2017. **91**(4): p. 896-913.

24. Yan, Y., X. Zuo, and D. Wei, *Concise Review: Emerging Role of CD44 in Cancer Stem Cells: A Promising Biomarker and Therapeutic Target.* Stem Cells Transl Med, 2015. **4**(9): p. 1033-43.

25. Korski, K., A. Malicka-Durczak, and J. Breborowicz, *Expression of stem cell marker CD44 in prostate cancer biopsies predicts cancer grade in radical prostatectomy specimens.* Pol J Pathol, 2014. **65**(4): p. 291-5.

26. Schmitt, M., M. Metzger, D. Gradl, G. Davidson, and V. Orian-Rousseau, *CD44 functions in Wnt signaling by regulating LRP6 localization and activation.* Cell Death Differ, 2015. **22**(4): p. 677-89.

27. Han, J., B. Gao, X. Jin, Z. Xu, Z. Li, Y. Sun, and B. Song, *Small interfering RNA-mediated downregulation of beta-catenin inhibits invasion and migration of colon cancer cells in vitro.* Med Sci Monit, 2012. **18**(7): p. BR273-80.

The neuroleptic drug fluphenazine induces a significant UVA-mediated cytotoxic effect on three human cancer cell lines through apoptosis

Luca Menilli, Aída Nelly García-Argáez, Lisa Dalla Via, Giorgia Miolo

The neuroleptic drug fluphenazine induces a significant UVA-mediated cytotoxic effect on three humancancer cell lines through apoptosis.
Photochem Photobiol Sci. 2019 Sep 1;18(9):2232-2239. doi: 10.1039/c9pp00023b.

Abstract

The cytotoxic activity of fluphenazine (FPZ) in combination with UVA light was evaluated on three human tumor cell lines, HeLa, MSTO-211H and A431. The photobiological effect was determined following the irradiation treatment in the presence or after the removal of the incubated FPZ. Under both conditions, FPZ proved to be very effective in killing tumor cells, with GI50 values in the micromolar range. However, when FPZ was present during irradiation, the photocytotoxicity was at least two times higher than after its removal suggesting the contribution of the drug both outside and inside the cells. The uptake of FPZ was very fast and, after only 15 minutes of incubation, the compound was accumulated inside lysosomes, as evidenced through fluorescence microscopy. FPZ distribution covered also the nucleus and the cytoplasm without significant plasma membrane association. After irradiation, the membrane of lysosomes in which FPZ was accumulated, loosed its integrity suggesting that the released lysosomal enzymes played an important role on the cell death, and mitochondria were damaged as well, following apoptosis. Indeed, cytofluorimetric studies demonstrated that apoptosis was the main mechanism of cell death. Finally, an extremely high production of ROS was found, indicating a significant photodynamic mechanism involved in the photocytotoxic effect of FPZ. Taken together, our data show that FPZ following UVA irradiation behaves as an effective photoantiproliferative compound inducing apoptosis on various human tumor cells.

1. Introduction

Fluphenazine (FPZ) is a neuroleptic and antidepressant drug widely used in psychotherapy for the treatment of psychotic patients affected by a variety of mental disorders, including schizophrenia, mania, severe anxiety, and disturbed behaviour.[1]

The most commonly occurring side effects of such treatments are extrapyramidal reactions, akathisia, agranulocytosis and, under the exposure of the patients to sunlight, photosensitization reactions, i.e. phototoxicity, with symptoms of an exaggerated sunburn, and photoallergy, resulting in the signs of contact hypersensitivity. The mechanism of photosensitization has been investigated through in vitro experiments, showing that this drug photosensitized lipid peroxidation damaging the cell membrane and mitochondria.[2]

Moreover, it was demonstrated that FPZ had the ability to irreversibly photobind to proteins through the trifluoromethyl group, highly susceptible to the attack of nucleophilic amino acids, thus explaining the in vivo immunological reaction triggered by the formed antigen. Additionally, the irreversible photobinding to calmodulin, that is preceded by a strong noncovalent binding to the protein, likely accounts for agranulocytosis.[3] The capacity of FPZ to externally bind salmon testes DNA and to photocleave pBR322 DNA, leading to single strand breaks, was found weak for FPZ in comparison with two other phenothiazine derivatives, thioridazine and perphenazine.4 Moreover, time-resolved absorption spectra of the drug in the presence of 2′-deoxiguanosine 5′-monophosphate (GMP) showed 100-folds lower reactivity of the FPZ radical cation with respect to perphenazine and thioridazine.[4]

Some studies have demonstrated that the highly cytotoxic singlet oxygen plus the phenothiazine cation radical and solvated electron, very reactive species towards biological substrates, can be formed in aqueous media, supporting the mechanism underlying the photosensitizing effects of FPZ.[5] Although FPZ easily undergoes degradation upon UV light yielding stable photoproducts (the main of them results from hydrolytic photocleavage of the trifluoromethyl group), they did not seem correlated to the potency of the parent compound. Indeed, photodegradation products of FPZ neither demonstrated toxicity in the dark nor under UVA light.[6]

In a previous in vitro study performed in the dark, FPZ inhibited human myeloblastic HL-60 cell line proliferation at pharmacologically relevant concentrations, i.e. in the 1-10 micromolar range, and showed a moderate cytotoxic activity also against the intraperitoneal L-1210 and P-388 leukemia murine tumour models, suggesting FPZ as potential drug in antileukemic treatments.[7] It has also been shown that FPZ is able to induce apoptosis in the dark in a B16 mouse melanoma cell line and to reduce in vivo the melanoma tumor growth.[8] The mechanism proposed for explaining the antiproliferative activity of FPZ was again the capacity to bind and thus to inhibit the action of calmodulin thereby blocking cell proliferation. In an attempt to clarify the possible antitumor mechanisms of FPZ, the action on signalling pathway members such as Wnt, MAPK and retinoic acid, all closely associated with tumours, and the indirect impact upon the tumour-associated target proteins CDK2, IGF1R, GSK3B, RARA, FGFR2 and MAPK10 were proposed.[9] Moreover, FPZ has been shown to inhibit P-glycoprotein (P-gp) and this effect allowed to consider this drug as an anti-cancer chemopreventive agent.[10]

The purpose of this study was to explore the cytotoxic effect of the combined action of FPZ with UVA light on three human tumor cell lines and to investigate the mechanism of cell death. The contribution of serum proteins and reactive oxygen species (ROS) were also examined. Finally, epifluorescence and confocal microscopy analyses were performed to examine the intracellular FPZ accumulation and the intracellular targets of photodamage.

2. Materials and Methods

2.1 Cell cultures

HeLa (human cervix adenocarcinoma cells) and A-431 (skin carcinoma squamous cells) were grown in Ham's Nutrient Mixture F-12 and Dulbecco's modified Eagle's medium respectively, supplemented with 10% heat-inactivated foetal bovine serum (Biowest, Nuaillé, France). MSTO-211H (human biphasic mesothelioma cells)

were grown in RPMI 1640 supplemented with 2.38 g L^{-1} Hepes, 0.11 g L^{-1} Na-pyruvate, 2.5 g L^{-1} glucose and 10% heat-inactivated fetal bovine serum. 1% antibiotic/antimycotic solution was added to the media. The cells were cultured at 37 °C in a moist atmosphere of 5% carbon dioxide. Culture media and supplements were purchased from Sigma Aldrich.

2.2 Irradiation procedure

UVA irradiation was carried out using Osram HQV 125W lamps, mainly emitting at 365 nm. The total energy delivered to the biological sample was determined for each experimental procedure by means of a radiometer equipped with a UV sensor (VarioControl and UV VarioSensor, Waldmann, Villingen-Schwenningen, Germany). The UVA radiant energy was about 1.44 mW cm^{-2}. Cells were irradiated in 24-well plates covered with the lid for about 14 minutes to reach 1.2 J cm^{-2} UVA dose. Light measurements were performed interposing the lid between the lamp and the sensor.

2.3 Viability assay

HeLa, A-431 and MSTO-211H cells (10^5) were seeded into each well of a 24-well cell culture plate. After incubation for 24 h two different treatments (Methods A and B) were used to determine the cell growth inhibition.

In Method A, the complete medium was replaced with an equal volume of DMEM without phenol red and various concentrations of fluphenazine (0.0 – 20.0 μM) were added. The cells were kept in the dark for 1 or 3 hours and then irradiated with a UVA dose of 1.2 J cm^{-2}. After irradiation, the DMEM containing the test compound was removed and the cells were incubated in complete medium for 24 h.

In Method B, cells were treated in complete medium with various concentrations of fluphenazine and were kept in the dark for 1, 3 or 8 hours. Then, the complete medium containing the test agent was replaced with an equal volume of Dulbecco's modified Eagle medium without phenol red and cells were irradiated with 1.2 J cm^{-2} of UVA light. After irradiation, the DMEM was removed and the cells were incubated in complete culture medium for 24 h.

For the experiments carried out in the dark, after seeding and incubation for 24 h, various concentrations of fluphenazine were added to the complete medium and the cells were incubated for further 24 h.

The trypan blue exclusion assay was performed to determine cell viability. Cytotoxicity data were expressed as GI_{50} values, i.e., the concentration of the test agent inducing 50% reduction in cell number compared with control cultures.

2.4 Evaluation of apoptotic cell death

To detect phosphatidylserine translocation from the inner face to the outer surface of plasma membrane, BD Pharmigen FITC Annexin V Apoptosis Detection Kit I (BD Biosciences, San Jose, CA USA) was used. HeLa cells (2.0×10^5) were seeded into each cell culture plate in complete growth medium. After incubation for 24 h, the same two treatments for irradiation (Methods A and B, already described above) were used to determine the apoptosis induction, except for the incubation time reduced to 18 h after irradiation. Then, in both methods the cells were centrifuged and resuspended at 106 cells/mL in binding buffer. Cell suspensions

(100 µL) were added with Annexin V-FITC and propidium iodide (PI) as indicated by the supplier's instructions and incubated for 15 min at room temperature in the dark. The populations of Annexin V-negative/PI-negative (viable), Annexin V-positive/PI-negative (early apoptosis), Annexin V-positive/PI-positive (late apoptosis) and Annexin V-negative/PI-positive (necrosis) cells were evaluated using BD FACSCanto II flow cytometer (BD Biosciences).

2.5 ROS generation

The assay was performed using DCFDA – Cellular Reactive Oxygen Species Detection Assay Kit (Abcam, Cambridge, UK) according to the manufacturer instructions. Briefly, HeLa cells (2.5×10^4) were seeded into each well of a 96-well black plate with a clear bottom (Corning, New York, USA) in the proliferation medium. After 24 h incubation, cultures were stained with 25.0 µM 2',7'-dichlorofluorescin diacetate (DCFDA) for 45 min and then incubated with various concentrations of FPZ (1.0 - 5.0 µM) for 1 h. Afterwards, the plate was irradiated with 1.2 J cm^{-2} of UVA light. Data were collected using Victor 3 fluorescence microplate reader (Ex/Em = 485/535, PerkinElmer, Waltham, Massachusetts, US). An untreated culture kept in the dark was taken as negative control, while a culture treated with 200.0 µM tertbutyl hydrogen peroxide (TBHP) was the positive control.

2.6 Drug localization

The localization of FPZ in the HeLa cells was determined by means of fluorescence microscopy. The native fluorescence of FPZ was detected in HeLa cells grown on coverslips, incubated with FPZ 20.0 µM for 15 and 60 minutes, and then fixed with 4% paraformaldehyde in PBS for 15 minutes. A sample of HeLa cells without treatment was used as control. The epifluorescence of FPZ was detected using a Zeiss Axio Observer Z1 fluorescence microscope.

2.7 Lysosome and mitochondria immunodetection

HeLa cells were grown on coverslips, incubated with 20.0 µM FPZ for 60 minutes at 37° C, then irradiated with 1.2 J cm^{-2} of UVA light, detached after 4 hours and fixed with 4% paraformaldehyde in PBS for 15 minutes. Permeabilization was performed with 0.1% Triton X-100 in PBS for 10 minutes. Non-specific binding sites were deactivated with 1% BSA in PBS overnight at 4°C. Lysosomes were labelled using rat anti-LAMP-1 monoclonal antibody (1D4B, 1:500, Abcam) overnight at 4° C and goat anti-rat secondary antibody conjugated to AlexaFluor 555 for 30 minutes at RT (1:500, Invitrogen, Carlsbad, CA, USA). Mitochondria were labelled with rabbit anti-Pyruvate Dehydrogenase E1-beta subunit monoclonal antibody (1:250, Abcam) and mouse anti-rabbit secondary antibody conjugated to AlexaFluor 488 for 30 minutes at RT (1:250, Invitrogen). Nuclei and actin filaments were stained with Hoechst 33342 (Invitrogen) and CF633 - phalloidin conjugates (Biotium, Fremont, CA, USA), respectively, in PBS for 5 minutes. Coverslips were then mounted with an antifading mounting medium. Samples were then imaged using SP5 confocal laser scanning microscope (Leica, Wetzlar, Germany).

3. Results and Discussion

3.1 Cytotoxic activity

The cytotoxic activity of FPZ was evaluated both in the dark and following UVA irradiation on three human tumour cell lines: HeLa (cervix adenocarcinoma), A431 (squamous carcinoma) and MSTO-211H (biphasic mesothelioma). The results, expressed as GI_{50} values, i.e. the concentration (μM) able to induce 50% cell death with respect to the control culture, are shown in Table 1.

Remarkably, the incubation of cells with FPZ up to 20.0 μM in the dark for 24 h was unable to induce any cytotoxic effect on cells, demonstrating the absence of toxicity of the drug in the dark in our experimental conditions.

Method	Cell Line GI_{50}[a] (μM)		
	HeLa	A431	MSTO-211H
Dark 24 h	> 20.0	> 20.0	> 20.0
A 1h	2.29 ± 0.28	4.64 ± 0.25	3.34 ± 0.45
B 1h	6.79 ± 0.53	10.01 ± 2.11	7.63 ± 0.36
A 3h	2.43 ± 0.07	3.84 ± 0.24	3.34 ± 0.06
B 3h	4.99 ± 0.89	9.22 ± 1.42	6.42 ± 0.62
B 8h	2.83 ± 0.35	8.31 ± 0.48	4.97 ± 0.43

Table 1. *GI_{50} values obtained from HeLa, A431 and MSTO-211H cells in the dark (24 h) and after increasing pre-incubation times (1 h, 3 h, 8 h) with different concentrations of FPZ (0.0 – 20.0 μM) then irradiated with UVA light (1.2 J·cm-2) using method A (FPZ present during the irradiation step) or B (cells washed from FPZ before the irradiation step).*

A preliminary investigation on the ability of FPZ to induce a photocytotoxic effect after UVA irradiation (1.2 J cm^{-2}) was carried out following an already established method, previously performed to investigate the photobiological activity of some well-known photochemotherapeutic drugs.[11] This experimental procedure (method A, 1 h) allowed us to highlight the ability of FPZ to provoke a significant photocytotoxicity on all tumor cells taken into consideration, the HeLa being the most sensitive, with GI_{50} values ranging from 2.29 to 4.64 μM. Prolonged incubation time in the presence of the test agent, i.e. 3 h instead of 1 h, gave comparable results, with GI50 values from 2.43 to 3.84 μM. This latter result raises the hypothesis that FPZ could be promptly accumulated inside the cells, i.e. within 1 h. Nevertheless, following method A it was not possible to make distinction between the contribution of irradiated FPZ inside and outside the cells. Therefore, a different experimental method (B) was performed, in which the drug was removed from the incubation medium just before irradiation (Table 1) in order to observe only the photodamaging effect of FPZ already internalized. The comparison between the GI50 values obtained with methods A and B after exposure to the

FPZ for the same period (1 or 3 h) clearly indicates a prominent effect when method A was carried out. Indeed, the GI_{50} values obtained when FPZ was absent during irradiation (method B) appeared about 2 times higher with respect to those attained by applying method A, and, interestingly, this behaviour was confirmed for all the cell lines studied. This result suggests that, following method A, a contribution to the overall photocytotoxic activity of FPZ external to the cells should be taken into account, and suggests that FPZ molecules remaining outside the cells were likely able to damage the neighbouring cell membrane components. Thus, besides the quite fast cell uptake of FPZ, both the outside and inside photobiological effects of FPZ on cells might explain the similar photocytotoxicity observed in cells irradiated after 1 or 3 h of incubation with method A (see Table 1, i.e. GI_{50} 2.29 ± 0.28 μM and 2.43 ± 0.07 μM after 1 and 3 h of incubation, respectively, for HeLa cells). In this connection, following method B, a certain increase in phototoxicity by increasing the incubation time was observed, particularly in HeLa cells (GI50 6.79 ± 0.53 μM; 4.99 ± 0.89 μM; 2.83 ± 0.35 μM, after 1 h, 3 h, 8 h, respectively) as the photobiological effect was exerted only by the internalized FPZ. Note that the incubation time could be extended to 8 h only with method B, where the cells could survive for longer times in the complete medium prior to the UVA treatment.

For obtaining all these results, 1.2 J cm^{-2} of UVA light was chosen as this dose was not toxic at all on all the three cell lines (see Fig. 1 for Hela cells). Indeed, the combined effect of FPZ plus UVA on cells could be more visible at a dose of UVA showing the lowest toxicity alone.

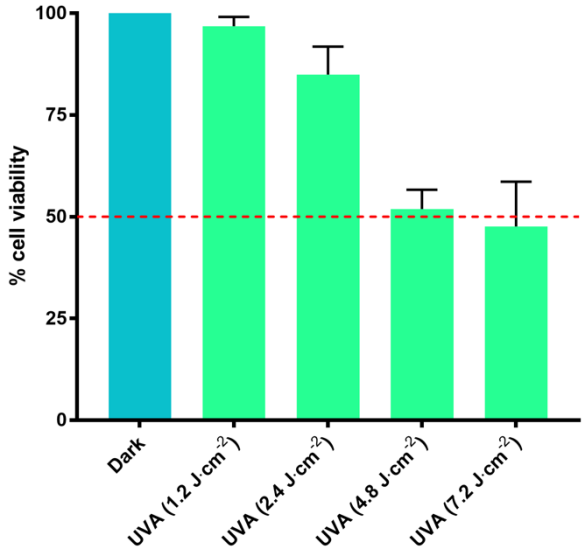

Figure 1. *Effect of increasing UVA doses on HeLa cells incubated with medium phenol red-free and without FPZ.*

3.2 Effect of foetal bovine serum proteins on FPZ antiproliferative effect

The lower photoantiproliferative activity observed by performing method B instead of A could have been due, besides the lack of contribution of FPZ external to the cells during irradiation, to the lower amount of drug available for the cells, as a result of a nonspecific binding of FPZ to foetal calf serum components. Actually, in method A, these latter were absent both during incubation and irradiation steps. Otherwise, in method B, the incubation with the drug occurred in complete medium, replaced just before irradiation with an essential one lacking serum. To verify this assumption, the photocytotoxic assay was performed on the most sensitive

HeLa cells following method B both in the presence and in the absence of serum. The obtained results, shown in Figure 2, highlighted the significant increase in phototoxicity in the absence of serum thus suggesting an interaction between FPZ and serum components capable of subtracting the drug from its action on cell targets. This hypothesis was also supported by literature data where the complexation of FPZ with human serum albumin was studied and the interactions occurring during binding process were analysed.[12]

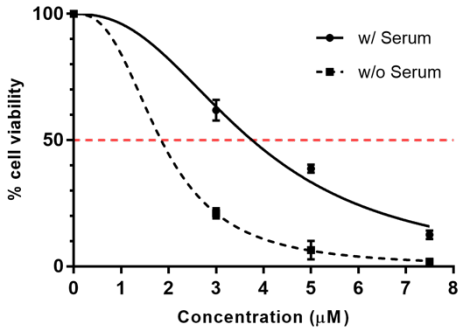

Figure 2. *Effect of foetal bovine serum on the photocytotoxic activity of FPZ on HeLa cells. Cells were incubated with FPZ (3.0, 5.0 and 7.5 μM) for 3 h in medium with serum (•) or without serum (■) and then irradiated with 1.2 J cm^{-2} of UVA light as described in method B. Cell viability was determined with Trypan blue assay.*

3.3 Evaluation of apoptosis

With the aim to investigate the mechanism responsible for cell death, flow cytofluorimetric experiments were performed on HeLa cells (the most sensitive among the three cell lines) in the presence of Annexin V-FITC and DNA-specific dye propidium iodide. In details, cells were treated for 1 h with FPZ and then irradiated with 1.2 J cm^{-2} UVA light, following method A or B, as indicated in Materials and Methods section (Fig. 3 and 4, respectively). Both dot plots representation (upper part) and histograms representing the percentage data (lower part) are shown.

As regard method A (Fig. 3), an increase in the concentration of FPZ caused a decrease in viable cells (Q4), along with a concurrent increase in apoptotic cells (both early and late apoptosis, Q3+Q2). Indeed, the percentage of viable cells was reduced from 84.8% (control) to 6.9% at 5.0 μM FPZ. Concurrently, the percentage of apoptotic cells increased from about 14% (control) to more than 90% (5.0 μM FPZ). Otherwise, the necrotic cell number (Q1) did not appear significantly affected by the treatment.

A similar behaviour was achieved by performing the experiments with method B (Fig. 4). Nevertheless, in this latter experimental condition, the effectiveness in inducing the apoptotic process appeared lower than with method A and indeed, at 5.0 μM FPZ, a percentage of apoptotic cells (Q3+Q2) of about 17% was reached, i.e., significantly lower with respect to that obtained with method A at the same concentration (Q3+Q2 ~ 90%). Overall, the above results indicate apoptosis as the main mechanism accountable for cell death induced by FPZ under UVA irradiation.

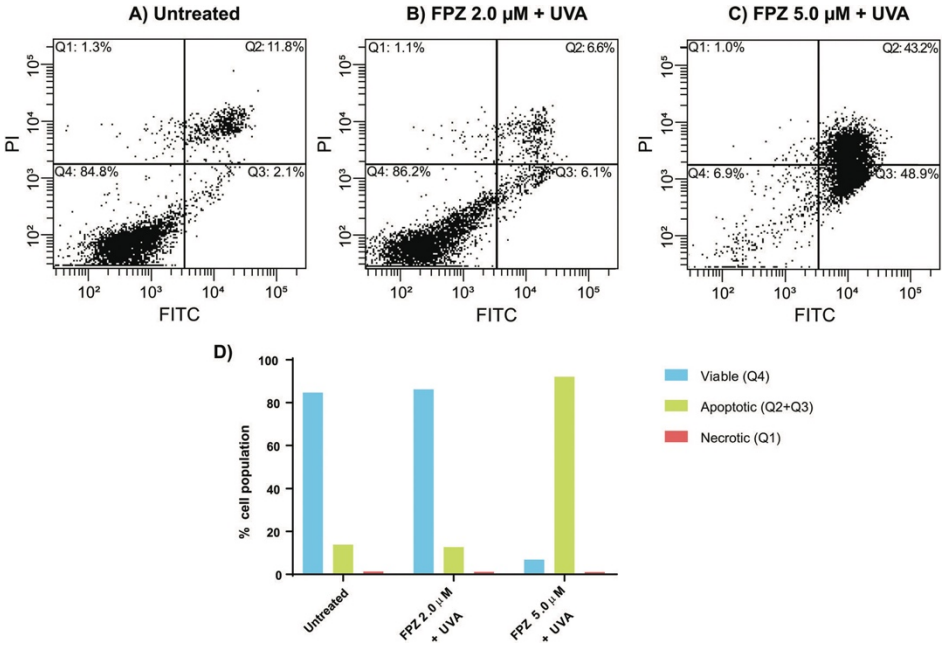

Figure 3. *Flow cytometric analysis of cell death induced by FPZ plus UVA light. HeLa cells were labelled with Annexin V - FITC (AnnV) and propidium iodide (PI) after treatment with different concentrations of FPZ and irradiation with 1.2 J cm^{-2} UVA, according to method A. Viable cells are gated in Q4 (AnnV - / PI -), early and late apoptotic cells are gated in Q3 and Q2 respectively (AnnV + / PI – and AnnV+ / PI +) and necrotic cells are gated in Q1 (AnnV - / PI +).*

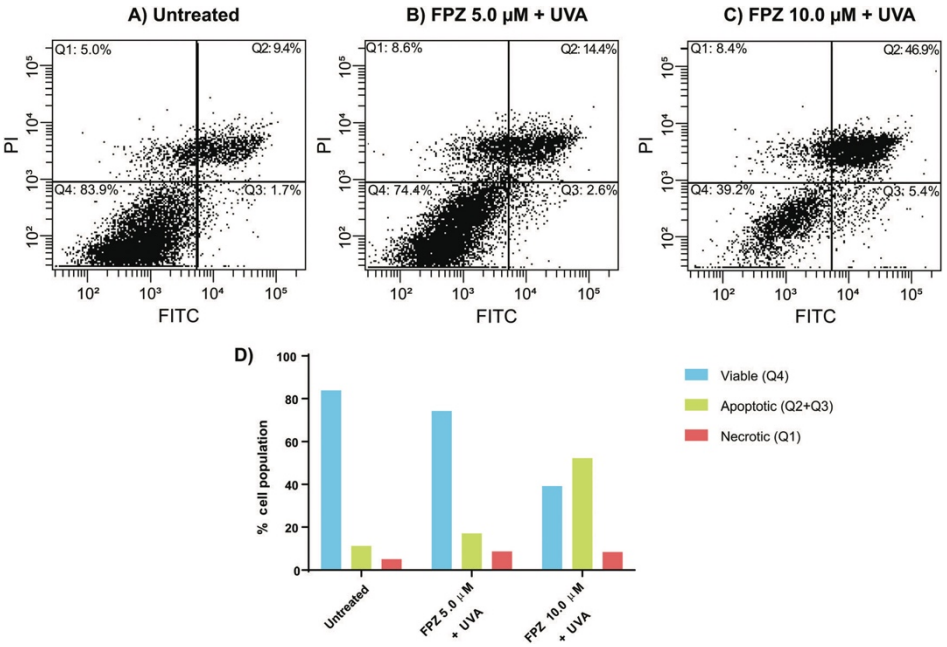

Figure 4. *Flow cytometric analysis of cell death induced by FPZ plus UVA light. HeLa cells were labelled with Annexin V - FITC (AnnV) and propidium iodide (PI) after treatment with different concentrations of FPZ plus 1.2 J cm^{-2} UVA, according to method B. Viable cells are gated in Q4 (AnnV - / PI -), early and late apoptotic cells are gated in Q3 and Q2 respectively (AnnV + / PI – and AnnV+ / PI +) and necrotic cells are gated in Q1 (AnnV - / PI +).*

3.5 Localization inside the HeLa cells

FPZ shows a weak native fluorescence (λ_{exc} = 330 nm and λ_{em} > 370 nm) that was detected under the UV irradiation of the fluorescence microscope used to localize the molecule inside the cells. At a first glance, the

FPZ epifluorescence images inside the HeLa cells (Fig. 5) showed small circular blue spots similar to vacuoles or lysosomes where FPZ accumulated very fast. In particular, after only 15 min of incubation FPZ was already concentrated inside the small vacuole-like structures, and after 60 minutes FPZ fluorescence was spread randomly in the cytoplasm, with some signals also inside the nucleus.

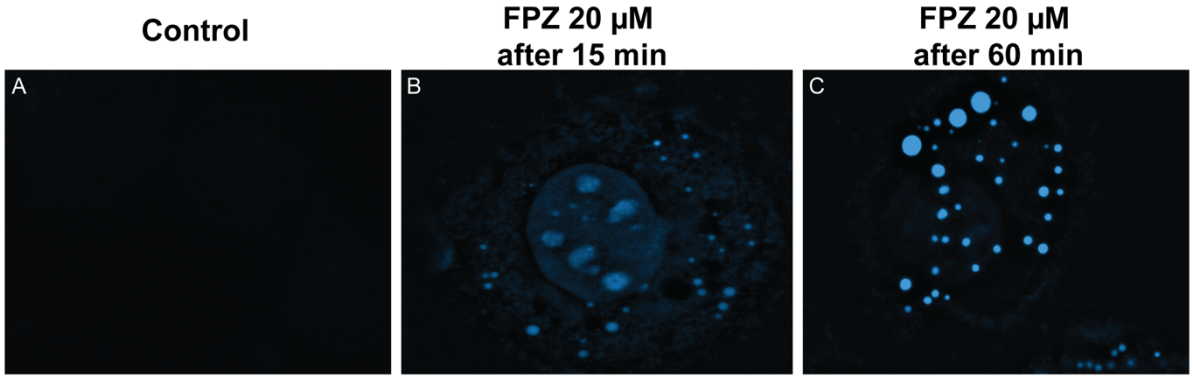

Figure 5. *Epifluorescence of FPZ in HeLa cells detected by fluorescence microscopy.*
A: cells not treated as control; 20.0 μM FPZ after 15 (B) and 60 (C) minutes of incubation.

3.6 Lysosome and mitochondria immunodetection

Anti-LAMP-1 and anti-Pyruvate dehydrogenase E1-beta subunit monoclonal antibodies were used to visualize by confocal microscopy the membrane of lysosomes and mitochondria, respectively, in untreated HeLa cells (Fig. 6A, E), cells irradiated with 1.2 J·cm-2 UVA (Fig. 6B, F), cells incubated with FPZ for 1 h (Fig. 6C, G) and cells incubated with FPZ for 1 h and irradiated with UVA (Fig. 6D, H).

As shown in Figure 6B, F after 1.2 J cm^{-2} UVA light excitation without the compound the cells were similar to the untreated sample (Fig. 5A) and seemed still unaffected by the treatment with UVA, thus confirming the viability assay results for this UVA dose. However, it was interesting to see the lysosomes (yellow) clearly swelled after 1 h of incubation with FPZ (Fig. 6C) most likely due to the presence of the compound inside (see Fig. 5). On the contrary, mitochondria seemed not affected from FPZ (Fig. 6G). Remarkably, the combined effect of UVA plus FPZ induced a dramatic impact to the integrity of the cells and their morphology (Fig. 6D, H). Indeed, both lysosomes and mitochondria lost their regular shape and their labeled membrane proteins were spread in the cytoplasm. Moreover, the cytoskeleton (red) seemed collapsed and the nucleus (blue) looked impaired with respect to the cells incubated with the drug only. These data are in good agreement with the previous cell viability experiments shown in Table 1.

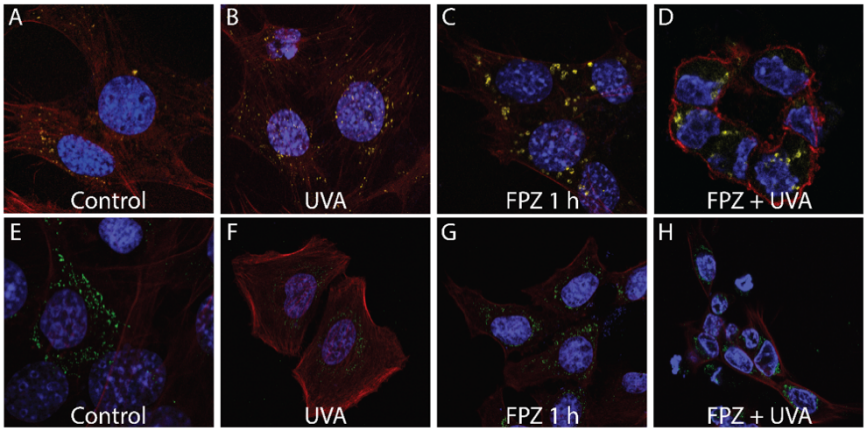

Figure 6. *Fluorescence microscopy of HeLa cells. A, E: untreated cells; B, F: cells irradiated with 1.2 J cm^{-2} of UVA; C, G: cells incubated 1 h with FPZ 20.0 μM; D, H: cells treated for 1 h with FPZ 20.0 μM and irradiated with 1.2 J cm^{-2} of UVA light. Yellow color represents lysosomes marked with anti-LAMP-1 primary antibody and secondary antibody linked to AlexaFlour 555; green color represents mitochondria stained with AlexaFlour 488; blue color represents the cell nucleus stained with Hoechst 33342; red color represents F-actin in the cytoskeleton, marked with phalloidin conjugated with CF633.*

3. 7 ROS generation

The involvement of ROS species in the photocytotoxic effect of FPZ was tested by using a specific assay able to detect ROS, including hydroxyl and peroxyl radical activity, within the cells. Cells treated with increasing concentrations of FPZ and kept in the dark did not exhibit any generation of ROS (Figure 7, dark bars not visible), as well as the irradiation of HeLa cells without FPZ exhibited a negligible production of ROS. On the contrary, cells treated with FPZ in the range 1.0 - 5.0 μM and irradiated with 1.2 J cm^{-2} of UVA, following method A, demonstrated a consistent ROS production, in a clear concentration dependent manner. Therefore, ROS could play a relevant role in the biological effect of FPZ in combination with UVA light. Indeed, it's noteworthy that the TBHP positive control formed ROS in an extent similar to 1.0 μM FPZ plus UVA alone and that 5.0 μM FPZ plus UVA produced ROS at least 6 folds higher than TBHP (Figure 7).

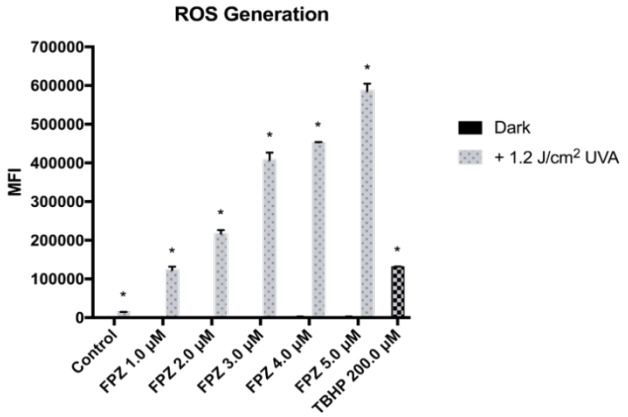

Figure 7. *ROS generation in HeLa cells, stained with 25.0 μM 2',7'-dichlorofluorescin diacetate (DCFDA) then incubated with various concentrations of FPZ (1.0 - 5.0 μM) and irradiated with 1.2 J cm^{-2} of UVA. Control samples: untreated cells kept in the dark (Control, FPZ 1.0 – 5.0 μM); cells treated with 200.0 μM tertbutyl hydrogen peroxide (TBHP, positive control).*

4. Conclusions

This contribution reports the notable cytotoxic effect of FPZ, at micromolar concentrations, in combination with a low UVA dose (1.2 J cm^{-2}) against three different human cancer cell lines. The use of two experimental methods to assess cell viability in combination with UVA light suggested that the removal of the free drug before irradiation induced a photocytotoxic effect about 2-fold smaller with respect to that observed when FPZ was present during irradiation, indicating an important contribution of FPZ molecules outside the cells to the overall activity. However, the presence of serum proteins in the medium left only in method B, able to strongly bind the drug12, strongly influenced the results obtained.

Remarkably, incubation of all the three cell lines up to 72 h with higher concentrations of FPZ (20.0 μM) in the dark did not cause significant reduction of the number of viable cells, indicating that FPZ was well tolerated by cells when the light was not applied.

Unlike previous studies performed in murine 3T3 fibroblasts in which plasma membrane seemed the main target of FPZ phototoxicity,[3] localization in HeLa cell plasma membrane appeared instead negligible, while lysosomes looked one of the main substrates after FPZ uptake. Therefore, it could be hypothesized that, as a result of disruption of lysosomal membranes upon illumination, the cells were digested by the released hydrolytic enzymes, leading to cell death. However, the effectiveness of lysosome-localized photosensitizers is generally significantly lower than in other organelles.[13] Indeed, the photodamage of FPZ also involved mitochondria indicating that the detrimental effect of this drug was extended to other cell targets. The minor localization inside the nucleus may be important to fully define the mechanism of the photoinduced cell death and it will worth to further examine the damage on DNA, both nuclear and mitochondrial. However, from previous studies FPZ did not seem so effective in photodamaging salmon testes DNA as other phenothiazines. Indeed, FPZ demonstrated to externally bind the DNA and not to be able to intercalate the macromolecule (probably due to the -CF_3 substituent in C2, inducing hindering and/or repulsive effects). Thus, its radical cation formed during irradiation could not react efficiently with the DNA bases.[4]

Furthermore, the formation of ROS inside the cells upon illumination suggested that a photodynamic mechanism was involved. This confirms the effective contribution of reactive oxygen species in FPZ photoantiproliferative activity, in agreement with previous results on 3T3 fibroblasts.[2]

As regards cell death, apoptosis was recognised as the main mechanism involved, accompanied by a very small fraction of necrotic cells.

Overall, our results indicate that the neuroleptic drug FPZ in combination with UVA light is able to kill different human cancer cell lines primarily through apoptosis. These properties make this drug a promising candidate for anticancer treatments in photochemotherapy.

References

1. A. Brayfield, Martindale: The Complete Drug Reference, Pharmaceutical Press, 39th edn., 2014.

2. C. Bastianon, R. Zanoni, G. Miolo, S. Caffieri and E. Reddi, Mitochondria and plasma membrane as targets of UVA-induced toxicity of neuroleptic drugs fluphenazine, perphenazine and thioridazine., Int. J. Biochem. Cell Biol., 2005, 37, 901–8.

3. S. Caffieri, G. Miolo, R. Seraglia, D. Dalzoppo, F. M. Toma and G. M. J. B. Van Henegouwen, Photoaddition of fluphenazine to nucleophiles in peptides and proteins. Possible cause of immune side effects, Chem. Res. Toxicol., 2007, 20, 1470–1476.

4. G. Viola, L. Latterini, D. Vedaldi, G. G. Aloisi, F. Dall'Acqua, N. Gabellini, F. Elisei and A. Barbafina, Photosensitization of DNA strand breaks by three phenothiazine derivatives., Chem. Res. Toxicol., 2003, 16, 644–51.

5. F. Elisei, L. Latterini, G. Gaetano Aloisi, U. Mazzucato, G. Viola, G. Miolo, D. Vedaldi and F. Dall'Acqua, Photochem. Photobiol., 2007, 75, 11–21.

6. G. Miolo, L. Levorato, F. Gallocchio, S. Caffieri, C. Bastianon, R. Zanoni and E. Reddi, In vitro phototoxicity of phenothiazines: involvement of stable UVA photolysis products formed in aqueous medium., Chem. Res. Toxicol., 2006, 19, 156–63.

7. M. Schleuning, V. Brumme and W. Wilmanns, Growth inhibition of human leukemic cell lines by the phenothiazine derivative fluphenazine., Anticancer Res., 13, 599–602.

8. I. Gil-Ad, B. Shtaif, Y. Levkovitz, J. Nordenberg, M. Taler, I. Korov and A. Weizman, Phenothiazines induce apoptosis in a B16 mouse melanoma cell line and attenuate in vivo melanoma tumor growth., Oncol. Rep., 2006, 15, 107–112.

9. L. Qi and Y. Ding, Potential antitumor mechanisms of phenothiazine drugs., Sci. China. Life Sci., 2013, 56, 1020–7.

10. A. Jaszczyszyn, K. Gąsiorowski, P. Swiątek, W. Malinka, K. Cieślik-Boczula, J. Petrus and B. Czarnik-Matusewicz, New fluphenazine analogues as inhibitors of P-glycoprotein in human lymphocyte cultures, Contemp. Oncol. (Poznan, Poland), 2012, 16, 332–337.

11. L. Dalla Via, S. Mammi, E. Uriarte, L. Santana, I. Lampronti, R. Gambari and O. Gia, New Furan Side Tetracyclic Allopsoralen Derivatives: Synthesis and Photobiological Evaluation, J. Med. Chem., 2006, 49, 4317–4326.

12. M. A. Cheema, P. Taboada, S. Barbosa, E. Castro, M. Siddiq and V. Mosquera, Energetics and Conformational Changes upon Complexation of a Phenothiazine Drug with Human Serum Albumin, Biomacromolecules, 2007, 8, 2576–2585.

13. N. L. Oleinick and H. H. Evans, The Photobiology of Photodynamic Therapy: Cellular Targets and Mechanisms, Radiat. Res., 1998, 150, S146–S156.

CONCLUSIONS AND FINAL REMARKS

The studies reported in this thesis aim to find new applications for already known photoactivatable compounds and drugs: 8-methoxypsoralen and 4,6,6'-trimethylangelicin, belonging to the psoralen + UVA (PUVA) class of photochemotherapeutic compounds, and fluphenazine, a neuroleptic drug known for its photosensitizing properties as adverse effects.

Focusing on psoralens, their application has been limited to superficial areas of the body until this moment. We were able to verify the reported evidence of psoralen activation with blue light and test this method on human cancer cells. In order to determine the differences between PUVA and our concept that we called PBL (Psoralen + Blue Light), blue light experiments were performed in parallel with UVA experiments. Both 8-MOP and TMA reported a remarkable antiproliferative action on our model prostate cancer cells, although the IC_{50} obtained were found to be higher when the two substances were activated with blue light. The experiments on plasmid pBR322 DNA demonstrated that blue light activation produce different amounts of DNA lesions, thus explaining the higher concentration required for PBL to induce the same amount of cell death obtained with PUVA experiments. The main difference between 8-MOP and TMA is that the latter was not able to form the highly mutagenic interstrand crosslink lesions under blue light, indicating that TMA could be considered safer than 8-MOP. Both compounds generated ROS under irradiation, indicating that photodynamic reactions are involved in the overall mechanism of action.

An important feature emerged from these compounds is their efficacy in targeting CSCs, cells responsible for tumoral self-renewal potential and formation of metastasis. CSCs are particularly difficult to eradicate, considering their resistance to chemotherapy (*i.e.* overexpression of efflux pumps) and radiotherapy (*i.e.* enhanced DNA repair mechanisms and overexpression of anti-apoptotic and pro-survival pathways). The inhibitory action on sphere formation and the reduced expression of CD44 receptors in treated cultures, both markers for stem-like features, clearly confirmed this important aspect of the global mechanism of action of these compounds. TMA proved to be very effective under both wavelength against $CD44^+$ cell population with respect to 8-MOP, a promising result that indicate that TMA could be successfully used for the treatment of solid tumours, possibly decreasing the risk of metastasis formation. Both 8-MOP and TMA induced prevalently apoptotic cell death and the underlying molecular mechanism revealed that the two compounds behaved with different effect on the phosphorylation of p38 (mediator of proapoptotic signalling, regulation of cell cycle checkpoint and autophagy activation) and p44/42 (ERK1/2, anti-apoptotic signalling) MAPKs. The observed evidence indicates that the different activation of MAPKs may be correlated to the type and the extent of DNA damage. Furthermore, TMA influence on CD44 expression was also related to the variation of nuclear β-catenin, a transcription factor that regulate the transcription of many oncogenes, indicating an existing relationship between CD44 receptors and the Wnt pathway, both involved in CSCs renewal and growth. Translating these results into a clinical application, TMA may be a good candidate for photochemotherapy against cancer. In particular, as BL is able to activate TMA without producing mutagenic cell lesions, the combination of this wavelength with TMA can be extended also to solid tumours. Indeed, BL can reach deeper areas of tissues as compared to UVA radiation and its delivery to the tumoral site can be easily performed with optical fiber, given that UVA requires materials with specific optical properties and are usually expensive.

As regards the antipsychotic drug fluphenazine, whose photoreactivity is well known under UVA irradiation in normal healthy cells, the study reported in this thesis evidenced its effectiveness in inducing cellular death following UVA irradiation also in three different human cancer cell lines used, with different IC_{50}, but still within the micromolar range. The different activity on the three cell lines may depend on tissue derivation. Indeed, the two cell lines from mucous tissue (HeLa and MSTO-211H) responded in a similar manner, while the cell line from epidermoid cancer (A431) was less sensitive.

As demonstrated by the DCFDA assay, fluphenazine formed high levels of intracellular ROS in concentration-dependent manner, indicating that reactive oxygen species could play a major role in cellular phototoxicity, along with the phenothiazine radical cation, as reported by Elisei *et al.*

The apoptotic cell death induced by the joint action of UVA and FPZ can be correlated to the damage observed in mitochondria and lysosomes and suggests that apoptosis may be activated via the intrinsic pathway. Overall results obtained until now indicate that fluphenazine can be a good candidate for superficial photochemotherapy, as its important side effects on the central nervous system can be avoided through its topical administration and by focused irradiation of the diseased area.

PARALLEL ACTIVITIES AND COMUNICATIONS

During these three years I was also involved in the study of photodegradation of abuse matrix, as light can induce photodegradative processes on molecules (*i.e.* drugs or illicit drugs). The results of these studies were published in the following papers:

- Miolo G, Stocchero G, Vogliardi S, Menilli L, Scrivano S, Montisci M, Favretto D. A Study on Photostability of Ethyl Glucuronide in Hair Irradiated under Artificial Sunlight. J Anal Toxicol. 2019 Jan 22. doi: 10.1093/jat/bky098.

- Miolo G, Tucci M, Menilli L, Stocchero G, Vogliardi S, Scrivano S, Montisci M, Favretto D. A Study on Photostability of Amphetamines and Ketamine in Hair Irradiated under Artificial Sunlight. Brain Sci. 2018 May 28;8(6). pii: E96. doi:10.3390/brainsci8060096.

I attended two important Photobiology congresses in Pisa (2017) and Barcelona (2019), where I presented two poster communications with the title:

- Intravescical photochemotherapy of bladder cancer: novel approaches based on local delivery of furocoumarins and phenothiazines (Menilli L, Sturaro G, Conconi MT, Miolo G);

- A photoproduct of ketamine was identified in hair samples irradiated with artificial light in a solar simulator (Menilli L, Tucci M, Miolo G, Favretto D).